GEOLOGICA ULTRAIECTINA

Mededelingen van de
Faculteit Aardwetenschappen
Universiteit Utrecht

No.195

Naturally Occurring Radioactive Materials in the gas and oil industry

Origin, transport and deposition of stable lead and ^{210}Pb from Dutch gas reservoirs

Arthur P. Schmidt

GEOLOGICA ULTRAIECTINA

Mededelingen van de
Faculteit Aardwetenschappen
Universiteit Utrecht

No. 195

Naturally Occurring Radioactive Materials in the gas and oil industry

Origin, transport and deposition of stable lead and ^{210}Pb from Dutch gas reservoirs

Arthur P. Schmidt

ISBN 90-393-2505-7

Naturally Occurring Radioactive Materials in the gas and oil industry

Origin, transport and deposition of stable lead and ^{210}Pb from Dutch gas reservoirs

Natuurlijk voorkomende radioactieve materialen in de gas- en olie-industrie

Herkomst, transport en afzetting van stabiel lood en ^{210}Pb
vanuit Nederlandse gasreservoirs

(met een samenvatting in het Nederlands)

Proefschrift

ter verkrijging van de graad van doctor
aan de Universiteit Utrecht
op gezag van de Rector Magnificus, Prof. Dr. H.O. Voorma
ingevolge het besluit van het College van Decanen
in het openbaar te verdedigen
op maandag 25 september 2000 des morgens te 10.30 uur

door

Arthur Pieter Schmidt

geboren op 24 november 1970, te Zwijndrecht

Promotor: Prof. Dr. R.D. Schuiling
Department of Geochemistry, Utrecht University
Utrecht, The Netherlands

Co-promotors: Dr. F.A. Hartog
Nuclear and Analytical Measurements
Shell Research and Technology Centre Amsterdam

Dr. S.R. van der Laan
Ceramics Research Centre
Corus Research, Development & Technology

The research described in this thesis was carried out at the Department of Geochemistry, Utrecht University, Budapestlaan 4, P.O. Box 80021, 3508 TA Utrecht, The Netherlands.
This study was supported by the Nederlandse Aardolie Maatschappij BV, Assen.

At the Home for Old Atoms...

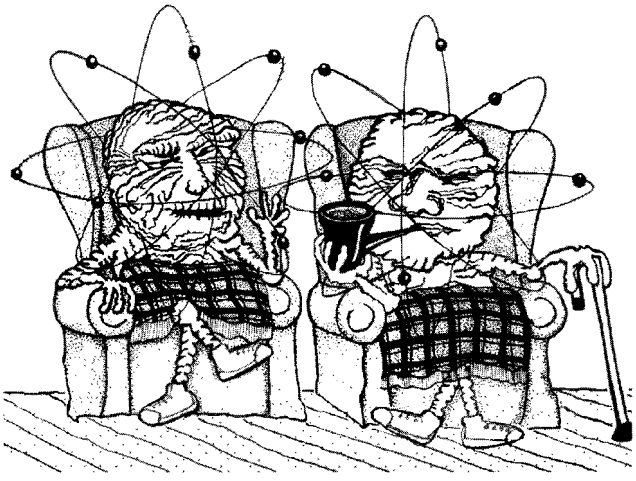

"When I was young I used to feel so alive, so dangerous! In fact, would you believe I started life as a Uranium-238? Then one day I accidentally ejected an alpha particle....now look at me, a spent old atom of Lead-206. Seems that all my life since then has been nothing but decay, decay, decay..."

Voor Odette

Contents

Prologue

Introduction

The omnipresence of Naturally Occurring Radionuclides (NORs) within the Earth is well-known. Since long, radioactive decay of NORs has been recognised as the primary source of our internal planetary heat, and driving force of volcanism and the movement of plates forming the Earth's crust. Since NORs are most abundant in the Earth's crust, from which all oil and gas are produced, it is no surprise to encounter NORs in the oil and gas industry.

Already at the beginning of the 20th Century, it became clear that NORs can be produced together with hydrocarbons. In oil and gas production facilities, enhanced quantities of some NORs can be found in the hydrocarbons themselves, in coproduced water, and in all kinds of waste materials such as mineral scales and sludges. Production water and deposits containing NORs have been termed NORM, i.e. Naturally Occurring Radioactive Materials, or TENORM, i.e. Technologically Enhanced NORM. The presence of NORM in production facilities can face oil and gas companies with large additional costs in maintenance, treatment and lost production, while extra care has to be taken regarding the environment and the health of production personnel. Therefore, management of NORM is essential to the oil and gas industry. Knowledge on the occurrence, origin and formation of NORM forms the basis of NORM management. Understanding NORM might assist in prediction or even prevention of NORM build-up in production facilities, leading to important risk and costs reductions.

This study was initialised to gain insight into the chemical behaviour and physical properties of primordial NORs U and Th and their decay products in hydrocarbon reservoirs and production facilities during production, processing and treatment of oil and gas. More specifically, three topics were selected in order to establish the influence of geochemical and production parameters on NORs, from subsurface to production facilities: a) accumulation of NORs in hydrocarbon source rocks and reservoir rocks, b) transport of NORs together with produced liquids and gases into production lines, and c) build-up of NORM in facilities. Focus of this study was the encounter of ^{210}Pb in the production of natural gas from Dutch reservoirs.

Summary

Chapter 1 of this thesis provides the reader with a background in the nature of oil and gas industry NORM. Based on an extensive literature search, this chapter deals with general aspects of the natural decay series, the history of oil and gas NORM, identifies the most relevant radionuclides, and investigates geochemical aspects of oil and gas NORM. Special attention is paid to the Netherlands and adjacent southern North Sea area. Focus of this thesis, production of stable Pb and ^{210}Pb with natural gas, was based on the conclusions of this literature search and on the encounter of ^{210}Pb-bearing scales in Dutch gas production facilities. Where relevant, results from this Ph.D. study are included in chapter 1.

In **Chapter 2** the distribution of NORs in Dutch Rotliegend and Kupferschiefer sediments is studied, in order to identify the origin of ^{210}Pb produced from Dutch gas reservoirs. In addition, a mechanism is proposed for the selective mobilisation of ^{210}Pb from the reservoir sediments.

Chapter 3 comprises a study on stable Pb in Dutch and German Rotliegend and Kupferschiefer sediments. A sequential extraction method is used to establish the distribution of Pb over five mineral phases in the sediments. Bulk chemistry, Pb distribution and stable Pb isotope signatures of the sediments are used to investigate whether Pb in Dutch Rotliegend gas reservoir brines can have originated from the Rotliegend sediments themselves.

Experimental determination of the solubilities of Pb and water in methane is studied in **Chapter 4,** in order to see whether enough Pb can be transported in a water saturated gas phase to explain the occurrence of Pb mineral deposits in gas production facilities where no reservoir brines are coproduced with natural gas. Solubilities are compared with observed Pb concentrations in Dutch natural gas production samples, and some remarks are made on the speciation of Pb in the hydrocarbon gas phase.

In **Chapter 5**, preliminary results are reported on the nature and deposition of a small number of Pb precipitates in Dutch gas production facilities. Final results from a detailed study on a much larger number of Pb deposits are presented in **Chapter 6**. Stable Pb isotope signatures of the deposits are used to investigate the origin of the Pb, while distribution of NORs in the deposits is studied in order to reveal the coprecipitation of NORs, and especially ^{210}Pb, in Pb-bearing precipitates. Also, deposition mechanisms of the Pb precipitates are studied, as are parameters influencing the deposition processes.

In **Chapter 7**, finally, a synthesis is presented on the origin, transport and deposition of NORM in Dutch gas production facilities. Combining results from chapters 1 through 6, answers are presented to questions posed at the start of this Ph.D. study. Based on the conclusions, suggestions for further research and recommendations regarding the production and deposition of NORM from natural gas reservoirs are given.

Acknowledgement - The author wishes to thank Nederlandse Aardolie Maatschappij (NAM) B.V. for providing sediment and scale samples, production data, and financial support for this Ph.D. research.

Chapter 1

NORM in the oil and gas industry - a geochemical review

A.P. Schmidt and F.A. Hartog

Abstract - A review of current geochemical knowledge on composition, origin and formation of Naturally Occurring Radioactive Materials (NORM) encountered during the production and processing of oil and gas is presented. Uranium and thorium are very insoluble under reduced hydrocarbon reservoir conditions, and will not be encountered in enhanced concentrations in hydrocarbon production streams. Daughter nuclides of ^{238}U and ^{232}Th, however, can be preferentially mobilised into reservoir brines. Mobilisation occurs through direct alpha recoil in combination with leaching. Because of high solubilities of radium, radon and lead in brines, mobilisation of Naturally Occurring Radionuclides (NORs) from the ^{226}Ra and ^{228}Ra sub-series into hydrocarbon formation waters can be very effective. As such, especially ^{228}Ra, ^{226}Ra and ^{210}Pb can be found in coproduced reservoir brines and subsequently become concentrated in various production wastes such as scales, sludges and reservoir materials. Preferential coprecipitation of ^{226}Ra and ^{228}Ra in sulphates and carbonates, and of ^{210}Pb in Pb-bearing scale minerals, will lead to ingrowth of shorter-lived daughter nuclides. Gaseous ^{222}Rn is transported in both hydrocarbon and water phases, and tends to concentrate in natural gas liquids during fractionation processes. Upon treatment and storage, ^{222}Rn daughter nuclides ^{210}Pb and ^{210}Po may be deposited on the inner surface of production facilities. In many cases, ^{210}Pb in scales and sludges is unsupported, due to separation from its parent ^{222}Rn in the course of the production process. Background concentrations of U and Th in reservoir sediments may lead to slightly enhanced concentrations of NORs from the ^{226}Ra and ^{228}Ra sub-series in associated reservoir brines. Higher concentrations of these daughter NORs are due to local enrichments of U and/or Th in reservoir sediments close to the perforations of oil and gas wells. Organic-rich shales and bituminous deposits, enriched in U, are frequently identified as sources of NORs coproduced with oil and natural gas.

To be submitted

Introduction

The presence of Naturally Occurring Radionuclides (NORs) in the Earth's crust is well-known. More than twenty primordial nuclides have been identified, most of them with half-lives exceeding the age of the Earth by several orders of magnitude (Kathren, 1998). Some primordial NORs, including ^{40}K, ^{87}Rb, ^{232}Th, ^{235}U, and ^{238}U, have half-lives roughly in the order of the age of the Earth. These NORs are potentially important on timescales governing geological processes such as the formation of hydrocarbon source-rocks and the generation and migration of oil and gas. Primordial nuclides ^{232}Th, ^{235}U, and ^{238}U are particularly important because they are heading the three natural decay series, which include a number of NORs with half-lives for all but one nuclide in the order of the oil and gas production time scale of days to decades (**Table 1.1**). It are these relatively short-lived NORs that, upon coproduction from oil and gas reservoirs, may be encountered in hydrocarbons themselves, in produced water, and in all kinds of hard and soft deposits in (sub)surface production facilities.

Strictly speaking, the acronym NORM, meaning Naturally Occurring Radioactive Materials, refers to natural materials containing NORs in non-enhanced concentrations. The acronym TENORM, meaning Technologically Enhanced NORM, has been introduced to distinguish NORM in the strict sense from materials with enhanced natural radioactivity as a result of human technology. Often, however, NORM is rather used to refer to any material which is radioactive due to the presence of natural radioactivity (Heaton and Lambley, 1995). Here we shall use the term NORM in this latter sense, comprising all oil and gas industry solids and liquids containing NORs. Of course, NORM is not restricted to the oil and gas industry but is encountered in any industry or process in which fluids or minerals are extracted from the Earth for energy or products such as fertiliser, building materials, paint pigments and ceramics (Gallup and Featherstone, 1995; Heaton and Lambley, 1995). An extensive but general overview of NORM sources and their origins has been given by Kathren (1998). In this paper we will only deal with oil and gas industry NORM, although many of the topics discussed are also relevant to NORM in other industries.

Natural decay series

Decay of radionuclides is described by the law of radioactive decay:

$$A_t = A_0 \cdot e^{-\lambda \cdot t}$$

where A_0 is the number of radionuclides at the time t = 0, A_t is the number of nuclides after a certain time t, and λ is the decay constant of the specific nuclide. The half life time $t_{½}$ of a radionuclide (**Table 1.1**) is inversely proportional to its decay constant:

$$t_{1/2} = \frac{\ln 2}{\lambda}$$

Table 1.1 - Natural decay series of ^{238}U, ^{235}U and ^{232}Th.

Atomic number	Element	Radionuclide	Half life	Radionuclide	Half life	Radionuclide	Half life
92	Uranium	**^{238}U**	$4.51 \cdot 10^9$ y	**^{235}U**	$7.04 \cdot 10^8$ y		
90	Thorium	^{234}Th	24.1 d	^{231}Th	25.5 h	**^{232}Th**	$1.41 \cdot 10^{10}$ y
91	Protactinium	^{234m}Pa (0.13%)	1.17 m	^{231}Pa	$3.28 \cdot 10^4$ y		
		^{234}Pa (99.87%)	6.75 h			^{228}Ra	5.76 y
		^{234}U	$2.45 \cdot 10^5$ y				
89	Actinium			^{227}Ac (98.6%)	21.8 y	^{228}Ac	6.13 h
		^{230}Th	$8.0 \cdot 10^4$ y	^{227}Th	18.7 d	^{228}Th	1.91 y
87	Francium			^{223}Fr (1.4%)	21.8 m		
88	Radium	^{226}Ra	$1.60 \cdot 10^3$ y	^{223}Ra	11.4 d	^{224}Ra	3.66 d
86	Radon	^{222}Rn	3.82 d	^{219}Rn	3.96 s	^{220}Rn	56 s
84	Polonium	^{218}Po (99.98%)	3.05 m	^{215}Po (~100%)	$1.78 \cdot 10^{-3}$ s	^{216}Po	0.15 s
82	Lead	^{214}Pb	26.8 m	^{211}Pb	36.1 m	^{212}Pb	10.6 h
85	Astatium	^{218}At (0.02%)	2 s	^{215}At (0.00023%)	~ 10^{-4} s		
83	Bismuth	^{214}Bi	19.7 m	^{211}Bi	2.15 m	^{212}Bi	60.6 m
		^{214}Po (99.98%)	$1.64 \cdot 10^{-4}$ s	^{211}Po (0.28%)	0.52 s	^{212}Po (64.0%)	$3 \cdot 10^{-7}$ s
81	Tellurium	^{210}Tl (0.02%)	1.32 m	^{207}Tl (99.7%)	4.77 m	^{208}Tl (36.0%)	3.1 m
		^{210}Pb	22.3 y				
		^{210}Bi	5.0 d				
		^{210}Po (~100%)	138.4 d				
		^{206}Tl (0.00013%)	4.20 m				
		^{206}Pb	Stable	**^{207}Pb**	Stable	**^{208}Pb**	Stable

Within a series of subsequent decay steps, ingrowth of a daughter nuclide from a parent is not only governed by the decay constant of the parent, but also by its own decay constant:

$$A_{d,t} = A_{p,0} \cdot \frac{\lambda_d}{\lambda_d - \lambda_p} \cdot (e^{-\lambda_p \cdot t} - e^{-\lambda_d t})$$

where *p* and *d* refer to parent and daughter nuclides, respectively. This equation can often be simplified, especially when the decay constant of the parent is much larger or smaller than that of the ingrowing daughter, and ingrowth is mainly governed by the decay constant of the longest-lived of the two nuclides.

When, within a geological system, daughter nuclides from the ^{238}U, ^{235}U and ^{232}Th decay series have the same activity concentrations ($Bq \cdot g^{-1}$) as their parents, the nuclides are said to be in radioactive or secular equilibrium. As a rule of thumb, daughter nuclides reach secular equilibrium with their parents in about five daughter half life times, provided that there is no migration of radionuclides in or out of the system. For instance, in such a closed system ^{226}Ra will have reached secular equilibrium with ^{230}Th in about 8,000 years (**Table 1.1**). A number of subsequent decay steps within one of the series is called a sub-series. When considering all radionuclides within a (sub-)series, the last member of the decay chain will be in secular equilibrium with the first one after five half life times of the longest-lived daughter nuclide involved. Therefore, within a closed system, the entire ^{238}U decay series will be in equilibrium after about one million years. However, since the chemical concentration ($mole \cdot g^{-1}$) of a nuclide is proportional to its half life time, nuclides with equal activity concentrations can have very different chemical concentrations. For instance, 50 $mBq \cdot g^{-1}$ for ^{238}U and ^{226}Ra correspond to concentrations of about 4 ppm for U and $1.4 \cdot 10^{-6}$ ppm for Ra. Likewise, a ^{222}Rn activity concentration of 10^4 $Bq \cdot m^{-3}$ corresponds to only $1.8 \cdot 10^{-10}$ $g \cdot m^{-3}$.

If radionuclides are able to migrate out of a system, leaving their parent nuclides behind, they are said to be unsupported. In their new environment, their concentration can only be sustained by influx from elsewhere, since there is no more *in situ* ingrowth via radioactive decay of their parents.

History of oil and gas NORM

The first reports on radioactivity associated with the production of hydrocarbons date back to the beginning of the 20th century. Only a few years after the discovery of radioactivity by Antoine Henri Becquerel in 1896 (Kathren, 1998), radon, then called radium emanation, was found in petroleum (Burton, 1904; Himstedt, 1904) and in natural gas (McLennan, 1904). Extensive reports on radon in natural gases from Europe and Canada were published some ten years later (Czakó, 1913; Satterly and McLennan, 1918). Another ten years later, the first report of radium in oil field waters (Tscherepennikov, 1928) greatly stimulated research on NORs in hydrocarbon

production waters, especially in the former Soviet Union, with the aim of radium production (Bobin, 1933; Nikitin and Merkulova, 1933; Komlev, 1933; Komlev *et al.*, 1933; Botset, 1934; Born, 1936; Alekseev *et al.*, 1958; Gutsalo, 1964; Lehnert and Just, 1979, and references therein). Outside the Soviet Union, several workers investigated the radioactivity of sedimentary rocks and associated petroleum (Bell *et al.*, 1940; Tiratsoo, 1949), which led to publication of the first general review on distribution and origin of NORs in petroleum, reservoir rocks and brines (Monicard and Dumas, 1952).

Renewed western interest in the subject in the 1950's partly resulted from the extensive Cold War search for uranium in the United States. The discovery of radon in natural gas from the Texas Panhandle gas field in 1949 led to a nationwide survey of NORs associated with hydrocarbons and reservoir formation waters (Faul *et al.*, 1952; Gott and Hill, 1953; Pierce *et al.*, 1956; Armbrust and Kuroda, 1956). Meanwhile, the presence of NORM scales in oil production facilities was first mentioned by Campbell (1951). He reported the frequent formation of radioactive crusts on the inside and the outside of well casings in the perforated zones. The same phenomenon was described from two wells of the Panhandle gas field (Faul *et al.*, 1952), while radium-rich scales and sludges were found in surface installations from the same field (Gott and Hill, 1953). From an oil production point of view, research on radioactive crusts continued especially in the former Soviet Union throughout the 1960's and 1970's (Lehnert and Just, 1979, and references therein). Meanwhile, however, in the the western world the subject apparently fell into oblivion again.

In the early 1970's, western interest in oil and gas NORM was raised again when radon was found to concentrate in light natural gas liquids such as ethane and propane during processing (Gray, 1993). This was followed by large surveys of radon contents of natural gas from a radiation protection point of view (Gesell, 1975; Tunn, 1975; Van der Heijde *et al.*, 1977). Although these surveys also revealed the (potential) presence in gas production facilities of sludges and scales containing ^{222}Rn daughter nuclides ^{210}Pb and ^{210}Po (Gesell,1975; Van der Heijde *et al.*, 1977), oil and gas NORM still was not a real issue. Some early environmental research was done on radium in oil production waters (Titayeva *et al.*, 1977; Landa and Reid, 1982; Kraemer and Reid, 1984), but otherwise the subject was more or less closed.

Oil and gas NORM again became an issue with the discovery, in 1981, of scales containing ^{226}Ra in North Sea oil production facilities (Smith, 1987). The subsequent 'first' discovery of ^{226}Ra-bearing scales in US oil production facilities in 1986 (Miller *et al.*, 1991) boosted still ongoing worldwide research on all possible aspects of NORM, including origin and nature, measurement techniques, environmental acceptability of operating procedures, disposal options, and site remediation methods (e.g. Smith, 1987; Bassignani *et al.*, 1991; Grice, 1991; Miller *et al.*, 1991; Gray, 1993; Testa *et al.*, 1994; Krishnan *et al.*, 1994; Jonkers *et al.*, 1997; Lysebo and Strand, 1997; Rood *et al.*, 1998; Zhuravel, 1999). Attention has been primarily focussed on oil production NORM containing ^{226}Ra and ^{228}Ra, which is common and quite easily detectable. Potential and actual occurrence of NORM scales and sludges containing ^{210}Pb and daughter products in gas facilities have only rarely been reported (Kolb and Wojcik, 1985; Gray, 1990; Bland and Chiu, 1996). The perhaps underestimated occurrence of this type of gas production NORM has been emphasised recently (Hartog *et al.*, 1995; idem, 1996).

Scope of this paper

Although coproduction of NORs with hydrocarbons has been known for almost a century and deposition of NORM in hydrocarbon production facilities for half a century, potential health, safety, environmental and financial risks of oil and gas NORM have only been realized since the 1980's (Smith, 1987). Since then, much time and money have been spent by the industry on development of NORM management (e.g. Miller *et al.*, 1991). As a result, extensive reviews are available on a large number of aspects of oil and gas NORM (e.g. Smith, 1992; API, 1992). However, with a few notable exceptions (Fisher, 1995; Jonkers *et al.*, 1997), existing reviews have shed rather insufficient light on geochemical aspects of the subject. Therefore, this paper presents a review of current geochemical knowledge on composition, origin and formation of oil and gas industry NORM.

Composition of oil and gas NORM

As has been mentioned above, NORs in the oil and gas industry may be encountered in both liquid and solid production streams. These can be divided into a) hydrocarbons themselves, being crude oil, natural gas, and natural gas liquids or hydrocarbon condensate, b) production water, which in general mainly consists of brine from the hydrocarbon reservoir, and c) secondary products and deposits. These include scales, sludges, scrapings, ferric dust from the inner surfaces of facilities, and hydrocarbon reservoir materials, together termed sand. Scales may be divided into hard scales and soft to medium hard scales, depending on their mineralogy, while scrapings are pieces or remnants of scale detached from the inner surface of facilities by inspection or cleaning tools (Jonkers *et al.*, 1997).

Due to the low isotopic abundance of ^{235}U and the very short half-lives of most of its daughter nuclides, NORs from the ^{235}U series are rarely encountered in the oil and gas industry and will not be further discussed. In general, only NORs from the ^{238}U and ^{232}Th decay series are important in oil and gas NORM (**Tables 1.2 and 1.3**). Of these series, primordial nuclides ^{238}U and ^{232}Th, plus the first four ^{238}U daughter nuclides ^{234}Th, ^{234}Pa, ^{234}U and ^{230}Th, are only encountered in non-enhanced, i.e. very low background concentrations. Important NORs all belong to the so-called ^{226}Ra and ^{228}Ra sub-series, of which ^{226}Ra, ^{222}Rn, ^{210}Pb and ^{210}Po (all ^{238}U daughters) and ^{228}Ra and ^{224}Ra (both ^{232}Th daughters) are commonly reported (Jonkers *et al.*, 1997). Due to ingrowth in scales and sludges or due to deposition from production streams, most of the other, often very short-lived, NORs of the two series will also be present in oil and gas NORM. If time has been long enough, ingrowing daughter nuclides will have reached secular equilibrium with their longer-lived parents. For most of these short-lived NORs, secular equilibrium is established within seconds to hours. So although these NORs will often be significantly present in oil and gas NORM, they are seldomly reported and therefore not mentioned in tables 2 and 3.

When looking at the different oil and gas production streams, large differences in NORs concentrations can be seen (**Table 2**). Significant amounts of NORs have not been reported for

crude oil. In contrast, high concentrations of NORs have been reported for natural gas, liquid hydrocarbons and produced water. Liquid hydrocarbons may contain large amounts of ^{222}Rn and daughter products ^{210}Pb and ^{210}Po (Jonkers *et al.*, 1997). Produced water can have high concentrations of ^{228}Ra and ^{224}Ra from the ^{232}Th series, and of ^{226}Ra and ^{210}Pb from the ^{238}U series.

Table 1.2 - Activity concentrations of NORs in produced hydrocarbons and water.

Radionuclide	Activity concentrations (mainly after Jonkers *et al.*, 1997) in:			
	crude oil ($Bq \cdot g^{-1}$)	natural gas ($Bq \cdot m^{-3}$)	hydrocarbon condensate / natural gas liquids ($Bq \cdot l^{-1}$)	production water ($Bq \cdot l^{-1}$)
^{238}U series				
^{238}U	0.0000001 - 0.01	n.r.	n.r.	0.0003 - 0.1
^{226}Ra	0.0001 - 0.04	n.r.	n.r.	0.002 - 1200
^{222}Rn	0.002 - 0.02*	5 - 200000	0.01 - 4200	n.r.
^{210}Pb	n.r.	0.005 - 0.02	0.3 - 230	0.05 - 190
^{210}Po	0 - 0.01	0.002 - 0.08	0.3 - 100	n.r.
^{232}Th series				
^{232}Th	0.00003 - 0.002	n.r.	n.r.	0.0003 - 0.001
^{228}Ra	n.r.	n.r.	n.r.	0.3 - 180
^{224}Ra	n.r.	n.r.	n.r.	0.5 - 40

* (Bell *et al.*, 1940). n.r.: not reported. Grey: significant enrichments; light grey: possibly significant enrichments.

In natural gas only enhanced concentrations of ^{222}Rn have been observed. Although reported ^{222}Rn concentrations in crude oil are low (Bell *et al.*, 1940) and ^{222}Rn concentrations in produced waters have not been reported at all, both due to release of ^{222}Rn upon depressurisation, we have reasons to believe that these can be significant too. In most oil fields crude oil, natural gas, natural gas liquids and water are produced together, while in most gas fields natural gas, natural gas liquids and water are produced together. Radon solubilities in both water and hydrocarbons are high, although solubility in petroleum (137 $g \cdot l^{-1}$ at STP, 0°C and 1 atm) is much higher than in water (0.5 $g \cdot l^{-1}$ at STP) (Clever, 1979; Gascoyne, 1992). Therefore, high ^{222}Rn activity concentrations in natural gas from oil fields also suggest high ^{222}Rn concentrations in crude oil from the same fields. In the same way, high ^{222}Rn activity concentrations in natural gas from gas fields suggest enhanced ^{222}Rn levels in produced water from these fields.

Waste products from oil and gas production, such as scales, sludges and coproduced reservoir material, may show enhanced concentrations of ^{226}Ra, ^{210}Pb and ^{210}Po from the ^{238}U series and ^{228}Ra from the ^{232}Th series (**Table 1.3**). Of these waste products, only ferric dust from the inner surface of NGL storage tanks and installations contains no radium isotopes. This difference is attributable to the absence of water in these facilities, as will be shown later. For produced sand only insignificant levels of ^{210}Pb have been reported, but enhanced levels are known to occur (F.A. Hartog, unpubl. res.).

Table 1.3 - Activity concentrations of NORs in waste products from oil and gas production.

Radionuclide	Activity concentrations (mainly after Jonkers *et al.*, 1997) in:					
	hard scales ($Bq \cdot g^{-1}$)	soft to medium hard scales ($Bq \cdot g^{-1}$)	sludges ($Bq \cdot g^{-1}$)	scrapings ($Bq \cdot g^{-1}$)	surface dust* ($Bq \cdot g^{-1}$)	sand** ($Bq \cdot g^{-1}$)
^{238}U series						
^{238}U	0.001 - 0.5	0.001 - 0.05	0.005 - 0.01	n.r.	n.r.	n.r.
^{226}Ra	0.1 - 15000	0.8 - 400	0.05 - 800	0.01 - 75	n.r.	0.0 - 22
^{210}Pb	0.02 - 75	0.05 - 2000	0.1 - 1300	0.05 - 50	4.8 - 1000	0.0 - 0.5
^{210}Po	0.02 - 1.5	n.r.	0.004 - 160	0.1 - 4	29	n.r.
^{232}Th series						
^{232}Th	0.001 - 0.002	0.001 - 0.07	0.002 - 0.01	n.r.	n.r.	n.r.
^{228}Ra	0.05 - 2800	0.05 - 300	0.5 - 50	0.01 - 10	n.r.	0.1 - 13

* (Bland and Chiu, 1996; Hartog *et al.*, 1996; Taylor and Cleghorn, 1996). ** (Randolph *et al.*, 1992; Lysebo and Strand, 1997). n.r.: not reported. Grey: significant enrichments; Light grey: possibly significant enrichments.

Absence of primordial nuclides ^{238}U and ^{232}Th and presence of NORs from the ^{226}Ra and ^{228}Ra sub-series in hydrocarbons, coproduced water and waste products can be readily explained from geochemical properties of the NORs and processes occurring on geological and/or hydrocarbon production time scales. Before looking at these properties and processes, however, we must first discuss the chemical and physical mechanisms by which radioactive disequilibrium within the ^{238}U and ^{232}Th decay series can be established in hydrocarbon production fluids.

Mobilisation of NORs from sediments into fluids

Radioactive or secular disequilibrium in hydrocarbon production fluids can only be caused by selective transfer of certain NORs from inside sediment grains to pore solutions. Transfer or mobilisation mechanisms of NORs from the ^{238}U and ^{232}Th natural decay series have been extensively investigated in a large number of geological settings, including hydrocarbon reservoirs (Rosholt *et al.*, 1963; Kigoshi, 1971; Kronfeld *et al.*, 1975; Asikainen, 1981; Bloch and Key, 1981; Osmond and Cowart, 1982; Andrews *et al.*, 1982; Fleischer, 1982; Kraemer and Reid, 1984; Rama and Moore, 1984; Åberg *et al.*, 1985; Laul *et al.*, 1985; Zukin *et al.*, 1987; Krishnaswami and Seidemann, 1988; Andrews *et al.*, 1989; Laul, 1992; Sun and Semkow, 1998).

Mobilisation can occur by four mechanisms, namely solid-phase diffusion, partial or complete dissolution, leaching, and direct alpha recoil. Of these mechanisms, solid-phase diffusion is not likely to be important, especially for the short-lived NORs from the ^{226}Ra and ^{228}Ra sub-series, because of too low diffusion coefficients of NORs in sediment grains (Bloch and Key, 1981). However, evidence for movement of divalent cations including Ca^{2+} in calcite at appreciable rates (Stipp *et al.*, 1999) may have implications for diffusion of U in carbonates because of

similarity in ionic radii for U^{4+} and Ca^{2+} (Kronfeld *et al.*, 1993). Partial or complete dissolution of grains may be important in some cases, such as the formation of secondary porosity in sandstones by corrosive fluids. However, dissolution processes are generally confined to certain stages of sediment diagenesis, and do not presently occur in hydrocarbon reservoirs. Dissolution can certainly not explain the constant supply of NORs from sediments into fluids required for continuous replenishment of short-lived NORs (Bloch and Key, 1981). In contrast, leaching or etching of NORs can be important because daughter isotopes within the decay series are either present in mineral lattice sites which have been subjected to radiation damage due to the previous decays (Rosholt *et al.*, 1963) or do not fit into the lattice because of crystal-chemical differences with their parent nuclides (Starik, 1938, and Cherdyntsev, 1971, both cited in Bloch and Key, 1981). Finally, alpha recoil, also known as the "Szilard-Chalmers" effect, is a second important mobilisation mechanism. Emmittance of an alpha, $^{4}_{2}He$, particle during radioactive decay gives the residual nucleus an amount of recoil energy that is far larger than chemical bond energies. As a result, the recoil atom may travel distances of 10^{-7} to 10^{-6} cm within mineral grains (Cherdyntsev, 1971, cited in Bloch and Key, 1981). Recoiled NORs that are situated close enough to the mineral surface may enter pore solutions or even adjacent mineral grains causing damage and facilitating later leaching (Fleischer, 1982).

In practice, mobilisation through leaching and direct alpha recoil operate simultaneously and are difficult to distinguish. However, in hydrocarbon reservoirs direct alpha recoil tends to be considered more important than leaching due to alpha recoil damage. For instance, excess activity concentrations of ^{228}Ra over its parent ^{232}Th in oil field brines are largely attributed to direct alpha recoil (Bloch and Key, 1981). Activity ratios of up to 10 for $^{234}U/^{238}U$ in oil field brines can be explained by alpha recoil of ^{234}Th from sediment grains into pore waters and subsequent decay of dissolved ^{234}Th to ^{234}U (Kronfeld *et al.*, 1975). Even if most of the ^{234}Th is quickly adsorbed on grain surfaces, produced ^{234}U may be readily dissolved (Andrews *et al.*, 1989). Further down the two decay series, excess activity concentrations of ^{224}Ra and ^{226}Ra over their respective parents ^{228}Th and ^{230}Th are attributed to the same processes (Bloch and Key, 1981; Laul *et al.*, 1985; Andrews *et al.*, 1989).

From the above examples it is clear that mobilisation of NORs from sediments through combined leaching and direct alpha recoil will only be effective if the nuclides have the right geochemical properties to stay into the pore solutions. The following section on distribution and geochemical behaviour of NORs in hydrocarbon reservoirs will therefore explain why especially NORs from the ^{226}Ra and ^{228}Ra sub-series are found in oil and gas NORM.

NORs in oil and gas reservoirs

Conditions in hydrocarbon reservoirs are generally very reducing. In such an environment, uranium is predominantly present in the +4 oxidation state. Dissolved oxidized U^{6+} (uranyl, UO_2^{2+}) forms strong complexes, particularly with carbonate, but U^{4+} does not and readily precipitates as UO_2, uraninite (Bloch and Key, 1981; Kraemer and Kharaka, 1986). Hence, ^{238}U concentrations in hydrocarbon reservoir brines are low, not exceeding 0.1 $Bq \cdot l^{-1}$ (**Table 1.2**)

which is equivalent to about 8 ppb.

Besides with carbonates, UO_2^{2+} also forms complexes with organic compounds such as humates and fulvates (Zielinski *et al.*, 1987). Because of this, sediments rich in humic substances, such as peat, lignite and coal, will adsorb U from ground waters with a partition coefficient as high as 10,000 (Szalay, 1958; Armands and Landergren, 1960). Once adsorbed, subsequent reduction of UO_2^{2+} to UO_2 and formation of organometallic complexes (Idiz *et al.*, 1986) may lead to U concentrations of up to 500 ppm in lignite or coal (Breger *et al.*, 1955; McKelvey *et al.*, 1955) and even up to 6000 ppm in peat (Zielinski and Meier, 1988). Typical U concentrations in hydrocarbon reservoir sediments such as sandstones, shales and carbonates are on the order of 2 to 4 ppm (Fisher, 1995). Due to the affinity of U for organic matter, U concentrations in black shales and oil shales range from 1 to 250 ppm (Asuen and Imasuen, 1990; Cortial *et al.*, 1990; Kronfeld *et al.*, 1993; Fisher, 1995). In contrast, U concentrations in crude oil (**Table 1.2**) are generally much lower than in reservoir sediments, since U is primarily present in the heavy asphaltene fraction of crude oil (Erickson *et al.*, 1954; Pierce *et al.*, 1964; Komarev *et al.*, 1967). Upon thermal diagenesis of hydrocarbon source rocks, usually only lighter hydrocarbons are able to migrate, leaving most of the U with the heavy, residual organic matter in the source rocks. Moreover, during conventional oil recovery most U that has been transported from the source rock to the reservoir will be contained in the bituminous residue that is not produced (Jonkers *et al.*, 1997).

In many geological settings, solid bitumens can be found containing very high levels of U. In most cases these bitumens are remnants of petroleum, derived by thermal alteration or bacterial degradation (Bloch and Key, 1981; Lomando, 1992). Scavenging of U from circulating ground waters over a long period of time led to U concentrations in these bitumens of up to 1 wt% (Curiale *et al.*, 1983). In a number of natural gas fields, the encounter of NORM in production fluids is (partly) attributed to the presence of such U-enriched solid bitumens in the reservoir sediments (Pierce *et al.*, 1964; Zhuravel, 1999; Schmidt *et al.*, 2000 / **Chapter 2**).

Thorium is generally considered to be a very insoluble and immobile element in ground water (Langmuir and Herman, 1980). Typical Th concentrations in hydrocarbon reservoir sediments range from 1 to 12 ppm in sandstones, shales and limestones (Fisher, 1995). Although Th, like U, may also be complexed by humic and fulvic acids, Th concentrations in organic-rich sediments such as peat or coal are not higher than in sediments with low organic matter contents. Even in the most organic-rich sediments, Th is mainly present in the inorganic fraction, in clay minerals or heavy minerals such as monazite (Kizil'shteyn and Levchenko, 1996). For these reasons, Th activity concentrations in crude oil and (produced) hydrocarbon reservoir brines are very low (**Table 1.2**). This holds not only for ^{232}Th, but also for ^{238}U daughter nuclides ^{234}Th and ^{230}Th. The only exception may be ^{228}Th from the ^{232}Th decay series. Elevated activity concentrations of ^{228}Th in brines may result from high concentrations of its parent ^{228}Ra, although in practice much of the very insoluble ^{228}Th is readily hydrolysed and adsorbed on grain surfaces (Zukin *et al.*, 1987; Andrews *et al.*, 1989).

In contrast to U and Th, Ra is very soluble in reduced hydrocarbon reservoir brines. High Ra concentrations in these brines (**Table 1.2**) can be partially explained by the formation of chloride complexes, which may account for about 60% of total dissolved Ra (Zukin *et al.*, 1987).

Correlation between salinity and Ra concentration in a number of hydrocarbon reservoir settings (Kraemer and Reid, 1984; Fisher, 1995) may point to better leaching of Ra by more saline waters (Kraemer and Reid, 1984) or to increased displacement of Ra on clay minerals by other cations (Tanner, 1964). Aided by the far better solubility of Ra compared with U and Th, Ra in (produced) hydrocarbon reservoir brines is generally highly unsupported. For oil field brines, $^{226}Ra/^{238}U$ activity ratios of up to 100,000 have been measured (Laul, 1992). In the same brines, $^{228}Ra/^{232}Th$ activity ratios tend to be less extreme (Laul *et al.*, 1985). This may be due to less effective leaching of ^{228}Ra compared to ^{226}Ra from recoil tracks in sediment grains, because ^{228}Ra is generated in the first alpha recoil step down the ^{232}Th decay chain.

As for the origin of Ra in hydrocarbon reservoir brines, there is general agreement that Ra is generated from U and Th in reservoir sediments close to the oil and gas well perforations (Kraemer and Reid, 1984; Smith, 1987; Fisher, 1995). Geologically short half lives of all Ra isotopes, slow flow velocities of basinal brines and too low U and Th concentrations in brines leave no other conclusion. According to Bloch and Key (1981), ^{226}Ra concentrations of up to 60 $Bq \cdot l^{-1}$ could be explained by mobilisation from reservoir sediments with slightly above average U contents. In many cases, however, ^{226}Ra concentrations are much higher and can only be explained by local U enrichments in the reservoir sediments. Organic-rich sediments with high U contents have been proposed as sources of ^{226}Ra in various hydrocarbon provinces such as Texas, the North Sea, and Ukraine (Pierce *et al.*, 1956; Smith, 1987; Zhuravel, 1999). In a similar way, high ^{228}Ra and ^{224}Ra concentrations must originate from local ^{232}Th enrichments in reservoir sediments.

As has been mentioned earlier, gaseous radon is very soluble in hydrocarbons and in reservoir brines. For this reason, in crude oil Rn can be present in unsupported state (Monicard and Dumas, 1952; Levorsen, 1958). Although Rn concentrations have not been reported for hydrocarbon production waters, Rn analyses are available for reduced brines that are comparable to hydrocarbon reservoir brines. These analyses show that ^{222}Rn is either in radioactive equilibrium with its parent ^{226}Ra, or has excess activity concentrations of up to about 5 (Laul *et al.*, 1985; Leslie *et al.*, 1991; Laul, 1992). In these cases, excess ^{222}Rn activity concentrations are attributed to sorption of ^{226}Ra from brine to rock (Leslie *et al.*, 1991; Laul, 1992). In general, ^{222}Rn in brines is either derived from decay of dissolved ^{226}Ra (Smith, 1987) or directly recoiled from ^{226}Ra in reservoir sediments. Due to the short half life of ^{222}Rn, only 3.8 d, for gas wells producing negligible amounts of liquid hydrocarbons it has been calculated that ^{222}Rn in produced gas must have been generated within a sphere of several tens of meters around the well perforations (Van der Heijde *et al.*, 1977; Jonkers *et al.*, 1997). In practice, not all ^{222}Rn may originate from reservoir sediments and/or brines. Some of it may also be generated from ^{226}Ra-bearing scales in or around perforations in the well tubings, which will be discussed later. In reservoir brines, short-lived ^{220}Rn from the ^{232}Th series, with a half life of only 55 s, will probably be in equilibrium with or slightly in excess of its parent ^{224}Ra. However, since natural gas surfacing times are usually on the order of several minutes, ^{220}Rn in natural gas will rarely reach the surface installations (Van der Heijde *et al.*, 1977). All ^{220}Rn progeny is very short-lived and, in reservoir brines, expected to be in secular equilibrium with ^{220}Rn, unless affected by sorption on sediments.

In the ^{238}U decay series, however, ^{210}Pb and, to a lesser extent, its daughter ^{210}Po may be significant constituents of hydrocarbon brines. Due to complexation by chloride and/or organic acids, Pb is very soluble in oil and gas brines (Giordano and Kharaka, 1994). Also, intermediate NORs between ^{222}Rn and ^{210}Pb are all very short-lived. Therefore, ^{210}Pb activity concentrations in these brines will not be significantly affected by sorption on sediment grains, and generally be equal to combined ^{222}Rn activity concentrations in hydrocarbon reservoir fluids. However, there are indications that increased flow velocities in reservoir sediments due to production of natural gas lead to enhanced mobilization of ^{222}Rn. During transport to the well perforations, decay of ^{222}Rn to ^{210}Pb leads to disequilibrium between ^{222}Rn and ^{210}Pb in reservoir brines, enabling production of brines carrying unsupported ^{210}Pb (Schmidt *et al.*, 2000 / **Chapter 2**).

The possibly significant ^{210}Pb daughter nuclide ^{210}Po has not been reported in (produced) reservoir brines. There are indications that ^{210}Po has an appreciable solubility in water (Taylor and Cleghorn, 1996), but its geochemical behaviour under oil and gas reservoir conditions is barely known, making its occurrence in reservoir brines rather difficult to predict.

Encounter of NORs during production and processing of oil and gas

The above explanation of behaviour of NORs in hydrocarbon reservoirs qualitatively explains the presence of unsupported ^{228}Ra, ^{224}Ra, ^{226}Ra, ^{222}Rn and ^{210}Pb in produced reservoir brines and of ^{222}Rn in produced natural gas. It should be stressed again that secular equilibrium between NORs in reservoir brines will only exist if static conditions in a reservoir system have not been disturbed within a time interval of about five half lives of the longest-lived nuclides involved. Production of hydrocarbons and brines from reservoirs obviously causes disruption of the system, because of increased fluid flow along preferential flow paths such as fractures and very permeable sediment layers. Increased fluid flow likely increases leaching of soluble NORs from sediments. Also, temperature and pressure changes during production, as well as contemporaneous production of fluids from several reservoir regions with their own local NORs distributions may cause large fluctuations in NORs concentrations over time (Leslie *et al.*, 1991). For these reasons it is very hard to quantitatively explain or predict NORs concentrations in produced hydrocarbons and brines. In general, however, production water volumes and salinity steadily increase with production time, as shown for example for North Sea gas fields (Jacobs and Marquenie, 1991). Because of increased leaching and solubility, concentrations of Ra and Pb nuclides are also expected to increase over time. Indeed, NORs concentrations tend to increase as wells age and amounts of produced water increase (Rood *et al.*, 1998). However, this effect is not generally visible, possibly due to deposition of NORs in installations (Jacobs and Marquenie, 1991). Of course, ^{222}Rn concentrations in natural gas are not affected by deposition of scales in tubing and surface installations. Since release of Rn from reservoir sediments into brines is constant and not influenced by any production parameter, ^{222}Rn concentrations in natural gas are expected to increase with decreasing pressure upon depletion of a gas reservoir. Attempts have been made to calculate ^{222}Rn concentrations in natural gas, but these were not very satisfactory (Van der Heijde *et al.*, 1977; Kolb and Wojcik, 1987).

Besides giving rise to general trends in NORs concentrations, production and processing of hydrocarbons and reservoir brines also leads to a typical distribution of NORs over production streams and wastes (**Tables 1.2 and 1.3**). In short, reservoir fluids enter the wellbore downhole through the perforations, and are transported via the tubing to the well head at the surface. Often, flows from several wells are mixed in the production manifold. Oil well fluids are then led to two or more separators to remove natural gas, after which water is separated from the oil in a dehydrator. Gas well fluids are first led to a gas separator and subsequently to a second separator where hydrocarbon condensate, i.e. liquid hydrocarbons or natural gas liquids, are separated from water.

As reservoir fluids are being transported to the surface, decreasing pressure and temperature often lead to separation of a liquid brine phase and a hydrocarbon gas phase. This may result in separation of ^{210}Pb from its parent ^{222}Rn, causing highly unsupported ^{210}Pb concentrations in gas production brines. However, to our knowledge no ^{210}Pb mass balance calculations have ever been reported for hydrocarbon production streams to check these considerations.

Produced ^{222}Rn from both oil and gas wells will be concentrated in separated natural gas, after which remaining ^{222}Rn will be concentrated in natural gas liquids because of the far better solubility in hydrocarbons than in water (Van der Heijde *et al.*, 1977). If individual constituents are separated from natural gas, ^{222}Rn will be preferentially concentrated in ethane and propane streams because the boiling point of Rn (-62°C) is between that of ethane (-88°C) and propane (-42°C) (Gesell, 1975; Van der Heijde *et al.*, 1977) and because of similarity in molecular size. In ethane and propane fractionators ^{222}Rn concentration factors on gas volume base of up to 20 have been measured (Gesell, 1975), and after liquefaction of up to 1000 (Jonkers *et al.*, 1997). Presence of ^{222}Rn in any of these hydrocarbon streams is not necessarily problematic because of the short half life of ^{222}Rn. However, when residence times of ^{222}Rn-bearing hydrocarbons in production or storage facilities are long enough, significant amounts of ^{210}Pb and subsequently ^{210}Po can be deposited on the inner surface of for instance fractionators or storage tanks (Gesell, 1975). Such deposits are often invisible to the naked eye, being present as films, coatings or plating (Gray, 1990) that can be detected by radiation surveys only. Deposits of this type are often reported as surface dust (**Table 1.3**) (Bland and Chiu, 1996; Hartog *et al.*, 1996; Taylor and Cleghorn, 1996). Besides in this surface dust, significant levels of ^{210}Pb and ^{210}Po may also be built up in natural gas liquids themselves (**Table 1.2**). Often, ^{210}Pb and ^{210}Po activity concentrations cannot be explained from concentrations of their parent nuclides ^{222}Rn and/or ^{210}Pb in the liquids, but the reason for this phenomenon is still not understood (Jonkers *et al.*, 1997). Evidently, somewhere along the gas treating process physical separation of parent and daughter nuclides must happen.

Accumulation of NORs in scales, sludges and reservoir materials

Changes of pressure and temperature upon production of hydrocarbons often lead to supersaturation of salts and metals in coproduced water. As a result mineral scales may be deposited throughout oil and gas production facilities. Most common scale minerals in both oil

and gas facilities are the less well soluble sulphates and carbonates of the Group IIA metals Ca, Sr and Ba. In practice, a whole range of other not very soluble compounds can be found, including SiO_2, Pb-Hg amalgams and Mg-carbonate, often in combination with the aforementioned sulphates and carbonates (e.g. Kaemmel *et al.*, 1978; Kolb and Wojcik, 1985; Smith, 1987; Basignani *et al.*, 1991). If sulphide is coproduced with hydrocarbons and brines, also sulphides of particularly Fe and Pb may be deposited (e.g. Kolb and Wojcik, 1985; Zhuravel, 1999). Metallic Pb has been found in several oil and gas production facilities, but this is a different type of scale since it is probably formed in a redox reaction with steel installation parts (Carpenter *et al.*, 1974; Kaemmel *et al.*, 1978; Hartog *et al.*, 1995; Schmidt, 1998; Schmidt *et al.*, submitted). With the exception of Hg compounds, which seem to be restricted to gas production facilities, all scale minerals can be found in both oil and gas facilities provided the right chemical and physical conditions are met. Injection of incompatible water into reservoirs to maintain production pressure during exploitation is the principal cause for deposition of sulphate scales in oil production facilities (Testa *et al.*, 1994).

Presence of NORs from the ^{226}Ra and ^{228}Ra sub-series in produced brines may lead to incorporation of NORs in scale minerals. Because Ra is also a Group IIA element, it will be readily incorporated in Ca, Sr and Ba sulphates and carbonates (Smith, 1987). Although the solubility of pure $RaSO_4$ is also very low, this compound will never be formed in nature because even in brines with the highest Ra activity concentrations, molar Ra concentrations are much too low (Langmuir and Melchior, 1985).

Sulphates and carbonates are the main minerals in so-called hard scales, and as such contain ^{226}Ra and ^{228}Ra as principal NORs (**Table 1.3**). If such scales do not contain additional minerals, and particularly Pb-bearing minerals, Ra daughter nuclides in the scales have most likely been generated in-situ. Taking into account the ^{222}Rn emanation factor, which for sulphate scales is on the order of 2 to 6% (Rood *et al.*, 1998), age and time of deposition of the scale may be calculated from its $^{226}Ra/^{210}Pb$ activity ratio (Jonkers *et al.*, 1997). Likewise, age and deposition time of ^{228}Ra-bearing scales may be calculated from their $^{228}Ra/^{228}Th$ ratio (Just *et al.*, 1981). Deposition of ^{226}Ra-bearing scales is widely observed in down-hole tubing and particularly in and around the tubing perforations of both oil and gas wells (Lehnert and Just, 1979). Depending on their ^{222}Rn emanation factor, these scales may significantly contribute to total ^{222}Rn in produced hydrocarbons and brines.

Soft to medium hard scales differ from hard scales in their overall composition and mineralogy, and may contain more than 50 wt% Pb (Jonkers *et al.*, 1997). Main NOR in these scales is ^{210}Pb, because of coprecipitation with stable Pb isotopes in for instance metallic Pb and Pb sulphide (Kolb and Wojcik, 1985; Hartog *et al.*, 1995; Schmidt, 1998 / **Chapter 5**; Schmidt *et al.*, submitted / **Chapter 6**). However, they often contain some ^{226}Ra and/or ^{228}Ra, likely in additional minerals such as barite (**Table 1.3**). Presence of ^{210}Po in soft to medium hard scales has not been reported, but is evident because of rapid ingrowth. There are at least three origins of ^{210}Pb in these scales: *in situ* decay of coprecipitated ^{226}Ra, decay of ^{222}Rn in natural gas, and direct transport of unsupported ^{210}Pb in coproduced water (Hartog *et al.*, 1995). Generally, decay of ^{222}Rn in natural gas will not be important because of very short residence times of natural gas in production facilities. If also too little ^{226}Ra is present in the scale, ^{210}Pb is

unsupported. As was mentioned above, unsupported ^{210}Pb in produced brines may result from transport distances too long for ^{222}Rn to be maintained in solution (Schmidt *et al.*, 2000), or from separation of a liquid and a gas phase during transport to the surface. However, part of it may be derived from decay of ^{222}Rn in water films on the inside of production facilities. The residence time of dissolved ^{222}Rn is likely higher than the residence time of ^{222}Rn in the gas phase.

Since scrapings primarily consist of pieces of mineral scales removed from the inner surface of facilities by cleaning or inspection tools, distribution of NORs in scrapings is identical to distribution in scales (**Table 1.3**). The same holds true for produced reservoir materials, since presence of NORs in these waste products is primarily due to the deposition of coatings of NORM scales on produced sediment grains. Distribution of NORs in sludges is more complex, since sludges are generally a mixture of liquid hydrocarbons, water, reservoir material and scale minerals, formed by settling in for instance separators and storage tanks (Gray, 1990). NORs found in sludges depend on the product streams from which the sludges settle. Sludges in gasoline plants and natural gas pipelines will primarily contain ^{222}Rn decay products, whereas sludge accumulating in crude oil terminals will contain ^{226}Ra, ^{228}Ra and their decay products (Gray, 1990; Roberts *et al.*, 1998).

Conclusions

Coproduction of NORs with oil and gas has been known for almost a century, and deposition of NORM in production facilities for half a century. Yet health, safety, environmental and financial risks of NORM were only fully realised in the 1980's. Geochemical research on oil and gas NORM has accumulated since the beginning of the 20th Century, and at present many questions can be answered.

Uranium and thorium are very insoluble under reduced hydrocarbon reservoir conditions, and therefore will not be produced from the reservoir in hydrocarbons or in coproduced reservoir brines. Daughter nuclides of ^{238}U and ^{232}Th, however, can be preferentially mobilized from sediments into reservoir brines. Two mobilisation mechanisms operate at the same time. Direct alpha recoil, by which daughter nuclides upon their generation are recoiled into fluid-filled pores between sediments grains, tends to be seen as somewhat more important than leaching. Leaching may occur where NORs are in lattice sites that are damaged by previous recoil processes or where NORs do not fit into lattice sites because of crystal-chemical differences with their parent nuclides.

Because of high solubilities of radium, radon and lead in brines, mobilisation is very effective for NORs from the ^{226}Ra and ^{228}Ra sub-series. As such, especially ^{228}Ra, ^{226}Ra and ^{210}Pb can be found in coproduced reservoir brines and in various production wastes such as scales, sludges and reservoir materials. Preferential coprecipitation of ^{226}Ra and ^{228}Ra in sulphates and carbonates, and of ^{210}Pb in Pb-bearing scale minerals, will lead to ingrowth of shorter-lived daughter nuclides upon aging of the scales. Gaseous ^{222}Rn is preferentially transported in natural gas and tends to concentrate in natural gas liquids. Boiling point and molecular size similarities of Rn with ethane and propane may lead to concentration factors of up to 1,000 after

liquefaction of separated hydrocarbons. Upon treatment and storage of the natural gas liquids ^{222}Rn daughter nuclides ^{210}Pb and ^{210}Po may be deposited on the inner surface of production facilities.

In many cases, ^{210}Pb in scales and sludges is unsupported. Presence of unsupported ^{210}Pb in coproduced brines may result from separation of gas and liquid phases during transport of fluids to the surface, or from transport distances too long for ^{222}Rn to be maintained in solution.

Background concentrations of U and Th in reservoir sediments may lead to slightly enhanced concentrations of daughter NORs in reservoir brines. Higher concentrations of NORs from the ^{226}Ra and ^{228}Ra sub-series are due to local enrichments of U and/or Th close to the oil and gas well perforations. Observed ^{222}Rn concentrations in natural gas can only be explained by generation of ^{222}Rn within a sphere of several tens of meters from the well perforations. Organic-rich shales and hydrocarbon residues, enriched in U, are often identified as sources of NORs coproduced with oil and natural gas.

References

Alekseev, F.A., V.I., E. and Filonov, V.A., 1958. Radioactive elements in oil field waters. Geochem. 3, 806-814.

Andrews, J.N. *et al.*, 1982. Radioelements, radiogenic helium and age relationships for ground waters from the granites at Stripa, Sweden. Geochim. Cosmochim. Acta 46, 533-1543.

Andrews, J.N., Ford, D.J., Hussain, N., Trivedi, D. and Youngman, M.J., 1989. Natural radioelement solution by circulating groundwaters in the Stripa granite. Geochim. Cosmochim. Acta 53, 1791-1802.

API, 1992. Bulletin on management of naturally occurring radioactive materials (NORM) in oil & gas production. Bulletin E2, Am. Petrol. Inst., Washington.

Armands, G. and Landergren, S., 1960. Geochemical prospecting for uranium in northern Sweden - enrichment of uranium in peat, International Geology Congress 21st session, Copenhagen, pp. 51-66.

Armbrust, B.F. and Kuroda, P.K., 1956. On the isotopic constitution of radium (Ra-224/Ra-226 and Ra-228/Ra-226) in petroleum brines. EOS, Trans. Am. Geophys. Union 37, 216-220.

Asikainen, M., 1981. State of disequilibrium between ^{238}U, ^{234}U, ^{226}Ra and ^{222}Rn in groundwater from bedrock. Geochim. Cosmochim. Acta 45, 201-206.

Asuen, G.O. and Imasuen, O.I., 1990. Occurrence and relationship of Mo, Nb, Th, U, Y and Zr in a typical oil shale (coaly shale) from Westfield Opencast Site, Scotland. Chem. Erde 50, 105-112.

Åberg, G., Löfvendahl, R., Nord, A.G. and Holm, E., 1985. Radionuclide mobility in thucholitic hydrocarbons in fractured quartzite. Can. J. Earth Sci. 22, 959-967.

Bassignani, A., Di Luise, G., Fenzi, A. and Finazzi, P.B., 1991. Radioactive scales in oil and gas production centers, Proc. first International Conference on Health, Safety and Environment, The Hague, 1991. Society of Petroleum Engineers, The Hague, pp. 527-537.

Bell, K.G., Goodman, C. and Whitehead, W.L., 1940. Radioactivity of sedimentary rocks and associated petroleum. AAPG Bull. 24, 1529-1547.

Bland, C.J. and Chiu, N.W., 1996. Accumulation of ^{210}Pb activity on particulate matter in LPG rail cars. Appl. Rad. Isot. 47, 925-926.

Bloch, S. and Key, R.M., 1981. Modes of formation of anomalously high radioactivity in oil-field brines. AAPG Bull. 65, 154-159.

Bobin, P.L., 1933. Thorium X content of water from well no. 1 in Ukhta oil field. Trav. Inst. Etat. radium,

USSR (in Russian) 2, 157-159.

Born, H.-J., 1936. Geochemische Zusammenhänge zwischen Helium-, Blei- und Radiumvorkommen in deutschen Salzlagerstätten. Kali Salze Erdöl 30, 41-45.

Botset, H.G., 1934. The radium content of some connate waters. Physics 5, 276-280.

Breger, I.A., Deul, M. and Rubinstein, S., 1955. Geochemistry and mineralogy of a uraniferous lignite. Econ. Geol. 50, 206-226.

Burton, E.F., 1904. Über ein aus Rohpetroleum gewonnenes radioaktives gas. Phys. Z. 5, 511-516.

Campbell, J.L., 1951. Radioactivity well logging anomalies. Petrol. Eng., B7-B12.

Carpenter, A.B., Trout, M.L. and Pickett, E.E., 1974. Preliminary report on the origin and chemical evolution of lead- and zinc-rich oilfield brines in entral Mississippi. Econ. Geol. 69, 1191-1206.

Clever, H.L., 1979. Krypton, xenon and radon - Gas solubilities. Solubility data series vol. 2. Pergamon Press, Oxford.

Cortial, F., Gauthier-Lafaye, F., Lacrampe-Couloume, G., Oberlin, A. and Weber, F., 1990. Characterization of organic matter associated with uranium deposits in the Francevillian Formation of Gabon (Lower Proterozoic). Org. Geochem. 15, 73-85.

Curiale, J.A., Bloch, S., Rafalska-Bloch, J. and Harrison, W.E., 1983. Petroleum-related origin for uraniferous organic-rich nodules of Southwestern Oklahoma. AAPG Bull. 67, 588-608.

Czakó, E., 1913. Über Heliumgehalt und Radioaktivität von Erdgasen. Z. Anorg. Chem. 82, 249-277.

Erickson, R.L., Myers, A.T. and Horr, C.A., 1954. Association of uranium and other metals with crude oil, asphalt, and petroliferous rock. AAPG Bull. 38, 2200-2218.

Faul, H., Gott, G.B., Manger, G.E., Mytton, J.W. and Sakakura, A.Y., 1952. Radon and helium in natural gas, 19th International Geological Congress, 9th session, Algiers, 339-348.

Fisher, R.S., 1995. Geologic, geochemical and geographic controls on NORM in produced water from Texas oil, gas and geothermal reservoirs, SPE/EPA exploration & production environmental conference. Society of Petroleum Engineers, SPE 29709, Houston, Texas, USA, 195-205.

Fleischer, R.L., 1982. Alpha-recoil damage and solution effects in minerals: uranium isotopic disequilibrium and radon release. Geochim. Cosmochim. Acta 46, 2191-2201.

Gallup, D.L. and Featherstone, J.L., 1995. Control of NORM deposition from Salton Sea geothermal brines. Geotherm. Sci. Tech. 4, 215-226.

Gascoyne, M., 1992. Geochemistry of the actinides and their daughters. In: M. Ivanovich and R.S. Harmon (Eds.), Uranium-series disequilibrium: Applications to earth, marine and environmental sciences. Clarendon Press, Oxford.

Gesell, T.F., 1975. Occupational radiation exposure due to ^{222}Rn in natural gas and natural gas products. Health Phys. 29, 681-687.

Giordano, T.H. and Kharaka, Y.K., 1994. Organic ligand distribution and speciation in sedimentary basin brines, diagenetic fluids and related ore solutions. In: J. Parnell (Ed.), Geofluids: Origin, migration and evolution of fluids in sedimentary basins. Special Publications of the Geological Society of London vol.78, 175-202.

Gott, G.B. and Hill, J.W., 1953. Radioactivity in some oil fields of southeastern Kansas. U.S.G.S. Bull. 988-E, 69-122.

Gray, P., 1990. Radioactive materials could pose problems for the gas industry. Oil & Gas J. 88 (26), 45-48.

Gray, P.R., 1993. NORM contamination in the petroleum industry. J. Petrol. Tech. 45, 12-16.

Grice, K.J., 1991. Naturally occurring radioactive materials (NORM) in the oil and gas industry.A new management challenge, First International Conference on Health, Safety and Environment In Oil and Gas Exploration and Production. Society of Petroleum Engineers of AIME, Richardson, TX, USA, the Hague, the Netherlands, 559-571.

Gutsalo, L.K., 1964. On the distribution of radium in the ground waters of the central part of the Dnieper-Donets basin. Geochem. Int. 9, 1177.

Hartog, F.A., Knaepen, W.A.I. and Jonkers, G., 1995. Radioactive lead: an underestimated issue?, API / GRI NORM conference, Houston, USA, 59-69.

Hartog, F.A., Jonkers, G. and Knaepen, W.A.I., 1996. The encounter and analysis of Naturally Occurring Radionuclides (NORs) in gas and oil production and processing, 7th International Symposium on Oil Field Chemicals, Geilo, Norway, 17-20.

Heaton, B. and Lambley, J., 1995. TENORM in the oil, gas and mineral industry. Appl. Rad. Isot. 46, 577-581.

Himstedt, F., 1904. Über die radioaktive Emanation der Wasser- und Ölquellen. Phys. Z. 5, 210-213.

Idiz, E.F., Carlisle, D. and Kaplan, I.R., 1986. Interaction between organic matter and trace metals in a uranium rich bog, Kern County, California, U.S.A. Appl. Geochem. 1, 573-590.

Jacobs, R.P.W.M. and Marquenie, J.M., 1991. Produced water from gas/condensate platforms: environmental considerations. First international conference on health, safety and environment. Society of Petroleum Engineers, The Hague, The Netherlands, 89-96.

Jonkers, G., Hartog, F.A., Knaepen, W.A.I. and Lancee, P.F.J., 1997. Characterisation of NORM in the oil and gas production (E&P) industry, International symposium on radiological problems with natural radioactivity in the non-nuclear industry, Amsterdam, the Netherlands.

Just, G., Lehnert, K. and Nebel, J., 1981. Abschätzung des Alters rezenter Radiumanreicherungen. Z. Geol. Wiss. 9, 1431-1436.

Kaemmel, T., Müller, E.P., Krossner, L., Nebel, J., Gommern, U.H. and Ungethüm, H., 1978. Sind $HgPb_2$ und (Hg,Pb), gebildet aus natürlichen Begleitkomponenten der Erdgase der Lagerstätten der Altmark, Minerale? Z. Angew. Geol. 24, 90-96.

Kathren, R.L., 1998. NORM sources and their origins. Appl. Rad. Isot. 49, 149-168.

Kigoshi, K., 1971. Alpha-recoil thorium-234: dissolution into water and the uranium-234/uranium-238 disequilibrium in nature. Science 173, 47-48.

Kizil'shteyn, L.Y. and Levchenko, S.V., 1996. The ecological aspect of the geochemistry of thorium in coals. Geochem. Int. 33, 74-82.

Kolb, W.A. and Wojcik, M., 1985. Enhanced radioactivity due to natural oil and gas production and related radiological problems. Sci. Tot. Env. 45, 77-84.

Kolb, W.A. and Wojcik, M., 1987. Dependence of radon concentration in natural gas on the geological and physical parameters of the gas reservoir. Math. Geol. 19, 309-317.

Komarev, V.L., Koshlyak, V.A. and Usmanov, M.G., 1967. Association of zones of high radioactivity with the water-oil interface in petroliferous sandstones. Doklady Akad. Nauk SSSR 172, 198-200.

Komlev, L.V., 1933. Origin of radium in oil-field waters. Trav. Inst. Etat. Radium, USSR (in Russian) 2, 207-221 (in English 222-223).

Komlev, L.V., Myatelkin, P. and Savchenko, V., 1933. Radioactivity of waters from the oil fields of Dagestan, Kuban and Azerbaidzhan. Trav. Inst. Etat. Radium, USSR (in Russian) 2, 176-206 (in English 206-207).

Kraemer, T.F. and Reid, D.F., 1984. The occurrence and behavior of radium in saline formation water of the U.S. Gulf coast region. Isot. Geosci. 2, 153-174.

Kraemer, T.F. and Kharaka, Y.K., 1986. Uranium geochemistry in geopressured-geothermal aquifers of the U.S. Gulf Coast. Geochim. Cosmochim. Acta 50, 1233-1238.

Krishnan, C., Kopperson, D. and Cuthill, T., 1994. Discovery of radioactive barium sulphate scale in PanCanadian Petroleum producing operations in southeastern Alberta. J. Can. Petr. Tech. 33, 49-54.

Krishnaswami, S. and Seidemann, D.E., 1988. Comparative study of ^{222}Rn, ^{40}Ar, ^{39}Ar and ^{37}Ar leakage from rocks and minerals: Implications for the role of nanopores in gas transport through natural

silicates. Geochim. Cosmochim. Acta 52, 655-658.
Kronfeld, J., Gradsztan, E., Muller, H.W., Radin, J., Yaniv, A. and Zach, R., 1975. Excess ^{234}U: an aging effect in confined water. Earth Planet. Sci. Lett. 27, 189-196.
Kronfeld, J., Minster, T. and Ne'eman, E., 1993. ^{238}U-series disequilibrium in the Upper Cretaceous oil shales of Israel as the primary source for the Dead Sea's ^{226}Ra anomaly. Terra Nova 5, 563-567.
Langmuir, D. and Herman, J.S., 1980. The mobility of thorium in natural waters at low temperatures. Geochim. Cosmochim. Acta 44, 1753-1766.
Langmuir, D. and Melchior, D., 1985. The geochemistry of Ca, Sr, Ba and Ra sulfates in some deep brines from the Palo Duro basin, Texas. Geochim. Cosmochim. Acta 49, 2423-2432.
Laul, J.C., Smith, R.M. and Hubbard, N., 1985. Behavior of natural uranium, thorium and radium isotopes in the Wolfcamp brine aquifers, Palo Duro Basin, Texas. Mat. Res. Soc. Symp. Proc. 44, 475-482.
Laul, J.C., 1992. Natural radionuclides in groundwaters. J. Radioanal. Nucl. Chem. 156, 235-242.
Lehnert, K. and Just, G., 1979. Sekundäre Gammastrahlungsanomalien in Erdgasfordersonden. Z. Geol. Wiss. 7, 503-511.
Leslie, B.W., Hammond, D.E. and Ku, T., 1991. Temporal changes in decay-series isotope concentrations in response to flow conditions in the SSDP well, Salton Sea, California. In: T.A. Abrajano and L.H. Johnson (Editors), Materials research society symposium proceedings. Scientific basis for nuclear waste management XIV. Materials Research Society, Pittsburgh, Pennsylvania, 719-726.
Levorsen, A.I., 1958. Geology of petroleum. W.H. Freeman and Co., San Francisco.
Lomando, A.J., 1992. The influence of solid reservoir bitumen on reservoir quality. AAPG Bull. 76, 1137-1152.
Lysebo, I. and Strand, T., 1997. NORM in oil production in Norway, International symposium on radiological problems with natural radioactivity in the non-nuclear industry, Amsterdam, the Netherlands.
McKelvey, V.E., Everhart, D.L. and Garrels, R.M., 1955. Origin of uranium deposits. Econ. Geol. 50th Ann. Vol., 464-533.
McLennan, J.C., 1904. On the radio-activity of natural gas. Nature 70, 151.
Miller, H.T., Bruce, E.D. and Cook, L.M., 1991. Management of occupational and environmental exposure to naturally occurring radioactive materials (NORM), 1991 SPE Annual Technical Conference and Exhibition., Pt. 2, Production Operations and Engineering. Soc of Petroleum Engineers of AIME, Richardson, TX, USA, 627-636.
Monicard, R. and Dumas, H., 1952. Radioactivité des roches sédimentaires, du petrole brut et des eaux de gisements. Revue I.F.P. 7, 96-102.
Nikitin, B.A. and Merkulova, M.S., 1933. Radium in field-waters and petroleum of Bibi-Eibat oil-field. Trav. Inst. Etat. Radium, USSR (in Russian) 2, 160-175 (in German 175-176).
Osmond, J.K. and Cowart, J.B., 1982. Groundwater. In: M. Ivanovich and R.S. Harmon (Eds.), Uranium series disequilibrium: applications to environmental problems. Clarendon Press, Oxford.
Pierce, A.P., Mytton, J.W. and Gott, G.B., 1956. Radioactive elements and their daughter products in the Texas Panhandle and other oil and gas fields in the United States. U.S.G.S. Prof. Paper 300, 527-532.
Pierce, A.P., Gott, G.B. and Mytton, J.W., 1964. Uranium and helium in the Panhandle gas field Texas, and adjacent areas. Geological Survey Prof. Pap. 454-G.
Rama, S.P. and Moore, W.S., 1984. Mechanism of transport of U-Th series radioisotopes from solids into ground water. Geochim. Cosmochim. Acta 48, 395-399.
Randolph, T.M. *et al.*, 1992. Radium fate and oil removal for discharged produced sand. In: J.P. Ray and F.R. Engelhart (Editors), 1992 International Produced Water Conference. Plenum Press, New York, San Diego, California, 267-279.
Roberts, C.J., Quinby, J.B., Duggan, W.P. and Yuan, Y., 1998. Disposal options and case-study pathway

analyses. Appl. Rad. Isot. 49, 241-258.

Rood, A.S., White, G.J. and Kendrick, D.T., 1998. Measurement of ^{222}Rn flux, ^{222}Rn emanation, and ^{226,228}Ra concentration from injection well pipe scale. Health Phys. 75, 187-192.

Rosholt, J.N., Shields, W.R. and Garner, E.L., 1963. Isotopic fractionation of uranium in sandstone. Science 139, 224-226.

Satterly, J. and McLennan, J.C., 1918. The radioactivity of the natural gases of Canada. Trans. Royal Soc. Can., Sec. III, 12, 153-160.

Schmidt, A.P., 1998. Lead precipitates from natural gas production facilities. J. Geochem. Expl. 62, 193-200 (**chapter 5** of this thesis).

Schmidt, A.P., Hartog, F.A., Van Os, B.J.H. and Schuiling, R.D., 2000. Production of ^{210}Pb from a Slochteren Sandstone gas reservoir. Appl. Geochem. 15, 1317-1329 (**chapter 2** of this thesis).

Schmidt, A.P., Hartog, F.A., Van Os, B.J.H. and Schuiling, R.D., submitted. Origin and deposition of stable lead and ^{210}Pb from Dutch natural gas systems (**chapter 6** of this thesis).

Smith, A.L., 1987. Radioactive-scale formation. J. Petr. Tech. 39, 697-706.

Stipp, S.L.S., Konnerup-Madsen, J., Franzreb, K., Kulik, A. and Mathieu, H.J., 1999. Spontaneous movement of ions through calcite at standard temperature and pressure. Nature 396, 356-359.

Sun, H. and Semkow, T.M., 1998. Mobilization of thorium, radium and radon radionuclides in ground water by successive alpha-recoils. J. Hydr. 205, 126-136.

Szalay, A., 1958. The significance of humus in the geochemical enrichment of uranium, 2nd Int. Conf. peaceful uses of atomic energy, Geneva, 182-186.

Tanner, A.B., 1964. Radon migration in the ground: a review. In: J.A.S. Adams and W.M. Lowder (eds.), The natural radiation environment. Chicago university press, Chicago, 161-190.

Taylor, G.L. and Cleghorn, M., 1996. Naturally occurring radioactive materials: Contamination and control in a world scale ethylene manufacturing complex, 8th Ethylene Producers Conference, 309-323.

Testa, C., Desideri, D., Meli, M.A., Roselli, C., Bassignani, A., Colombo, G. and Fresca Fantoni, R. , 1994. Radiation protection and radioactive scales in oil and gas production. Health Phys. 67, 34-38.

Tiratsoo, E.N., 1949. The radioactivity of sediments. Radioactivity and petroleum. Petroleum 12, 313-315.

Titayeva, N.A., Taskayev, A.I., Ovchenkov, V.Y., Aleksakhin, R.M. and Shuktomova, I.I., 1977. U, Th and Ra isotope composition in soils in prolonged contact with radioactive stratal waters. Geochem. Int. 14, 57-63.

Tscherepennikov, A.A., 1928. The occurrence of radioactivity in the Uchta area (in Russian). Vestnik Geologiceskogo Komiteta Leningrad 3, 18-28.

Tunn, W., 1975. Untersuchungen über Spurenelemente in Gasen aus deutschen Erdgas- und Erdöl-Feldern, Compendium Vorträge der Haupttagung der Deutsche Mineralölwissenschaft und Kohlechemie. Deutsche Gesellschaft fur Mineralölwissenschaft, 96-111.

Van der Heijde, H.B., Beens, H. and De Monchy, A.R., 1977. The occurrence of radioactive elements in natural gas. Ecotox. Environm. Safety 1, 49-87.

Zhuravel, N.E., 1999. Ukrainian oil field NORM contamination examined. Oil Gas J. 97, 103-105.

Zielinski, R.A., Otton, J.K., Wanty, R.B. and Pierson, C.T., 1987. The geochemistry of water near a surficial organic-rich uranium deposit, northeastern Washington State, U.S.A. Chem. Geol. 62, 263-289.

Zielinski, R.A. and Meier, A.L., 1988. The association of uranium with organic matter in Holocene peat: an experimental leaching study. Appl. Geochem. 3, 631-643.

Zukin, J.G., Hammond, D.E., Ku, T. and Elders, W.A., 1987. Uranium-thorium series radionuclides in brines and reservoir rocks from two deep geothermal boreholes in the Salton Sea Geothermal Field, southeastern California. Geochim. Cosmochim. Acta 51, 2719-2731.

Chapter 2

Production of ^{210}Pb from a Slochteren Sandstone gas reservoir

A. P. Schmidt, F.A. Hartog, B.J.H. van Os and R.D. Schuiling

Abstract - Recently, precipitates of metallic lead and galena in gas production facilities have been reported to contain ^{210}Pb. In the North Sea area, uranium-bearing Kupferschiefer or Carboniferous coal measures have been suggested as possible source of ^{210}Pb. Through coproduction of formation water with natural gas, ^{210}Pb may enter production facilities together with non-radioactive lead, and precipitate as metallic lead or galena. In this study, bituminous sandstones with up to 2.8 wt% organic carbon from a ^{210}Pb producing Permian, Slochteren Formation gas reservoir have been found to contain up to 330 ppm uranium. The sandstones show a complex diagenetic history, during which migrating U-enriched hydrocarbons were trapped in secondary pores. Continuing enlargement of pore space and the wetting characteristics of the reservoir fluids lead to a preferred distribution of hydrocarbon rims around quartz grains, creating fluid filled voids between the grains. Subsequently, finely grained uranium oxide precipitated along the bitumen - fluid boundaries. U-Pb chemical age dating of uranium oxide grains at around 246 Ma and the close association of abundant anhydrite with the bitumen impregnations point to a Zechstein source for U-enriched bitumen. The metal-rich Kupferschiefer is the most likely candidate. One of the bituminous sandstones shows a marked depletion of ^{210}Pb with respect to ^{238}U and ^{226}Ra, probably caused by the production of natural gas from the reservoir. Production started at the end of the nineteen sixties and induced fluid flow throughout the reservoir. This enabled transport of ^{222}Rn and its decay product ^{210}Pb away from the uranium oxide grains. The observed uranium concentrations and permeabilities make the bituminous sandstones in this reservoir probably a more important source of ^{210}Pb than the overlying Kupferschiefer or underlying Carboniferous coal measures.

Slightly modified from Applied Geochemistry 15 (2000), 1317-1329

Introduction

Recently, precipitates of metallic lead and galena in natural gas production facilities have been reported to contain ^{210}Pb from the ^{238}U natural decay series. In these Naturally Occurring Radioactive Material (NORM) scales ^{210}Pb is frequently unsupported, i.e. there is no *in situ* ingrowth from its nearest long-lived parent ^{226}Ra (Schmidt, 1998 / **Chapter 5**). Barite or calcite scales containing unsupported ^{226}Ra are a common phenomenon in the oil and gas industry (e.g. Bassignani *et al.*, 1991; Ford *et al.*, 1996), but lead scales containing ^{210}Pb have only recently drawn attention (Hartog *et al.*, 1995, 1996). Because of the half life of ^{210}Pb of 22.3 y (Ivanovich *et al.*, 1992) and the resulting short transport distances, the origin of this radionuclide must be looked for close to the well perforations, even under production conditions. According to Smith (1987), ^{238}U-enriched shales, such as the Zechstein Kupferschiefer, or Carboniferous coal measures are the most likely sources in the North Sea area. Often, however, U enrichments can also be found in reservoir bitumens, i.e. the solid residues of migrated hydrocarbons. Examples are uraniferous organic-rich nodules in rocks from the Texas Panhandle gas field (Pierce *et al.*, 1964), in Permian red beds from Oklahoma (Curiale *et al.*, 1983) and in Carboniferous rocks from North Wales (Parnell and Swainbank, 1990).

In the current study two sediment cores from a northeastern Netherlands' gas field were examined for the distribution of Naturally Occurring Radionuclides (NORs) in the Rotliegend reservoir sediments, as an attempt to explain the origin, mobilisation and transport of ^{210}Pb produced from this gas field.

Location and geological setting

The gas field is situated in the former transition zone between the Silverpit Claystone Formation and the Slochteren Sandstone Formation, both deposited in Late Rotliegend times. The Slochteren Sandstone locally forms a 150 m thick gas reservoir sequence, overlain by the Ten Boer Claystone (**Fig. 2.1**). This tongue of the Silverpit Claystone is in turn overlain by the Zechstein Kupferschiefer. Since the reservoir is formed by an eastward dipping horst block, the Slochteren Sandstone is juxtaposed to Zechstein salts and carbonates on the west .

The Late Rotliegend sediments of the northeastern Netherlands were deposited in a south to north direction on the southern flank of the Southern Permian Basin (Staüble and Milius, 1970). In the basin centre, clays and evaporites were deposited in a desert lake environment. At the basin margin, in the core area, alluvial fans and wadi systems carried detritus from the Variscan Mountains to the basin. The resulting sands and conglomerates were partly reworked by west to southwest directed winds (Van Wijhe *et al.*, 1980).

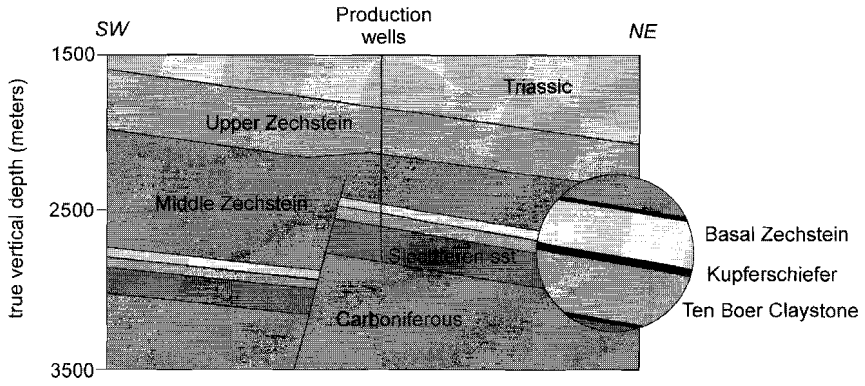

Figure 2.1 - Stratigraphic sketchmap of the gas field.

Sampling and methods

Sample description

Samples were taken from 4" sediment cores of two production wells. Both wells, horizontally separated by about 700 meters, produce natural gas from the same reservoir. Core C1, from a well drilled in 1996, comprises the Ten Boer Claystone and the Slochteren Sandstone (**Fig. 2.1**), from 2750 to 2900 m depth. The section consists of alternating conglomerates, coarse to fine sandstones, and shales, all indicative of a fluviatile deposition environment. The sequence shows light-coloured, reduced sediments of the Slochteren Sandstone in the bottom part of the core, while red, oxidized shales of the Ten Boer Claystone become more frequent in the uppermost 40 m. Discoloration of red sandstones is common in gas reservoirs, and caused by the reduction of iron oxide grain coatings. Between 2800 and 2830 m, several intervals of brownish grey sandstone contain dark, bituminous layers, ranging in thickness from one mm to over 30 cm. Between 2812 and 2814 m, the core shows an intense overprint of up to 2 cm large white anhydrite spots. These spots are less abundant from 2800 to 2812 m, and hardly occur between 2814 and 2830 m. Based on radiation readings three of the thickest bituminous layers were sampled for detailed investigation because of their relatively high natural radioactivity (**Table 2.1**, samples 2-4). Because the second layer lies at around 2813 m, this bituminous sandstone shows abundant anhydrite spots. For comparison, a non-bituminous grey sandstone sample was taken from the same core (sample 1).

Core C2, from a well drilled in 1990, comprises the same sediments as the first core, but in addition shows the locally 40 cm thick black Kupferschiefer on top of the Ten Boer Claystone, and a few meters of grey Carboniferous shales underneath the Slochteren Sandstone (**Fig. 2.1**). The total section ranges from 3235 to 3470 m depth. Bitumen impregnations occur between 3290 m and 3327 m, but do not show any white overprints. Radiation analysis revealed

enhanced levels of radioactivity in the Kupferschiefer, a Slochteren Sandstone conglomerate and the Carboniferous shales, which were all sampled (**Table 2.1**, samples 5, 9 and 10). In addition, samples were taken from three bituminous layers of the Slochteren Sandstone for comparison with the bituminous sandstones of core C1 (samples 6-8).

Table 2.1 - Sample description

Core	Sample no. and type		Depth (m)
C1	1	Grey sandstone	2790.34
	2	Bituminous sandstone	2810.62
	3	Bituminous sandstone	2813.33
	4	Bituminous sandstone	2826.85
C2	5	Kupferschiefer	3240.38
	6	Bituminous sandstone	3296.05
	7	Bituminous sandstone	3298.70
	8	Bituminous sandstone	3326.45
	9	Conglomerate	3460.30
	10	Carboniferous shale	3466.50

Microprobe and bulk chemical analysis

Polished thin sections of untreated samples were carbon-coated and examined using a Jeol JXA 8600 electron microprobe in back-scattered mode and wavelength dispersive spectral (WDS) analysis at an accelerating voltage of 15 kV and a current of 10 nA. In order to investigate the diagenetic history of the sample sediments, detailed textural observations were made of the bituminous sandstone samples from cores C1 and C2. Quantitative analyses on individual mineral grains from all samples were performed against in-house mineral standards. Counting times were 20 s per element, except for U minerals, for which counting times of 100 s per element were used. U minerals were analysed for U and Pb, in order to calculate U-Pb ages of the minerals. Detection limits of the elements were on the order of 0.2 wt% at counting times of 20 s, and on the order of 0.1 wt% at counting times of 100 s. U and Pb analyses of U minerals were accurate within 0.2 wt%.

Subsamples of just over 10 g of sediment were ground in a mechanical mortar. Major and trace element concentrations were determined by x-ray fluorescence (XRF) spectroscopy on a ARL8410 spectrometer, with an accuracy of better than 5% for major elements and better than 2% for trace elements. Precision was better than 1% for both major and trace elements. Samples were heated to 700° C in a Ströhlein CS-5500 combustion furnace, and total carbon contents were determined from CO_2 production with a CS-MAT 5500 analyzer within limits of ± 1.5% relative. Organic carbon contents were measured by heating samples to 500° C in a Ströhlein I-05 combustion assembly and analyzing the produced CO_2 with a C-MAT 5500 with an accuracy of ± 1.3% relative. $C_{carbonate}$ was calculated from the difference between C_{total} and $C_{organic}$.

Porosity and permeability measurements

Porosity and permeability measurements were carried out on an orientated plug from one of the bituminous sandstones from core C1, to see whether migration of fluids and released radionuclides from the sandstone is theoretically possible. The plug was cleaned by means of extraction of soluble hydrocarbons with a mixture of methanol and water (95/5%). Additional cleaning with toluene was done in order to remove any residual oil. Porosity and horizontal and vertical permeability were measured both before and after cleaning with toluene. For comparison, porosity and permeability were also determined for an oriented plug of the non-bituminous grey sandstone from the same core.

Gamma-ray spectroscopy

Naturally occurring radionuclides (NORs) were determined on ground and homogenised subsamples of 20 g of sediment using standard gamma-ray spectroscopy techniques (Knaepen *et al.*, 1995). Detection limits were 0.02 Bq/g for all radionuclides. Standard deviations (2σ) were ± 10% for ^{238}U, ^{226}Ra and ^{210}Pb.

Activities of ^{238}U were determined via the 63.3 keV emission (γ-yield: 3.81%) of its daughter isotope ^{234}Th and the 1001.0 keV emission (γ-yield: 0.79%) of a second daughter isotope, ^{234m}Pa. Activities of ^{210}Pb were determined via its emissions at 46.5 keV (γ-yield 4.00%). The efficiency calibration (22-1800 keV) of the hpGe detector was done using a mixed radionuclide reference solution (QCY.48 from Amersham Int. Ltd.) to which a certified amount of ^{210}Pb has been added. The accuracy of the counting unit was tested with two IAEA certified reference materials, U and Th ores, which are both in complete secular equilibrium. To correct for self-absorption of the samples, the two reference materials were irradiated with a point source containing all relevant radionuclides. Self-absorption corrections are checked regularly with a sample from the interlaboratory test programme described in Knaepen *et al.* (1995). Test sample activities found for ^{234}Th (63.3 keV) and ^{210}Pb (46.5 keV) usually do not differ more than 3-5% from their theoretical values. In practice, both 63.3 keV ^{234}Th and 46.5 keV ^{210}Pb emissions can be measured with a combined precision/accuracy of better than 10% (Knaepen *et al.*, 1995).

Results

Texture

The bituminous sandstones from cores C1 and C2 mainly consist of well-sorted (0.5 - 0.8 mm), well-rounded grains of detrital quartz and some feldspar, with some small laminae of moderately rounded, bimodally to badly sorted grains, indicative of a mixed aeolian and fluviatile deposition environment. Most grain contacts clearly show the effects of eogenetic and mesogenetic

compaction and pressure solution (Gaupp *et al.*, 1993), which destroyed much of the initial porosity of the sandstone (**Micrograph A**). Quartz and feldspar grains are coated with fine-grained clay mineral rims. Between compactional grain contacts these rims form thin, squeezed films, suggesting that clay mineral formation occurred before compaction took place. As these coatings are radial, the clay minerals probably grew from connate interstitial Rotliegend porewaters (Goodchild and Whitaker, 1986). Some detrital feldspar grains are dissolved, while others are completely preserved. Secondary pores of the bituminous sandstones from core C1 are mainly filled with bitumen and clay mineral booklets, but locally also with mineral cements (**Micrograph B**). Bituminous sandstone sample 4 contains a large number of cement 'nodules' (**Micrograph C**), causing the white overprint in the hand specimen. Secondary pores of the bituminous sandstones from core C2 clearly contain more mineral cements than bitumen and clay minerals, but no cement nodules. Whereas most secondary pores are no larger than 500 µm in diameter, the three bituminous sandstones from core C1 contain a number of very large secondary pores, up to several millimeters in diameter. Some of these pores are completely filled with solid bitumen (**Micrograph D**), but in others the bitumen forms approximately 100 µm thick rims around highly or even completely dissolved quartz grains. Along the voids between the bitumen rims massive arrays of up to 10 µm large crystals occur (**Micrograph E**). A third type of large secondary pores is filled with remnant flakes of detrital quartz and feldspar, floating in the bitumen (**Micrograph B**). This kind of pores might be small-scale deformation bands, often observed in porous sandstone reservoirs as a result of cataclastic deformation (Fossen and Hesthammer, 1998).

The grey sandstone from core C1 is not well sorted and mainly coarse-grained. It contains some large fragments of grey shale, but no bitumen or large secondary pores. The Kupferschiefer from core C2 is a finely laminated black shale, whereas the Carboniferous shale from the same core still contains large amounts of detrital quartz and feldspar grains in a matrix of clay minerals. The conglomerate from the second core, finally, shows no marked textural features.

Microanalysis and mineralogy

All quartz and feldspar grains of the bituminous sandstones from core C1 are coated with fine-grained clay mineral rims of chlorite (sample 2), mixed illite/chlorite (sample 3) or chlorite followed by illite (sample 4). Secondary pores are mainly filled with bitumen and kaolinite booklets, but locally also with Fe-Mg carbonate cement and barite. The massive arrays of fine crystals along the voids between bitumen rims appear to be uranium oxides, with an average composition resembling that of gummite, UO_3 (**Table 2.2**). In a few cases, these grains contain a small amount of titanium, while in one pore of sample 4 an array of TiO_2 crystals appears. Minor anhydrite can be found in all bituminous sandstones, but in sample 3 forms the large cement nodules of the white overprint (**Micrograph C**).

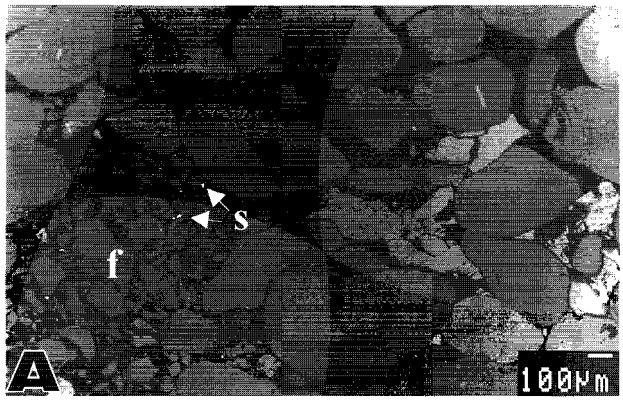

Micrograph A - Closely packed quartz grains caused by early diagenetic compaction and pressure solution (upper left). Remnant flakes (f) of quartz and feldspar grains, associated with small crystals of Cu-Sn sulphide (s) floating in a matrix of bitumen (bottom left).

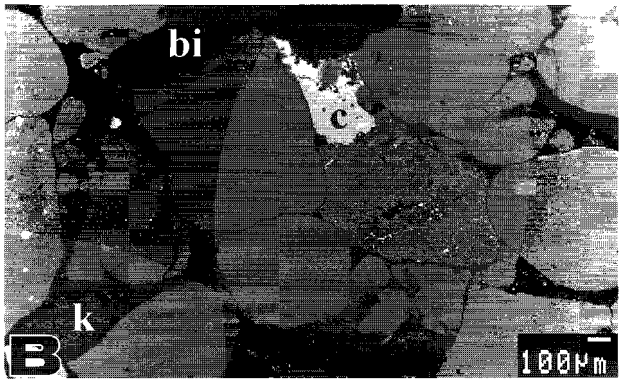

Micrograph B - Secondary pores filled with bitumen (bi), kaolinite booklets (k) and Fe-carbonate cement (c).

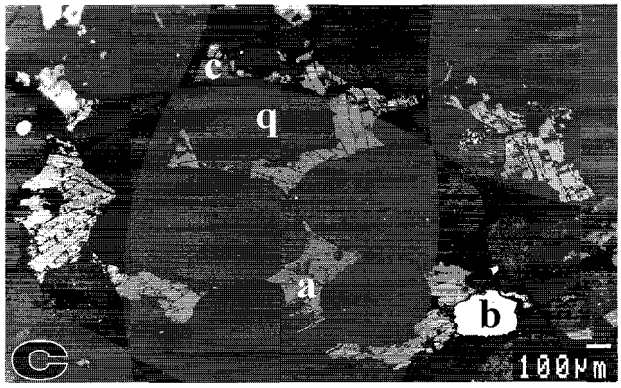

Micrograph C - Quartz grains (q) enclosed by a nodule of anhydrite cement (a). Barite (b) is closely associated with anhydrite, and some remnants of Fe-carbonate cements (c) can be found in the secondary pores.

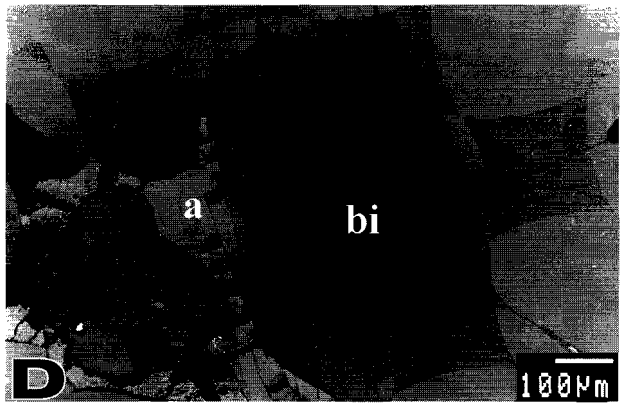

Micrograph D - Large secondary pore containing anhydrite (a) and bitumen (bi).

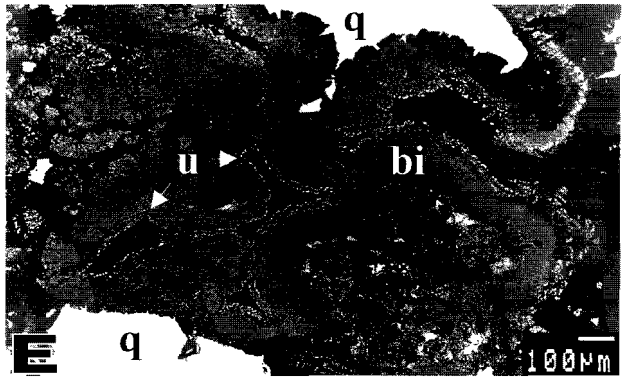

Micrograph E - Large secondary pore showing highly dissolved quartz grains (q) surrounded by rims of bitumen (bi). Large arrays of small uranium oxide grains (u) mark the boundaries between the bitumen rims and remaining pore space.

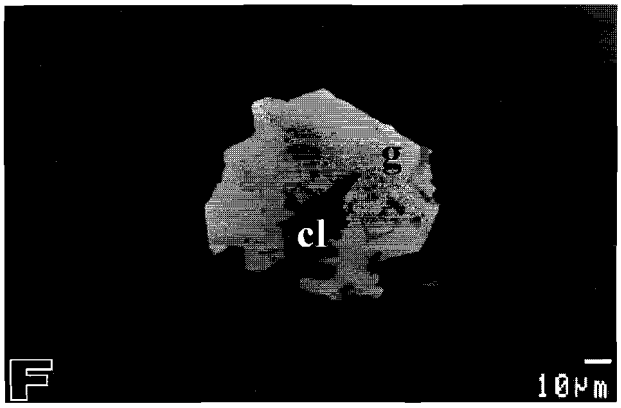

Micrograph F - Galena grain (g), partially dissolved, associated by a small crystal of clino-safflorite, $(Co,Ni)As_2$, (cl).

are almost completely dissolved (**Micrograph D**), but not in the large pores filled with floating grain flakes. Bitumen in the latter pores contains many small crystals of Cu-Sn sulphide, possibly kuramite, Cu_3SnS_4, or mohite, Cu_2SnS_3 (**Micrograph A**). In addition, barite can be found on both quartz and K-feldspar grains. Galena, PbS, is present on quartz grains in samples 2 and 4. All galena grains are partly dissolved and are associated with small grains of clinosafflorite (**Micrograph F**).

The bituminous sandstones from core C2 can be easily distinguished from those of core C1. The secondary pores of core C2 mainly contain (Fe-)dolomite cements and clay minerals. Only little anhydrite is present, and uranium oxides, as well as arsenides and sulphides are absent in these sandstones. The other samples from cores C1 and C2 do not show any bitumen, uranium oxides or sulphides. The Kupferschiefer is the only exception, containing finely dispersed pyrite and some sulphides of Pb and Cu.

U-Pb chemical ages

Microprobe analysis of U, Th and Pb contents of U minerals may be used to calculate an age of the minerals, on the assumption that all Pb in the grains is radiogenic, i.e. derived from the decay of U and Th, and no Pb is lost. In the present study, U-Pb ages were calculated based on U and Pb contents of uranium oxide grains from bituminous sandstones of core C1, following the method of Bowles (1990). The Th concentrations in the grains were all below the detection limit of 0.1 wt%. The accuracy of the Pb analyses of 0.2 wt% corresponds to errors of 20 Ma for chemical ages.

Table 2.2 - Composition and chemical age of uranium oxide grains

Sample	Grain size (µm)	Composition (wt%)									
		UO_3	TiO_2	PbO	ThO_2	As_2O_5	FeO	CaO	SiO_2	Total	Age (Ma)
3	4 x 2	89.95	0.35	2.78	b.d.	0.66	0.55	2.36	0.83	96.88	241
3	4 x 2	87.41	0.36	2.75	b.d.	0.75	0.52	2.12	1.06	94.97	244
3	6 x 2	90.44	0.47	2.86	b.d.	0.77	0.55	2.24	0.98	98.31	246
3	5 x 2	88.49	0.54	2.98	b.d.	0.60	0.63	2.33	0.91	96.48	260
3	5 x 3	89.67	0.99	2.72	b.d.	0.37	0.68	2.29	0.83	97.55	235
3	5 x 2	89.62	1.07	2.75	b.d.	0.36	0.70	2.23	0.98	97.71	238
3	5 x 3	89.03	0.94	2.91	b.d.	0.34	0.67	2.31	0.87	97.07	255
3	5 x 2	89.54	0.50	2.07	b.d.	0.77	0.57	2.04	1.11	96.60	180
3	5 x 3	89.36	0.51	2.31	b.d.	0.83	0.38	1.56	1.28	96.23	202
4	3 x 2	90.66	1.08	2.17	b.d.	0.24	0.76	2.11	1.63	98.65	186
4	4 x 2	85.11	4.45	2.22	b.d.	0.39	0.70	1.53	1.19	95.59	204

b.d. : below detection limit

Ages of uranium oxide grains all fall within a range of approximately 180 to 260 Ma (**Table 2.2**). Since all grains, except two, from sample 3 show about the same age, their mean of 246 ± 20 Ma is taken as the age of uranium oxide formation. Younger ages of uranium oxide grains from samples 3 and 4 are either caused by loss of radiogenic lead or of ^{238}U daughter nuclides, or reflect a later formation of the grains.

Bulk chemical analysis

The Kupferschiefer and the Carboniferous shale can clearly be distinguished from the other samples by their low SiO_2 and high TiO_2, Al_2O_3 and K_2O concentrations, indicative of the high clay mineral contents (**Table 2.3**). The high Fe_2O_3 (2.01 - 5.12 wt%) and MgO (0.29 - 1.36 wt%) contents of the bituminous sandstones of core C2 reflect the presence of large amounts of Fe-dolomite cements, whereas the minor presence of these cements in the bituminous sandstones of core C1 is confirmed by their low Fe_2O_3 (0.35 - 0.45 wt%) and MgO (0.10 - 0.19 wt%) contents.

Table 2.3 - Major elements (wt%)

Core	Sample no. and type	SiO_2	TiO_2	Al_2O_3	Fe_2O_3	MgO	MnO	CaO	K_2O	Na_2O	P_2O_5	LOI*	Total
C1	1 Grey sandstone	82.79	0.20	7.01	1.89	0.49	0.04	0.39	2.35	0.74	0.08	2.91	98.89
C1	2 Bituminous sst.	87.38	0.09	4.76	0.45	0.12	0.01	0.70	1.82	0.66	0.07	3.37	99.43
C1	3 Bituminous sst.	82.22	0.08	4.16	0.40	0.10	0.01	2.98	1.61	0.56	0.07	6.17	98.36
C1	4 Bituminous sst.	86.55	0.08	5.09	0.35	0.19	0.01	0.46	1.95	0.65	0.07	4.14	99.54
C2	5 Kupferschiefer	42.71	0.68	13.84	3.65	3.52	0.15	9.53	3.61	0.77	0.17	25.13	103.75
C2	6 Bituminous sst.	84.35	0.10	5.20	5.12	0.69	0.09	0.29	1.91	0.66	0.07	4.22	102.69
C2	7 Bituminous sst.	86.00	0.12	2.92	2.01	1.36	0.12	4.04	0.97	0.37	0.07	5.52	103.50
C2	8 Bituminous sst.	87.29	0.08	5.16	2.22	0.29	0.03	0.73	1.87	1.01	0.07	2.98	101.74
C2	9 Conglomerate	80.33	0.12	3.30	6.53	2.14	0.09	3.90	0.71	0.22	0.11	5.71	103.17
C2	10 Grey shale	59.38	1.05	23.58	3.79	0.67	0.01	0.00	4.35	0.55	0.05	5.37	98.78

* : loss on ignition

Trace element composition and carbon contents of the samples (**Table 2.4**) further show the difference between the bituminous sandstones from both cores. Arsenic (up to 296 ppm), Cu, V, U (up to 327 ppm) and organic carbon concentrations (0.77 - 2.77 wt%) are much higher in the first core, whereas Ni (average of 45 ppm) and Pb (average of 32 ppm) contents are clearly higher in bituminous sandstones 2 and 4, reflecting the presence of Co-Ni arsenides and Pb sulphides in these samples. Cobalt contents of the samples are difficult to interpret because of contamination by the W-carbide grinding equipment. The high concentrations of metals in the Kupferschiefer, such as Cu (1.44 wt%), Pb (714 ppm) and U (52 ppm) are not surprising, because this shale is well-known for its high metal concentrations throughout north-western Europe and Poland (e.g. Piestrzyński, 1990; Sun and Püttmann, 1996, 1997).

Table 2.4 - Trace elements (ppm) and carbon contents (wt%)

Core	Sample no. and type	As	Co	Cu	Ni	Pb	V	S	Ba	Th	U	C_{total}	$C_{organic}$	$C_{carbonate}$
C1	1 Grey sandstone	4	221	10	16	9	28	0	441	11	0	0.55	0.27	0.28
C1	2 Bituminous sandstone	296	323	26	46	34	45	1882	555	6	36	1.42	0.77	0.65
C1	3 Bituminous sandstone	29	237	75	12	11	31	12478	322	10	327	4.19	2.77	1.42
C1	4 Bituminous sandstone	240	268	42	43	30	84	485	1034	9	139	2.51	1.65	0.86
C2	5 Kupferschiefer	140	334	14390	218	714	2243	12806	311	3	52	12.08	9.87	2.21
C2	6 Bituminous sandstone	2	319	10	26	15	14	588	709	8	0	1.25	0.55	0.70
C2	7 Bituminous sandstone	4	195	8	12	12	18	4675	1000	8	5	1.45	0.27	1.18
C2	8 Bituminous sandstone	5	204	6	15	9	15	1745	1340	9	0	0.81	0.50	0.31
C2	9 Conglomerate	8	258	10	13	10	46	670	2081	7	2	1.39	0.17	1.22
C2	10 Grey shale	5	65	13	67	13	130	0	524	20	5	0.04	0.02	0.02

Porosity and permeability

The porosity and permeability were only tested for the grey sandstone (sample 1) and one of the bituminous sandstones (sample 4) of core C1 (**Table 2.5**). Surprisingly, the porosities of 16.6% and 16.7% after cleaning with the methanol/water mixture are the same for both samples, and normal for sandstones. The horizontal permeability of the bituminous sandstone, 94 mD after cleaning with toluene, is only half the horizontal permeability of the grey sandstone, probably because of the impregnation with bitumen. The vertical permeability of the bituminous sandstone, 48 mD, is about half the horizontal permeability. The additional cleaning with toluene had little effect on the porosity and permeability of the bituminous sandstone, because the bitumen appeared almost insoluble in toluene and only little residual oil was removed. The initial porosity of 16.7 vol% was increased to 17.4 vol%.

Table 2.5 - Porosity and permeability of two sandstone samples from core C1

Sample no. and type	Cleaning step	Porosity (vol%)	Horizontal permeability (mD)	Vertical permeability (mD)
1 Grey sandstone	methanol/water	16.6	181	n.d.
4 Bituminous sandstone	methanol/water	16.7	87	42
	toluene	17.4	94	48

n.d. : not determined

Naturally Occurring Radionuclides

In seven out of the ten investigated samples the activities of all radionuclides of the three natural decay series were below or just slightly above detection limits. The remaining three samples, all bituminous sandstones from core C1, only showed activities for radionuclides from the ^{238}U-series. In two of these reservoir materials, radioactive daughter nuclides ^{226}Ra and ^{210}Pb are in

secular equilibrium with ^{238}U (samples 2 and 4). In sample 3, ^{238}U and ^{226}Ra are in secular equilibrium, but ^{210}Pb shows a deficiency of 30 ± 14 % compared to ^{226}Ra (**Table 2.6**). There seems to be a discrepancy between the U concentration and the ^{238}U activity of the bituminous sandstones from core C1, as shown in **Tables 2.4 and 2.6**. However, both analyses were performed on different subsamples and different amounts of material, the heterogeneous nature of the samples giving rise to widely variable analytical results.

Table 2.6 - Naturally occurring radionuclides in the bituminous sandstones from core C1.

Sample	^{238}U (Bq/g)	^{238}U (ppm)	^{226}Ra (Bq/g)	^{210}Pb (Bq/g)
2	2.20 ± 0.22	177 ± 18	2.30 ± 0.23	2.40 ± 0.24
3	2.80 ± 0.28	226 ± 23	3.00 ± 0.30	2.10 ± 0.21
4	2.80 ± 0.28	226 ± 23	3.00 ± 0.30	2.90 ± 0.29

Discussion

Diagenesis

Diagenesis of Upper Rotliegend sandstones has been extensively studied in the north-east Netherlands (e.g. Van Wijhe *et al.*, 1980; Lee, 1985; Lee *et al.*, 1989) and north-west Germany (e.g. Gaupp *et al.*, 1993; Platt, 1994). In addition, some general overviews of Rotliegend sandstone diagenesis are available for north-west Germany (e.g. Burri *et al.*, 1993; Hock *et al.*, 1995). Early diagenetic clay mineral coatings are common in alluvial, fluvial and aeolian Rotliegend sandstones (e.g. Goodchild and Whitaker, 1986; Gaupp *et al.*, 1993). In addition, grain-rimming dolomite cements, infiltrating illitic clay and hematite frequently form early cements in the alluvial fan deposits of north-west Germany (Platt, 1994), while early carbonate cements are particularly common in wadi sandstones, or associated aeolian deposits (Nagtegaal, 1979; Gage, 1980). Upon burial, clay mineral growth, iron carbonate precipitation and feldspar dissolution dominate mesogenetic processes. Illite, and locally dickite (high-T kaolinite), are the most important clay mineral phases. Late phases of calcite and anhydrite cementation occur after clay mineral growth (Platt, 1994).

In this study, diagenesis of the investigated sediments was deduced from the textural and mineralogical observations of the bituminous sandstone samples from both cores. In general, diagenesis followed the sequence summarized above (**Fig. 2.2**). Before compaction, early diagenesis was characterized by overgrowth of radial Mg-Fe-smectite and/or illite on detrital quartz and feldspar grains. They probably grew as a result of an early phase of grain dissolution by alkaline, oxidizing Rotliegend groundwaters (Goodchild and Whitaker, 1986), the Mg-Fe-smectite being transformed into chlorite during later diagenesis (Hillier, 1994). There is no trace of early diagenetic cements such as dolomite, carbonate or hematite. These cements were most likely dissolved during the later generation of secondary porosity.

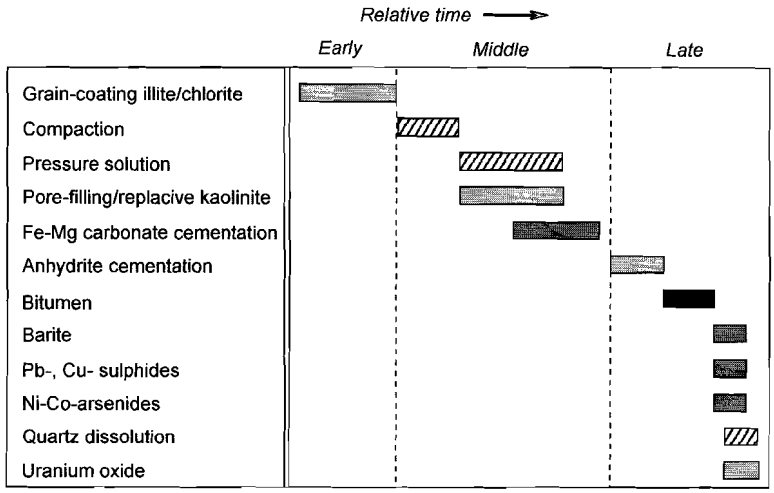

Figure 2.2 - Diagenetic history of the bituminous sandstones.

Upon burial, extensive pressure solution gave rise to many sutured grain contacts (**Micrograph A**), a phenomenon frequently observed in Rotliegend sandstones rich in illite grain coatings (Gaupp *et al.*, 1993). In a next stage, dissolution of lithic fragments created secondary porosity, which was partly filled-in with kaolinite formed in the same process. After this, Fe-Mg carbonates precipitated, especially in the bituminous sandstones from core C2, followed by anhydrite, $CaSO_4$ (**Micrograph C**) in the sandstones of core C1. Anhydrite cementation was most intense in the middle of the three bituminous sandstones of this core. Only minor anhydrite cementation occurred in the other two bituminous sandstone layers. Anhydrite probably precipitated as gypsum from hypersaline waters originating from juxtaposed Zechstein sediments. Although average $\delta^{34}S$ values of $+7.8 \pm 3.4‰$ for Rotliegend anhydrite samples from the Netherlands (Holser, 1979) suggest overall mixing of Rotliegend and Zechstein fluids, significant influx of Zechstein fluids into Rotliegend sediments especially occurred on or near horst blocks in northern Germany (Platt, 1994).

In a next stage the remaining pore space was filled with bitumen, sometimes taking up kaolinite that was already present (**Micrograph B**). Metals such as Ni, Co, Cu, Sn and As, which precipitated as arsenides and sulphides on grains or as inclusions within the bitumen of core C1, were transported in fluids accompanying the hydrocarbons. Reducing, acidic oil and gas field brines are often highly enriched in metals which they may have extracted from oxidized sediments during migration (e.g. Carpenter, 1979; Sverkjensky, 1984). Sulphide was probably derived from the dissolution of anhydrite and subsequent reduction of SO_4^{2-} to HS^-. Clearly, most anhydrite crystals show signs of dissolution upon contact with the hydrocarbons (**Micrograph C**). Therefore, the absence of sulphides in the bituminous sandstones of core C2 may be explained by the initial absence of anhydrite in these samples. Ba was also carried into the

sandstones of core C1 and precipitated as large crystals of barite upon contact with anhydrite (**Micrograph C**).

In the middle bituminous sandstone layer of core C1, reoxidation occurred soon after influx of the hydrocarbons, likely because of a surplus of SO_4^{2-}. This resulted in dissolution of sulphide and arsenide precipitates on detrital grains, which is reflected by the relatively low Co, Ni, Pb en As concentrations in sample 3, compared to the other two bituminous sandstones from the first core (**Table 2.4**). Because SO_4^{2-} was much less abundant in the other two layers, here sulphides and arsenides were only reoxidized to a minor extent, as shown by the presence of partly dissolved crystals of galena and clinosafflorite on quartz grains (**Micrograph F**). As a result, high Co, Ni, Pb en As concentrations were retained in samples 2 and 4. High Cu concentrations in all three bituminous sandstones of the first core suggest that Cu-Sn sulphides were not affected by re-oxidation, either because they were restricted to bitumen-filled pores and had not precipitated on detrital grains, or because of an insufficiently large redox gradient.

Origin and deposition of uranium and bitumen

As described above, uranium oxide minerals are restricted to the largest secondary pores in the bituminous sandstones from core C1. These pores are not entirely filled with bitumen, but some pore space was preserved by the formation of rims of bitumen around detrital grains. Quartz and feldspar grains enclosed by these rims show very sharp edges (**Micrograph E**), suggesting that the fluids associated with the hydrocarbons were capable of dissolving these grains. The presence of 'empty' bitumen rims also points to grain dissolution after entrapment of the hydrocarbons. This enlargement of pore space and the wetting characteristics of the fluids lead to a preferred distribution of bitumen rims around quartz grains, and created fluid-filled voids between these grains. Microprobe analysis revealed that all bitumen contains uranium and titanium, yet only in the largest secondary pores, where quartz dissolution occurred after hydrocarbon entrapment, uranium oxide, and to a lesser extent titanium oxide, precipitated along the bitumen rims (**Micrograph E**). These two processes seem to be coupled, and the fluid-filled voids between the bitumen rims were probably required to establish the redox and pH conditions to dissolve quartz grains and precipitate uranium oxide at the same time. After entrapment, thermal cracking transformed the liquid hydrocarbons slowly into bitumen. Uranium oxide may have played a role as well, as it has been suggested that radiations from decay of uranium and its daughter products cause polymerization and dehydrogenation of organic matter (e.g. Pierce *et al.*, 1964; Curiale *et al.*, 1983, Parnell, 1993b).

The almost linear correlation between U and C_{org} in the three bituminous sandstones from core C1 (**Fig. 2.3**) suggests that U was already present in the hydrocarbons when they became trapped in the sandstones. Given the depositional age of the sandstones and the local geological setting, there are three possible source rocks for the U-bearing hydrocarbons. First, hydrocarbons may have been generated in the underlying Carboniferous coal seams. Based upon tectonic reconstructions and vitrinite reflection data, Van Wijhe *et al.* (1980) estimated that the generation of Rotliegend gas in the Carboniferous coal strata started as early as 200 MA.

Any oil generation in the Carboniferous must have started long before. Second, the Zechstein Kupferschiefer, which was deposited around 256 MA (Harland *et al.*, 1990), may have provided the hydrocarbons, while the overlying Zechstein carbonates form the third possibility. The observed association of bitumen and abundant anhydrite in core C1 suggests that both fluids followed the same migration path and probably originated from the same source. Since anhydrite must have originated from juxtaposed Zechstein salts, a Zechstein source rock for the bitumen is most likely. Assuming that U enrichment of the organic matter in the source rock was syngenetic, the average U-Pb chemical age of 246 ± 20 Ma of the uranium oxide grains from sample 3 also suggests a Zechstein source rock. The metal-rich (**Table 2.4**) Kupferschiefer then is a likely candidate for providing hydrocarbons, uranium, barium and the other metals found in the bituminous sandstones. In a recent diagenetic study of a Rotliegend gas field in the southern North Sea, the authors also reported precipitation of anhydrite from Zechstein fluids (Gluyas *et al.*, 1997). Barite precipitation in the same field, however, was attributed to mixing of sulphate-rich Zechstein formation water and barium-rich Carboniferous formation water.

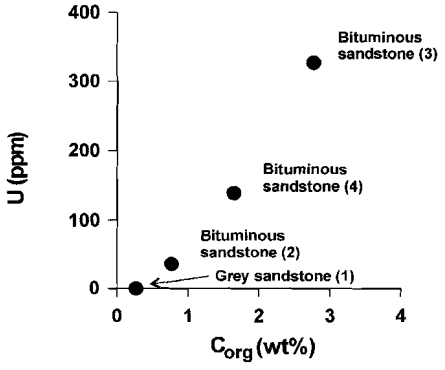

Figure 2.3 - U versus C_{org} contents of the samples from core C1.

^{238}U-series disequilibrium

Disequilibrium within the ^{238}U decay series is a common phenomenon in natural systems, due to the different chemical behaviour of the radionuclides involved. In the Dead Sea ^{226}Ra is considerably in excess of its parent ^{238}U, due to the high solubility of radium, especially in brines (Kronfeld *et al.*, 1993). Brines from the Salton Sea Geothermal Field, California, always contain ^{226}Ra far in excess of ^{238}U, but often ^{222}Rn is in excess of ^{226}Ra as well, due to the gaseous nature of radon (e.g., Zukin *et al.*, 1987; Leslie *et al.*, 1991).

In this study, bituminous sandstones nos. 2 and 4 show secular equilibrium between ^{238}U and ^{210}Pb (**Table 2.6**). In contrast, in sample 3 ^{210}Pb is depleted by 30 ± 14% relative to ^{226}Ra and ^{238}U. This suggests that ^{210}Pb has been removed from the host rock by percolating fluids. However, since all except two uranium oxide grains of sample 3 yield the same chemical age

of 246 Ma, secular equilibrium in the sandstone must have been disturbed very recently. This can be explained by the production of gas from the reservoir. In a steady state gas reservoir fluid flow is almost zero. ^{222}Rn emanating from uranium oxide grains enters the fluid filled voids, but decays before it can diffuse through the fluids. Its decay product ^{210}Pb will then be quickly re-adsorbed onto uranium oxide mineral grains (Rama and Moore, 1984) (**Fig. 2.4A**).

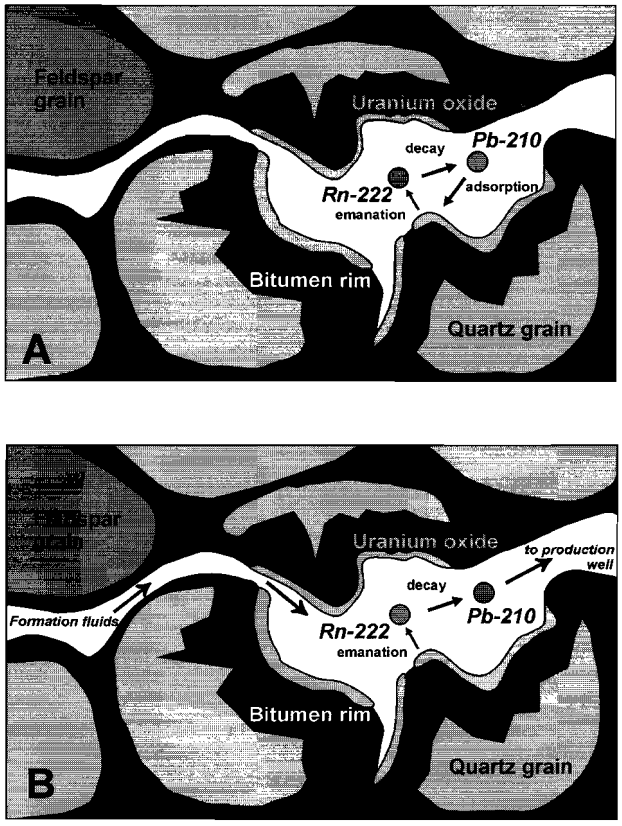

Figure 2.4 - Mobilisation of ^{210}Pb from U oxide in a bituminous reservoir sandstone. **A**: In a steady state reservoir ^{210}Pb from emanated ^{222}Rn is preferrentially readsorbed onto uranium oxide grains and retained in the system. **B**: Production of natural gas induces fluid flow, removing ^{210}Pb from the system and preventing adsorption onto uranium oxide grains.

However, production of natural gas from the investigated reservoir started in the end of the nineteen sixties, generating large-scale fluid flow throughout the reservoir, including the area of the studied production wells. Under these conditions ^{222}Rn emanating from uranium oxide grains may be transported by the percolating fluids, removing its decay product ^{210}Pb from the system (**Fig. 2.4B**). The observed porosity of 16.7% and horizontal permeability of 87 mD show that bituminous sandstone sample 3 is still a good gas reservoir rock, despite its heavy bitumen

impregnation. Percolation of reservoir fluids through the bituminous sandstones should therefore be no problem. Direct leaching of ^{210}Pb from the surface of uranium oxide grains is not a likely explanation, because it should also have a significant effect on the ^{226}Ra activity of the sample. We have no indication of leaching of ^{226}Ra, since the sample shows secular equilibrium between ^{226}Ra and ^{238}U well within the standard deviations of our analyses.

From the disequilibrium between ^{210}Pb and ^{226}Ra in sample 3 we can calculate the amount of time needed to produce such a disequilibrium, assuming that during this time interval all newly produced ^{210}Pb was removed from the system as ^{222}Rn. With a half life of 22.3 years for the decay of ^{210}Pb, a time interval of around 11.5 years is needed to explain the amount of disequilibrium observed. However, this is a minimum value, because not all produced ^{222}Rn will have been emanated from the uranium oxide grains. Typical ^{222}Rn emanation factors for uranium minerals such as pitchblende (UO_2) or carnotite, $K_2(UO_2)_2(VO_4)_2.1\text{-}3H_2O$, may reach 25% or higher at room temperature, depending on the crystalline nature and the internal surface area of the minerals (e.g., Giletti and Kulp, 1955; Krishnaswami and Seideman, 1988). When the temperature is raised from room temperature to 200° C, ^{222}Rn emanation largely increases due to the increasing diffusion coefficient of ^{222}Rn (Giletti and Kulp, 1955).

Conclusions

Bituminous sandstones from two production cores from a Permian, Slochteren Sandstone gas reservoir have been found to contain up to 2.8 wt% organic carbon and up to 330 ppm uranium. The sandstones show a complex diagenetic history, during which migrating hydrocarbons were trapped in secondary pores of the reservoir sandstone. Continuing enlargement of pore space and the wetting characteristics of the reservoir fluids led to a preferred distribution of hydrocarbon rims around quartz grains, which created fluid filled voids between the grains. Subsequently, precipitation of finely grained uranium oxide, UO_3, occurred along the bitumen - fluid boundaries. Chemical age dating of uranium oxide grains at around 246 Ma and the close association of anhydrite, sulphides and arsenides with the bitumen impregnations point to a Zechstein source for bitumen, uranium and metals precipitated in the sulphides and arsenides. The metal-rich Zechstein Kupferschiefer is the most probable source rock for U-enriched hydrocarbons, Ba and other metals such as Cu, Ni and Pb.

One of the bituminous sandstones shows a marked depletion of ^{210}Pb with respect to ^{238}U and ^{226}Ra, probably caused by the production of natural gas from the reservoir. Production started at the end of the nineteen sixties, inducing fluid flow throughout the reservoir, and enabling transport of ^{222}Rn and its decay product ^{210}Pb away from the uranium oxide grains. Since the bituminous sandstones were recovered from actual production wells, transport times in the reservoir and decay of ^{210}Pb during transport to the well are reduced to a minimum. Through production of formation water together with natural gas, ^{210}Pb may enter production facilities together with stable, non-radioactive lead and coprecipitate, forming scales of metallic lead or galena. The observed permeabilities and uranium concentrations make the bituminous sandstones in this reservoir an important source of ^{210}Pb, probably more important than the

overlying Kupferschiefer, renowned for its radioactive character, or the underlying Carboniferous coal measures.

Acknowledgement - The authors would like to thank Dr. Sieger van der Laan for many valuable discussions. The manuscript greatly benefitted from his critical and constructive remarks. This is publication #990902 of the Netherlands Research School of Sedimentary Geology.

References

Bassignani, A., Di Luise, G., Fenzi, A. and Finazzi, P.B., 1991. Radioactive scales in oil and gas production centers. In: Proc. 1st International Conference on Health, Safety and Environment, The Hague, 1991, v. 2. Society of Petroleum Engineers, The Hague, pp. 527-537.

Bowles, J.F.W., 1990. Age dating of individual grains of uraninite in rocks from electron microprobe analyses. Chem. Geol. 83, 47-53.

Burri, P., Faupel, J. and Koopmann, B., 1993. The Rotliegend in northwest Germany, from frontier to fairway. In: J. R. Parker (Ed.), Proc. 4th Conference on Petroleum Geology of Northwest Europe. The geological Society, pp. 741-748.

Carpenter, A.B., 1979. Interim report on lead and zinc in oilfield brines in the central Gulf Coast and in southern Michigan, Society of mining engineers of AIME.

Curiale, J.A., Bloch, S., Rafalska-Bloch, J. and Harrison, W.E., 1983. Petroleum-related origin for uraniferous organic-rich nodules of Southwestern Oklahoma. AAPG Bull. 67, 588-608.

Ford, W.G.F., Gadeken, L.L., Callahan, T.J. and Jackson, D., 1996. Solvent removes downhole NORM-contaminated $BaSO_4$ scale. Oil Gas J. 94, 65-68.

Fossen, H. and Hesthammer, J., 1998. Deformation bands and their significance in porous sandstone reservoirs. First Break 16, 21-25.

Gage, M., 1980. A review of the Viking Gas Field. In: Halbouty, M. T.(Ed.), Am. Assoc. Petrol. Geol. Mem., v. 4, pp. 39-48.

Gaupp, R., Matter, A., Platt, J., Ramseyer, K. and Walzebuck, J., 1993. Diagenesis and fluid evolution of deeply buried Permian (Rotliegende) gas reservoirs, Northwest Germany. AAPG Bull. 77, 1111-1128.

Giletti, B.J. and Kulp, J.L., 1955. Radon leakage from radioactive minerals. Amer. Mineral. 40, 481-496.

Gluyas, J., Jolley, L. and Primmer, T., 1997. Element mobility during diagenesis: Sulphate cementation of Rotliegend sandstones, Southern North Sea. Marine Petrol. Geol. 14, 1001-1011.

Goodchild, M.W. and Whitaker, J.H.M., 1986. A petrographic study of the Rotliegendes sandstone reservoir (Lower Permian) in the Rough Gas Field. Clay Miner. 21, 459-477.

Harland, W.B., Armstrong, R.L., Cox, A.V., Craig, L.E., Smith, A.G. and Smith, D.G., 1990. A geologic time scale 1989. Cambridge University Press, Cambridge.

Hartog F. A., Jonkers G., and Knaepen W. A. I. (1996) The encounter and analysis of Naturally Occurring Radionuclides (NORs) in gas and oil production and processing. Proc. 7th International Symposium on Oil Field Chemicals, Geilo, Norway, pp. 17-20.

Hartog F. A., Knaepen W. A. I., and Jonkers G. (1995) Radioactive lead: an underestimated issue? Proc. API / GRI NORM Conference, Houston, USA, pp. 59-69.

Hillier S. (1994) Pore-lining chlorites in siliciclastic reservoir sandstones: electron microprobe, SEM and XRD data, and implications for their origin. Clay Minerals 29, 665-679.

Hock, M., Kraft, T., Kloas, F. and Stowe, I., 1995. Lithology and sandstone diagenesis types from petrophysical well logs - a tool for improved reservoir characterization in the Rotliegend formation, Permian basin, Northwestern Germany. First Break 13, 441-450.

Holser W. T. (1979) Rotliegend evaporites, Lower Permian of Northwestern Europe. Erdöhl und Kohle 32, 159-162.

Ivanovich M., Latham A. G., and Ku T.-L. (1992) Uranium-series disequilibrium applications in geochronology. In: Ivanovich, M. and Harmon, R. S. (eds.), Uranium-series disequilibrium: Applications to earth, marine and environmental sciences. Clarendon Press, Oxford (Chapter X).

Knaepen, W.A.I., Bergwerf, W., Lancee, P.J.F., Van Dijk, W., Jansen, J.F.W., Janssen, R.G.C., Kiezenberg, W.H.T., Van Sluijs, R., Tijsmans, M.H., Volkers, K.J. and Voors, P.I., 1995. State-of-the-art of NORM nuclide dtermination in samples from oil and gas production: Validation of potential standardization methods through an interlaboratory test programme. J. Radioanal. Nucl. Chem. 198, 323-341.

Krishnaswami, S. and Seidemann, D.E., 1988. Comparative study of ^{222}Rn, ^{40}Ar, ^{39}Ar and ^{37}Ar leakage from rocks and minerals: Implications for the role of nanopores in gas transport through natural silicates. Geochim. Cosmochim. Acta 52, 655-658.

Kronfeld, J., Minster, T. and Ne'eman, E., 1993. ^{238}U-series disequilibrium in the Upper Cretaceous oil shales of Israel as the primary source for the Dead Sea's ^{226}Ra anomaly. Terra Nova 5, 563-567.

Lee, M., Aronson, J.L. and Savin, S.M., 1985. K/Ar dating of time of Gas Emplacement in Rotliegende Sandstone, Netherlands. AAPG Bull. 69, 1381-1385.

Lee, M., Aronson, J.L. and Savin, S.M., 1989. Timing and conditions of Permian Rotliegende sandstone diagenesis, Southern North Sea: K/Ar and oxygen isotopic data. AAPG Bull. 73, 195-215.

Leslie, B.W., Hammond, D.E. and Ku, T., 1991. Temporal changes in decay-series isotope concentrations in response to flow conditions in the SSDP well, Salton Sea, California. In: Abrajano, T.A. and Johnson, L.H. (Eds.), Materials research society symposium proceedings: Scientific basis for nuclear waste management XIV, Pittsburgh, Pennsylvania, pp. 719-726.

Nagtegaal, P.J.C., 1979. Relationship of facies and reservoir quality in Rotliegendes desert sandstones, southern North Sea region. J. Petrol. Geol. 2, 145-158.

Parnell, J. and Swainbank, I., 1990. Pb-Pb dating of hydrocarbon migration into a bitumen-bearing ore deposit, North Wales. Geology 18, 1028-1030.

Parnell, J., 1993. Chemical age dating of hydrocarbon migration using uraniferous bitumens, Czech-Polish border region. In: Parnell, J., Kucha, H. and Landais, P. (Eds.), Bitumens in ore deposits. Special Publications of the Society for Geology Applied to Mineral Deposits, v. 9. Springer-Verlag, Berlin, pp. 510-517.

Pierce, A.P., Gott, G.B. and Mytton, J.W., 1964. Uranium and helium in the Panhandle gas field Texas, and adjacent areas, Geological Survey Professional Paper 454-G.

Piestrzynski, A., 1990. Uranium and thorium in the Kupferschiefer formation, Lower Zechstein, Poland. Mineral. deposita 25, 146-151.

Platt, J.D., 1994. Geochemical evolution of pore waters in the Rotliegend (Early Permian) of northern Germany. Marine Petrol. Geol. 11, 66-78.

Rama, S.P. and Moore, W.S., 1984. Mechanism of transport of U-Th series radioisotopes from solids into ground water. Geochim. Cosmochim. Acta 48, 395-399.

Schmidt, A.P., 1998. Lead precipitates from natural gas production installations. J. Geochem. Expl. 62, 193-200 (**chapter 5** of this thesis).

Smith, A.L., 1987. Radioactive-scale formation. J. Petr. Techn. 39, 697-706.

Stäuble, A.J. and Milius, G., 1970. Geology of Groningen gas field. In: Halbouty, M.T. (Ed.), Geology of giant petroleum fields. AAPG Mem., v. 14, pp. 359-369.

Sun, Y. and Püttmann, W., 1996. Relationship between metal enrichment and organic composition in Kupferschiefer hosting structure-controlled mineralization from Oberkatz Schwelle, Germany. Appl. Geochem 11, 567-581.

Sun, Y. and Püttmann, W., 1997. Metal accumulation during and after deposition of the Kupferschiefer from the Sangerhausen Basin, Germany. Appl. Geochem. 12, 577-592.

Sverjensky, D.A., 1984. Oil field brines as ore-forming solutions. Econ. Geol. 79, 23-37.

Van Wijhe, D.H., Lutz, M. and Kaasschieter, J.P.H., 1980. The Rotliegend in the Netherlands and its gas accumulations. Geologie en Mijnbouw 59, 3-24.

Zukin, J.G., Hammond, D.E., Ku, T. and Elders, W.A., 1987. Uranium-thorium series radionuclides in brines and reservoir rocks from two deep geothermal boreholes in the Salton Sea Geothermal Field, southeastern California. Geochim. Cosmochim. Acta 51, 2719-2731.

Chapter 3

Distribution and isotopic composition of lead in Rotliegend and Kupferschiefer sediments: the origin of lead in Dutch Rotliegend gas reservoir brines

A.P. Schmidt, B.E. van Dalen, B.J.H. van Os en S.R. van der Laan

Abstract - Rotliegend sandstones, conglomerates and mudstones from three gas fields in the northern Netherlands and southern North Sea area and from outcrops in northern Germany show Pb concentrations comparable to average sandstones and shales. Sequential extraction of Pb shows that feldspars are the main Pb-bearing mineral fraction in all types of sediment, containing up to 92% of total Pb. Fe-oxide grain coatings may account for up to 20% of total Pb, while carbonate cements may contain 10-40% of Pb in sandstones. Elevated Pb concentrations in bituminous sandstones from one of the gas fields are due to the presence of Pb-sulphide associated with the bitumens. Stable Pb isotope signatures of the reservoir sediments and signatures corrected for ingrowth of Pb from decay of U and Th since sediment deposition provide a Pb evolution curve of the sediments. Isotopic signatures of Pb minerals deposited from the reservoir brines plot on this Pb evolution curve, supporting large scale mobilization of Pb from Rotliegend sediments into Rotliegend brines between the time of deposition and the present. Reported Pb concentrations in Dutch gas reservoir brines of up to 150 ppm can be explained by dissolution of feldspars and Fe-oxides from an average Rotliegend sediment. Mobilization of Pb from Rotliegend sediments was probably a single large scale event, controlled by diagenetic fluid fluxes.

Submitted

Introduction

Produced waters from Dutch Rotliegend gas fields sometimes show remarkably high concentrations of Pb. For instance, in the Akkrum Field in the province of Friesland, the Rotliegend brine had a Pb concentration of 108 $mg \cdot l^{-1}$ (Carpenter, 1989). Some wells even produce brines with up to 150 $mg \cdot l^{-1}$ Pb (F.A. Hartog, pers. comm.). Due to corrosion of steel parts, or changes in temperature and pressure during gas production, presence of Pb in produced waters may result in the deposition of metallic Pb or Pb sulphide in production facilities (Schmidt, 1998/ **Chapter 5**; Schmidt *et al.*, submitted / **Chapter 6**). The origin of Pb in Rotliegend formation waters has never fully been investigated, but it has been suggested that Pb was derived from the Rotliegend sediments themselves (Carpenter, 1989; Hallager *et al.*,1991). Stable Pb isotope signatures of a Rotliegend brine and of metallic Pb and galena scales deposited from Rotliegend brines in Dutch gas facilities showed Late Carboniferous to Early Cretaceous model ages, and the hypothesis was put forward that Pb in the brines was mainly derived from feldspars in the Rotliegend sediments (Schmidt *et al.*, subm. / **Chapter 6**).

This hypothesis can be tested by comparing isotopic signatures of the brine and scales with those of Rotliegend sediments. However, data on the distribution and isotopic composition of Pb in Rotliegend sediments are very rare. To our knowledge, Pb concentrations have only been reported for some Rotliegend sediments in northern Germany (Hartmann, 1963; Knoke, 1968;Tunn, 1975). Stable Pb isotope compositions have never been reported for Rotliegend sediments, and are only known for Dutch Kupferschiefer sediments from one core in the Groningen gas field (Wedepohl *et al.*, 1978).

In order to elucidate the origin of Pb in Rotliegend formation waters, this study presents detailed investigations on the distribution and isotopic composition of Pb in Dutch Rotliegend and Kupferschiefer sediments, taken from sediment cores from three gas fields in the southern North Sea and northeastern Netherlands area. For comparison, a number of Rotliegend and Kupferschiefer sediments from representative outcrops in northern Germany were sampled as well. Stable Pb isotope signatures of the Dutch gas reservoir sediments are compared with isotope signatures of Pb mineral scales deposited from brines from the same reservoirs (Schmidt *et al.*, subm. / **Chapter 6**). Combined with bulk Pb concentrations and the distribution of Pb over mineral fractions of the sediments, isotopic data are used to investigate whether Pb in Dutch Rotliegend brines has been derived from local Rotliegend sediments, and if so, which mineral fraction or fractions contributed to Pb in these gas reservoir brines.

Geological setting

The Rotliegend sediments of the northeastern Netherlands and southern North Sea area were deposited in a south to north direction on the southern flank of the Southern Permian Basin (Staüble and Milius, 1970). The Southern Permian Basin (**Fig. 3.1**) developed as a result of thermal subsidence following the Saalian tectonic phase, a long period of non-deposition and regional uplift (Van Wijhe *et al.*, 1980; Ziegler, 1990). Recent models suggest that Upper

Rotliegend sedimentation started when the basin had already subsided some 700 to 1000 m below global sea level (Van Wees *et al.*, 2000). In the basin centre, clays and evaporites were deposited in a desert lake environment. At the basin margin, alluvial fans and wadi systems carried detritus from the Variscan Mountains to the basin. The resulting alluvial sands and conglomerates were partly reworked by west to southwest directed winds (Van Wijhe *et al.*, 1980). Rotliegend deposition ended when the entire basin was flooded during the Zechstein marine transgression, caused by the formation of a rift zone between Greenland and Scandinavia (Ziegler, 1990).

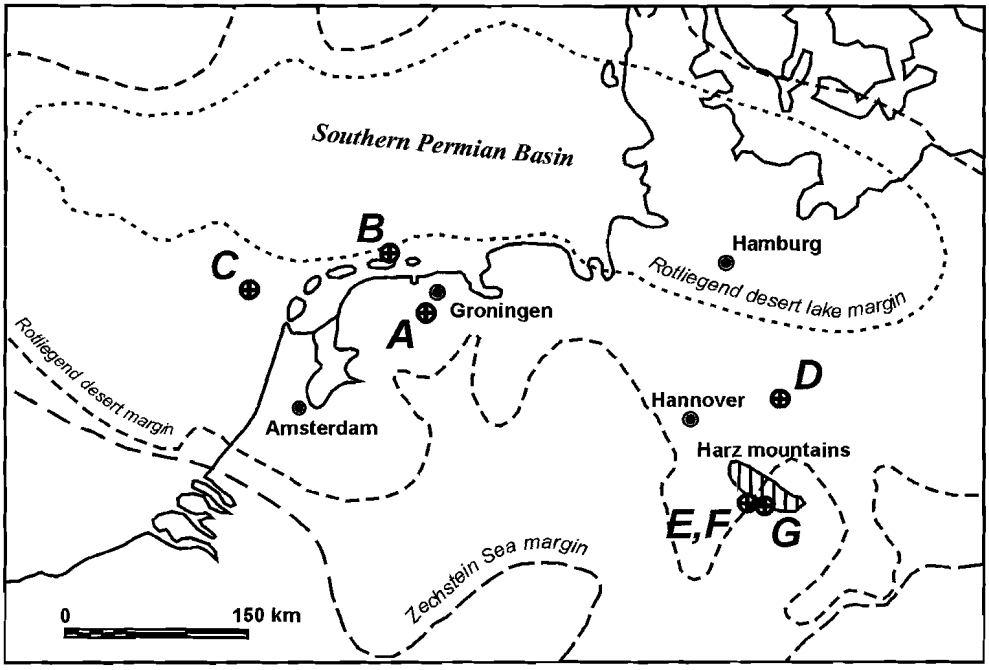

Figure 3.1 - Permian palaeogeographical map of the Netherlands and northern Germany (after Ziegler, 1990; McCann, 1998) showing the locations of the gas reservoirs A-C and outcrops D-G.

Gas fields A through C (**Fig. 3.1**) are situated in the Late Rotliegend transition zone between the Silverpit Formation of the basin centre and the Slochteren Formation of the basin margin (**Fig. 3.2**). The gas reservoir at location A consists of the locally 150 m thick non-divided Slochteren Member, which is overlain by the Ten Boer Member and the Z1 Kupferschiefer Member. Since the reservoir is formed by an eastward dipping horst block, the Slochteren Member is juxtaposed to Zechstein salts and carbonates on the west.

At location B, the gas reservoir consists of the 90-100 m thick Upper Slochteren Member. It is underlain by the Ameland Member, and overlain by the Ten Boer Member, both part of the Silverpit Formation. The reservoir is formed by a south dipping fault block, and flanked by two other Rotliegend gas reservoirs to the north and the south. The reservoir at location C is again formed by the Upper Slochteren Member, locally about 130 m thick. This reservoir is formed by a southwest tilted fault block, which causes juxtaposition of the Slochteren Member to Zechstein sediments on the northeast.

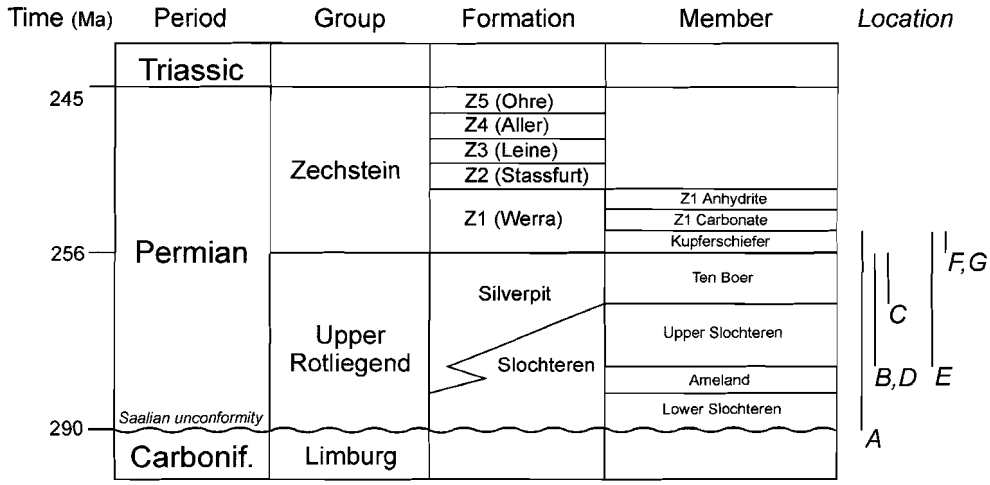

Figure 3.2 - Generalized Permian stratigraphy of the northern Netherlands and southern North Sea area (after Van Adrichem Boogaert and Kouwe, 1993) with sampled sediments at the different locations.

Location D is an outcrop near the village of Bebertal, representing the uppermost about 130 m section of the Rotliegend. The mainly fluviatile sandstones are part of the Hannover Formation, which is equivalent to the Upper Slochteren and Ten Boer Members in The Netherlands (Verdier, 1996). Location E is an outcrop in the village of Elrich, representing the Upper Rotliegend sequence boundary. Aeolian dunes of the uppermost part of the Hannover Formation are capped by about 50 cm of dark grey Kupferschiefer, but with a locally 1 m thick Zechstein conglomerate in between. Location F is a Kupferschiefer outcrop in the village of Walkenried, about 1 km from location E. At location G, finally, the Zechstein conglomerate and the sampled Kupferschiefer were deposited on Early Rotliegend volcanics of the Schneverdingen Formation. Deposition of these volcanics occurred during the tectonic events causing the Saalian unconformity in The Netherlands.

Samples and methods

Sample description

Twenty-two sediment samples were collected from four cores (A1, A2, B and C) of gas reservoirs A, B and C. In addition, eight sediment samples were collected at four north German outcrops D through G. Sediment samples comprise mudstones, fine to coarse sandstones, bituminous sandstones, conglomerates and black shales (Kupferschiefer). Mineralogy of these samples corresponds with the general composition of these types of sediment (e.g., Oszczepalski, 1986; McCann, 1998). Major minerals in the Rotliegend sediments are quartz and feldspars in the sandstones, and clay minerals (mainly illite), feldspars and quartz in the mudstones. Kupferschiefer sediments primarily consist of calcium carbonate and clay minerals. Major and accessory minerals of the different types of sediment are listed in **Table 3.1**. Detailed mineralogical descriptions of Kupferschiefer and most Rotliegend samples from cores A1 and A2 can be found elsewhere (Schmidt *et al.*, 2000 / **Chapter 2**).

Table 3.1 - Mineralogical composition of sediment types.

Sediment types	Major minerals	Accessory minerals
Fine to coarse sandstones	Quartz, feldspars	Illite, kaolinite, calcite, dolomite, barite, anhydrite, Fe-oxides
Bituminous sandstones	Quartz, feldspars	Illite, kaolinite, bitumen, U-oxides, barite, Fe-oxides, Cu-/Ni-/Pb-sulphides, calcite, anhydrite
Mudstones	Illite, feldspars, quartz	Kaolinite, Fe-oxides
Conglomerates	Quartz, feldspars, carbonates	Illite, kaolinite, Fe-oxides
Black shales (Kupferschiefer)	Illite, carbonates, organic matter	Pyrite, Cu-, Pb-, Zn-sulphides, phosphates

Analytical procedures

Upon sampling, sediments were stored in geochemical sample bags until further use. Quantities of about 100 g were dried at 60°C, ground in a mechanical mortar and divided into several subsamples. Subsamples of 10 g were pressed into tablets, and major and trace element concentrations were determined by X-ray fluorescence (XRF) spectroscopy on an ARL8410 spectrometer. Accuracy was better than 5% for major elements and better than 2% for trace elements. Loss on ignition of the sediments was measured by glowing at 970°C.

Subsamples of 0.25 g were totally dissolved by acid digestion ($HCl/HF/HNO_3/HClO_4$) in sealed Teflon containers in a microwave oven at 180°C. Concentrations of a number of relevant elements in both bulk samples and all leachates from the sequential extraction procedure were determined using a VG Plasmaquad PQ2+ ICP-MS. Precision (2σ) was better than 2%. Stable Pb isotopes of both bulk samples and leachates were measured with the same ICP-MS at a concentration of 30 to 50 ppb Pb. Ten runs were measured for each sample. For mass bias

correction NBS 981 standard was run after each batch of 6 samples. Relative standard deviations (2σ) for isotope ratios are separately reported for each sample. Further details on the ICP-MS analysis procedure can be found in Walraven *et al.* (1997).

Sequential leaching procedure

Based on the mineralogical composition of the samples (**Table 3.1**) and earlier investigations of Pb distribution in sediments, likely important Pb-bearing mineral phases in our samples are carbonates, sulphides, Fe-oxides, clay minerals, and feldspars (Hartree and Veizer, 1982; Zielinski *et al.*, 1983). In addition, Pb may be present in exchangeable sites on clays and in organic matter (Zielinski *et al.*, 1983; Bunzl *et al.*, 1995). Therefore, a method was set up for the sequential leaching of Pb in five steps: as an exchangeable cation (step 1), associated with carbonates (step 2), with organic matter and sulphides (step 3), and with Fe-oxides (step 4), and present in residual matter such as clay minerals and feldspars (step 5). The leaching procedure was largely developed from extraction procedures for trace elements from soils and sediments (Gatehouse *et al.*, 1977; Vidal and Rauret, 1995; Crespo *et al.*, 1996; Cave and Harmon, 1997). The following reagents and order of application were chosen for the extraction of Pb from subsamples of 1 g of sediment:

1. ***Exchangeable Pb***. The samples were leached with 10 ml 1 M $MgCl_2$ of pH 7 at room temperature for 1 h.

2. ***Pb associated with carbonates***. Residues from step 1 were leached for 5 h at room temperature with 5 ml 1 M ammonium acetate, adjusted to pH 4.5 with 96% acetic acid.

3. ***Pb adsorbed to organic matter and from sulphides***. About 4 ml 30% H_2O_2 was added to the residues from step 2 and allowed to react at 60°C until no more gas development could be seen. Subsequently 5 ml 30% H_2O_2 was added to the suspensions which were left overnight at 60°C. Before centrifugation, suspensions were heated to 80°C for 10 minutes to destruct remaining H_2O_2, and 5 ml 1 M ammonium acetate of pH 5 was added.

4. ***Pb adsorbed to or precipitated in amorphous and crystalline Fe-oxides***. The residues from step 3 were leached at 70°C for 24 h with 6 ml of Tamm's reagent (12.6 g oxalic acid and 24.9 g ammonium oxalate in 1 l of solution) at pH 3. The solid residues were dried in a stove at 80°C and weighed.

5. ***Pb in clays and feldpars***. About 0.25 g of the dried residues from step 4 were put in sealed teflon containers and totally dissolved by acid digestion ($HCl/HF/HNO_3/HClO_4$) in a microwave oven for 2 h.

Further details on the leaching procedure are reported in **Appendix 3.1**. It must be stressed here that although all of the reagents used in our leaching procedure have been successfully applied in other extraction schemes before, selective reagents are never fully specific for one mineral phase (Cave and Harmon, 1997). Strictly speaking, extracted phases are operationally defined. Therefore, selectivity must be thoroughly checked by using mineralogical and chemical data of the leached sediments. Also, the leaching process will not quantitatively extract true trace element concentrations from target phases because of readsorption of many trace

elements onto the rock matrix during leaching steps (Cave and Harmon, 1997). Again, careful evaluation of the extraction results is needed to overcome this general shortcoming of selective extraction methods.

Distribution of Pb

Total Pb contents of different sediment types

Concentrations of major elements and selected trace elements in bulk sediments from the four Dutch cores are given in **Table 3.2**, while bulk chemistry of sediments from the north German outcrops is given in **Table 3.3**. In general, Pb concentrations in sandstones, conglomerates and mudstones are comparable to values for average sandstone (7 ppm) and shale (20 ppm) reported by Wedepohl (1956) (**Fig. 3.3**). Two of the bituminous sandstones from core A1 have rather high Pb concentrations, of about 30 ppm. The mineralogy of these samples suggests that these high amounts of Pb are due to the presence of Pb-sulphide (**Table 3.1**). Pb concentrations in our samples are also comparable to German Rotliegend sandstones from literature, which generally contain between 1 and 15 ppm Pb (Hartmann, 1963; Knoke, 1968; Tunn, 1975).

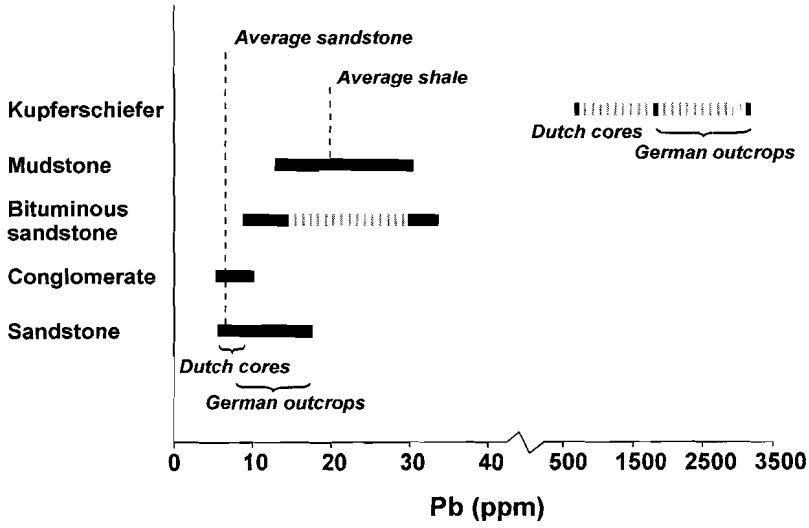

Figure 3.3 - Pb concentrations in five different sediment types from Dutch natural gas reservoir cores and German outcrops. Average sandstone and shale values from Wedepohl (1956).

Table 3.2 - Bulk chemistry of samples from Dutch Rotliegend gas reservoir sediments.

Core	Sample no. and type	Member	Depth (m)	SiO_2	TiO_2	Al_2O_3	Fe_2O_3	MgO	MnO	CaO	K_2O	Na_2O	P_2O_5	LOI*	Total	Cu	Pb	Th	U
A1	1 Red mudstone	TB	2759.91	54.1	0.8	20.5	5.8	0.8	0.0	0.0	5.1	0.9	0.1	6.3	94.5	13	19	1	1
	2 Red mudstone	TB	2767.33	50.9	0.9	17.6	4.6	2.7	0.2	5.8	4.6	2.5	0.1	12.2	102.0	26	18	11	3
	3 Red mudstone	TB	2789.92	54.9	0.9	21.2	4.4	0.9	0.0	0.8	5.3	0.9	0.1	5.7	95.2	22	20	3	2
	4 Coarse grey sandstone	TB	2790.34	82.8	0.2	7.0	1.9	0.5	0.0	0.4	2.4	0.7	0.1	2.9	98.9	7	9	2	1
	5 Fine grey sandstone	TB	2790.62	75.3	0.3	6.9	1.8	2.1	0.2	3.8	2.0	1.0	0.1	7.5	101.0	6	9	5	2
	6 Bituminous sandstone	US	2810.62	87.4	0.1	4.8	0.5	0.1	0.0	0.7	1.8	0.7	0.1	3.4	99.4	27	36	3	30
	7 Bituminous sandstone	US	2813.33	82.2	0.1	4.2	0.4	0.1	0.0	3.0	1.6	0.6	0.1	6.2	98.4	84	9	3	261
	8 Bituminous sandstone	US	2826.85	86.6	0.1	5.1	0.4	0.2	0.0	0.5	2.0	0.7	0.1	4.1	99.5	45	33	3	102
	9 Grey conglomerate	US	2897.71	69.1	0.1	2.2	2.0	4.6	0.2	9.2	0.6	0.1	0.1	12.7	100.9	6	7	2	1
A2	10 Black shale	K	3240.10	48.5	0.7	16.5	4.5	2.4	0.1	5.6	3.9	0.7	0.2	19.9	102.9	14317	728	10	23
	11 Black shale	K	3240.38	42.7	0.7	13.8	3.7	3.5	0.2	9.5	3.6	0.8	0.2	25.1	103.8	16422	770	9	51
	12 Bituminous sandstone	S	3296.05	84.4	0.1	5.2	5.1	0.7	0.1	0.3	1.9	0.7	0.1	4.2	102.7	6	11	3	1
	13 Bituminous sandstone	S	3298.70	86.0	0.1	2.9	2.0	1.4	0.1	4.0	1.0	0.4	0.1	5.5	103.5	6	10	2	1
	14 Bituminous sandstone	S	3326.45	87.3	0.1	5.2	2.2	0.3	0.0	0.7	1.9	1.0	0.1	3.0	101.7	5	8	2	1
	15 Conglomerate	S	3460.30	80.3	0.1	3.3	6.5	2.1	0.1	3.9	0.7	0.2	0.1	5.7	103.2	9	9	3	2
B	16 Red mudstone	TB	4131.22	55.4	0.9	19.1	5.5	1.2	0.0	0.8	4.9	3.0	0.2	5.2	96.2	79	30	3	2
	17 Fine white sandstone	US	4226.01	83.3	0.1	7.9	0.4	0.2	0.0	0.4	1.3	1.8	0.1	3.2	98.4	5	7	0	1
C	18 Red mudstone	TB	4055.65	59.7	0.7	14.7	4.9	1.8	0.1	3.7	3.1	0.5	0.2	8.4	97.9	6	14	9	5
	19 Grey mudstone	TB	4056.83	54.8	1.0	24.0	1.9	0.7	0.0	0.3	5.8	0.7	0.2	5.8	95.1	5	18	1	2
	20 Red mudstone	TB	4056.87	53.0	0.9	21.5	5.1	1.0	0.1	1.6	5.0	0.6	0.2	6.3	95.1	7	25	8	4
	21 Red mudstone	TB	4060.76	67.7	0.6	15.8	2.8	0.7	0.0	0.7	2.7	0.4	0.1	4.5	96.0	3	11	1	1
	22 Fine grey sandstone	TB	4060.80	80.7	0.1	5.6	1.6	1.8	0.1	3.8	0.5	0.1	0.1	6.5	100.9	3	5	3	1

Major elements determined by XRF (wt%), trace elements by ICP-MS (ppm). * Loss on ignition. TB: Ten Boer; US: Upper Slochteren; K: Kupferschiefer; S: Slochteren.

Table 3.3 - Bulk chemistry of samples from north German Permian outcrops.

Location	Sample no. and type		SiO_2	TiO_2	Al_2O_3	Fe_2O_3	MgO	MnO	CaO	K_2O	Na_2O	P_2O_5	LOI*	Total	Cu	Pb	Th	U
D (Bebertal)	23	Upper Rotliegend sandstone	73.6	0.4	8.6	2.2	0.2	0.1	5.1	2.3	1.6	0.2	n.d.	94.1	9	18	n.d.	5
E (Ellrich)	24	Upper Rotliegend sandstone	72.5	0.2	11.8	1.1	0.4	0.0	1.4	3.7	0.2	0.1	2.1	93.3	6	14	n.d.	1
	25	Upper Rotliegend sandstone	77.2	0.2	10.8	1.0	0.3	0.0	0.5	3.7	0.1	0.1	n.d.	93.8	8	8	n.d.	2
	26	Upper Rotliegend sandstone	76.4	0.2	11.0	1.8	0.3	0.0	0.5	3.5	0.1	0.1	n.d.	93.8	10	10	n.d.	1
	27	Upper Rotliegend sandstone	74.8	0.1	8.2	0.7	0.4	0.1	5.8	2.1	0.1	0.1	n.d.	92.4	14	10	n.d.	0
	28	Kupferschiefer	27.8	0.4	6.9	2.4	8.4	0.4	18.6	2.0	0.4	0.1	32.4	99.7	70	1828	n.d.	10
F (Walkenried)	29	Kupferschiefer	42.3	0.7	12.9	3.7	3.8	0.4	9.2	3.6	0.3	0.1	n.d.	77.0	2799	3145	n.d.	39
G (Ilfeld)	30	Kupferschiefer	34.5	0.5	10.2	5.2	4.7	0.4	9.9	2.4	0.4	0.3	33.1	101.5	357	20227	n.d.	24

Major elements (wt%) and trace elements (ppm) determined by XRF. * Loss on ignition; n.d.: not determined.

An exception to these moderate Pb values are some sandstones within several centimeters or decimeters of the Kupferschiefer, which may contain Pb concentrations up to 140 ppm due to the presence of Pb-sulphides (Knoke, 1968). The Dutch Kupferschiefer samples from core A2 clearly contain much less Pb than their German equivalents, but all samples fall within the wide range of Pb concentrations (~10 to ~10,000 ppm) which have been reported for the Kupferschiefer (e.g. Wedepohl, 1964; Sun and Püttmann, 1996).

Distribution of Pb in mineral fractions

Before discussing the distribution of Pb in mineral fractions, the applied extraction procedure should be evaluated. Cumulative Pb recovery in the five leachates of the extraction procedure amounted to 95 ± 13% (2σ) of total Pb in bulk sediments, with the exception of samples 6 and 7 (**Table 3.4**). Likely reasons for minor excursions in Pb recovery are adsorption of Pb on filters, and errors in ICP-MS analyses. Large excursions in Pb recovery from samples 6 (148%) and 7 (386%) are probably caused by the use of different subsamples and the very inhomogeneous nature of these sandstones, which was noticed before (Schmidt *et al.*, 2000 / **Chapter 2**).

Effectivity and selectivity of the leaching procedure can be properly checked by looking at leaching results for Ca, Cu and Fe. These are key elements for three of the five target phases, i.e. carbonates (step 2), organic matter and sulphides (step 3), and Fe-oxides (step 4), respectively. Cumulative 2σ recoveries of Ca, Cu and Fe were determined for five different sample types, and mean recoveries amounted to 90 ± 13% for Ca, 94 ± 7% for Cu, and 87 ± 8% for Fe (**Table 3.4**). Excursions from theoretical values of 100% can be attributed to the same effects causing minor excursions in Pb recoveries.

Percentages of Ca, Cu and Fe leached per step were calculated for a normal sandstone, sample 5, and for an organic-rich, bituminous sandstone, sample 8 (**Fig. 3.4**). Percentages show that the extraction procedure successfully separates carbonates from Fe-oxides and residual minerals in both sample types. These results are in agreement with extraction results on Permian red bed sediments by Cave and Harmon (1997), who used identical reagents for extraction of carbonates and Fe-oxides and found that they were very selective for their target phases. In sample 8, the large fraction of Ca in the exchangeable fraction is caused by the dissolution of anhydrite, which is an abundant cement in the bituminous sandstones from core A1. In the same sample, the low amount of Fe in the Fe-oxides leachate compared to the residual minerals leachate illustrates the almost complete absence of Fe-oxides, also evidenced by the very low Fe_2O_3 concentration of the bituminous sandstone (**Table 3.2**).

In contrast to carbonates and Fe-oxides, selective extraction of sulphides and organic matter from organic-rich sediments is not very successful, as evidenced by the percentages Cu in leachates of sample 8. From the mineralogy of these sediments it is clear that Cu-sulphides are the main source of Cu in organic-rich sediments. Therefore, the organic matter and sulphide leachate should contain the highest amount of Cu from all leachates. However, the carbonates leachate of sample 8 contains around 50% of total Cu, while also the Fe-oxides leachate contains more Cu than the organic matter and sulphide leachate.

Table 3.4 - Leached amounts of Pb per sequential extraction step and cumulative recovery of Pb and key elements Ca, Cu and Fe.

Core	Sample no. and type	Bulk Pb (ppm)	Pb recovery in sequential leaching steps (ppm)					Sum 1-5 (ppm)	Recovery (%)			
			Step 1	Step 2	Step 3	Step 4	Step 5		Pb	Ca	Cu	Fe
A1	1 Red mudstone	18.5	0.5	0.6	1.5	0.8	16.3	19.7	106	n.d.	n.d.	n.d.
	2 Red mudstone	18.0	-	2.7	0.7	-	15.3	18.6	103	n.d.	n.d.	n.d.
	3 Red mudstone	20.5	-	2.8	0.1	0.6	16.4	20.0	97	n.d.	n.d.	n.d.
	4 Coarse grey sandstone	9.3	-	1.3	-	2.4	7.6	11.3	121	111	87	98
	5 Fine grey sandstone	9.4	0.2	1.1	1.3	2.0	6.8	11.4	122	92	101	90
	6 Bituminous sandstone	36.0	-	26.3	11.3	6.3	9.4	53.4	148	n.d.	n.d.	n.d.
	7 Bituminous sandstone	8.6	-	20.6	2.5	2.2	7.9	33.2	386	n.d.	n.d.	n.d.
	8 Bituminous sandstone	33.0	-	13.6	3.7	4.0	6.8	28.1	85	91	94	85
	9 Grey conglomerate	6.8	-	0.7	0.2	0.3	6.1	7.2	107	78	102	77
A2	10 Black shale (Kupf.)	727.8	0.4	231.1	57.1	32.5	337.2	658.3	90	n.d.	n.d.	n.d.
	11 Black shale (Kupf.)	770.3	0.3	345.9	47.5	-	316.5	710.2	92	n.d.	n.d.	n.d.
	12 Bituminous sandstone	11.1	-	3.1	-	0.4	7.9	11.4	102	n.d.	n.d.	n.d.
	13 Bituminous sandstone	9.5	-	3.5	0.1	0.4	4.7	8.7	91	n.d.	n.d.	n.d.
	14 Bituminous sandstone	8.5	-	1.5	0	0.3	5.5	7.4	87	n.d.	n.d.	n.d.
	15 Conglomerate	9.2	-	1.1	0	0.6	6.0	7.8	84	n.d.	n.d.	n.d.
B	16 Red mudstone	29.9	-	3.6	0.1	1.0	25.0	29.7	99	n.d.	n.d.	n.d.
	17 Fine white sandstone	6.8	-	1.7	0.3	1.2	3.5	6.7	97	79	88	85
C	18 Red mudstone	14.0	-	1.5	-	0.5	10.8	12.9	92	n.d.	n.d.	n.d.
	19 Grey mudstone	17.9	-	1	0	0.2	13.7	14.8	83	n.d.	n.d.	n.d.
	20 Red mudstone	25.0	-	1	-	1.1	18.5	20.6	82	n.d.	n.d.	n.d.
	21 Red mudstone	11.3	-	0.9	-	0.5	10.0	11.4	101	n.d.	n.d.	n.d.
	22 Fine grey sandstone	5.3	-	1.1	-	0.0	3.3	4.4	83	n.d.	n.d.	n.d.
							mean recovery (%, 2σ)		95 ± 13	90 ± 13	94 ± 7	87 ± 8

n.d.: not determined

In analogy to Cu, selective extraction of Pb from sulphides in organic-rich sediments may be unsuccessful with the reagents applied in our extraction scheme. In conclusion, cumulative recovery of Pb and leaching results for Ca, Cu and Fe indicate that the leaching procedure is a reliable method for sequentially extracting Pb from sediments with low organic matter contents and no sulphides. However, leaching results for Cu from an organic-rich sandstone suggest that selective leaching of Pb from sulphides in organic-rich sediments may be impossible with the applied reagents.

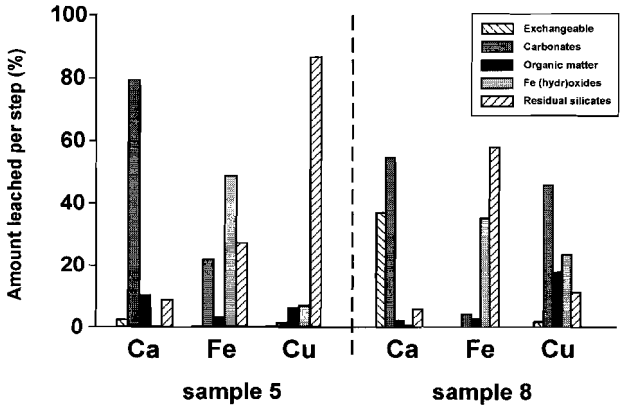

Figure 3.4 - Percentages of Ca, Fe and Cu sequentially leached from a fine grey sandstone (sample 5) and an organic-rich, bituminous sandstone (sample 8).

Instead of using absolute amounts of Pb leached per extraction step (**Table 3.4**), distribution of Pb in mineral fractions can be better discussed by using relative amounts. In general, Pb in sandstones from all four cores and bituminous sandstones from core A2 is mainly present in carbonates (10-40%) and in residual minerals (52-75%) (**Fig. 3.5**). This Pb distribution is no surprise, since carbonates and feldspars are the two major mineral groups, besides sulphides, in which Pb is frequently found. In carbonates, Pb replaces Ca, in feldspars Pb replaces K and perhaps also some Ca (Boyle, 1959). No examples of Pb-bearing carbonates in Rotliegend sandstones have been published, but Pye and Krinsley (1986) reported carbonate cements with up to 2.1 wt% CuO and 1.1 wt% ZnO. Lead concentrations in feldspars generally range from 10 to 100 ppm, with an average of 38 ppm (Gmelin, 1976). The Fe-oxides fraction is only important in sandstone samples 4, 5 and 17 (18-21%). This result is a bit puzzling for sample 17, since this sandstone contains much less Fe_2O_3 than samples 4 and 5 (**Table 3.2**). The minor importance of the Fe-oxides fraction for the total Pb content of the sediments is further stressed by the absence of a relationship between Fe oxidation state and associated Pb concentrations. Reduced, grey mudstone sample 19 has a much lower trivalent Fe concentration than most oxidized mudstones, but Pb concentrations are comparable. Also, oxidized German sandstone sample 24 has the same Pb distribution pattern as Dutch reduced sandstone sample 22, but a Pb concentration more than twice as high.

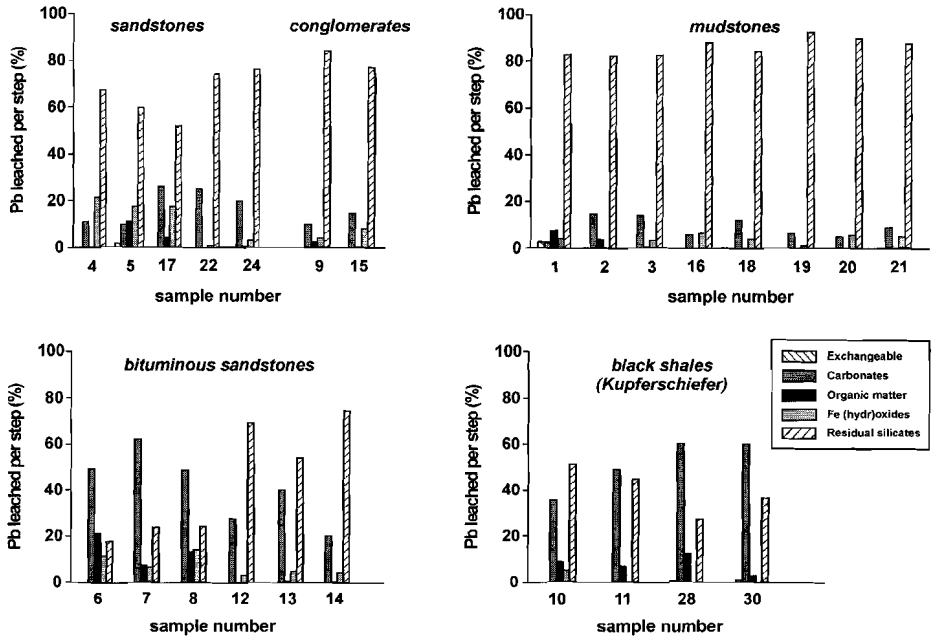

Figure 3.5 - Pb distribution in mineral phases of Rotliegend and Kupferschiefer sediments.

Bituminous sandstones from core A1, samples 6-8, clearly differ from all other sandstones. In these sandstones, Pb is mainly leached in the carbonates step (49-64%). The residual minerals fraction only contains 18-24% of total Pb, the organic matter fraction 6-21%. This different Pb distribution is caused by larger total Pb amounts in these sandstones due to the presence of Pb-sulphides. However, instead of being leached in the organic matter and sulphides fraction, Pb-sulphides, like Cu-sulphides, appear to be leached together with carbonates. Kupferschiefer samples, in which Pb-sulphides are expected to be the most important Pb-bearing minerals, show the same behaviour. The carbonate fraction contains 35-60% of totally leached Pb, while the organic matter and sulphides fraction contains only 3-12%. In addition, the residual mineral fraction contains 27-51%. This latter percentage seems very high, but feldspars in the Kupferschiefer have been reported to contain up to 2 wt% PbO, and kaolinite about 0.5 wt% PbO as a result of isomorphic substitution upon contact with metal-rich brines (Kucha, 1985). In conglomerates and mudstones, finally, residual minerals are by far the most important Pb-bearing fraction, accounting for 77-92% of total Pb. This Pb must be mainly present in feldspars, which are abundant in both conglomerates and mudstones. Illite, most abundant clay mineral in mudstones, generally contains only insignificant amounts of structural Pb (Gmelin, 1976). This is also evidenced by major loss of structural Pb from smectites upon their diagenetic transition into illites (Hallager *et al.*, 1991).

Stable Pb isotopes

Stable Pb isotope ratios with respect to ^{204}Pb are known to be inaccurate in ICP-MS analysis because of interference of ^{204}Hg with the ^{204}Pb signal. We therefore report only $^{206}Pb/^{207}Pb$, $^{208}Pb/^{207}Pb$ and $^{206}Pb/^{208}Pb$ ratios, which are not sensitive to variable Hg contents of the samples. Analysed stable Pb isotope ratios of sediments from Dutch gas reservoir formations form a close range (**Table 3.5**). Except for bituminous sandstone samples 6, 7 and 8, which show 'anomalously' high ^{206}Pb values compared to ^{207}Pb and ^{208}Pb, $^{206}Pb/^{207}Pb$ ratios range from 1.186 to 1.208, and $^{208}Pb/^{207}Pb$ from 2.459 to 2.482. In order to elucidate the origin of Pb in Dutch gas reservoir brines, it is useful to correct analysed ratios for ingrowth of Pb from decay of U and Th since deposition of the sediments. This is obvious for samples 6 through 8, containing high amounts of U, but also for the other samples, since the correction needed is larger than the standard deviations of the analyses. Corrections were calculated using depositional ages and U, Th and Pb concentrations of the sediments. Ages for Kupferschiefer (256 Ma) and Upper Slochteren and Ten Boer formations (both 270 Ma) were taken from Harland *et al.* (1990). For bituminous sandstone samples 6 through 8 an age of 246 Ma was taken, calculated from U/Pb ratios of uranium oxide grains in postgenetic bitumen impregnations (Schmidt *et al.*, 2000 / **Chapter 2**). Uranium, Th and Pb concentrations were taken from **Table 3.2**. Average U,Th and Pb concentrations of the two Kupferschiefer samples from core A2 were used to correct Pb isotope ratios for an additional Kupferschiefer sample from the Groningen gas field (Wedepohl *et al.*, 1989). Further details on the correction procedures and an example of the calculations are given in **Appendix 3.2**.

Corrected stable Pb isotope ratios for the sediments are also given in **Table 3.5**. Variation in corrected ratios is somewhat larger than in original ratios, mainly because of analytical errors in U, Th and Pb concentrations of the sediments. Samples 6, 7, 8 and 18 could not be corrected properly and will be further left out of the discussion. Corrected isotope ratios of mudstone sample 18 are anomalously low, probably because of its anomalously high U concentration compared to the other mudstones from this study. Proper correction of isotope ratios for bituminous sandstones 6 through 8 proved to be impossible, likely because of postgenetic Pb and U deposition and subsequent remobilisation of Pb in these samples (Schmidt *et al.*, 2000 / **Chapter 2**). Remobilisation of Pb was most intense in sample 7 (sample 3 from Schmidt *et al.*, 2000 / **Chapter 2**), resulting in calculated ingrowth concentrations higher than present Pb isotope concentrations in this sandstone.

Origin of Pb in Rotliegend brines

Testing the hypothesis that Pb in Rotliegend gas reservoir brines has been primarily derived from feldspars in the Rotliegend sediments involves three steps. First, stable Pb isotope ratios of the gas reservoir sediments should be compared with those of metallic Pb and galena deposits from gas production facilities (Schmidt *et al.*, submitted / **Chapter 6**).

Table 3.5 - Stable Pb isotope ratios of bulk sediments from Dutch gas reservoirs.

Core	Sample no. and type	$^{206}Pb/^{207}Pb$	$^{208}Pb/^{207}Pb$	$^{206}Pb/^{208}Pb$	Age (Ma)	$^{206}Pb/^{207}Pb$ corrected	$^{208}Pb/^{207}Pb$ corrected	$^{206}Pb/^{208}Pb$ corrected
A1	1 Red mudstone	1.199 ± 0.002	2.476 ± 0.007	0.484 ± 0.001	270	1.192	2.473	0.482
	2 Red mudstone	1.205 ± 0.003	2.478 ± 0.005	0.486 ± 0.001	270	1.178	2.446	0.482
	3 Red mudstone	1.208 ± 0.004	2.481 ± 0.007	0.487 ± 0.001	270	1.193	2.474	0.482
	4 Coarse grey sandstone	1.194 ± 0.005	2.461 ± 0.005	0.485 ± 0.002	270	1.167	2.450	0.476
	5 Fine grey sandstone	1.206 ± 0.004	2.475 ± 0.005	0.487 ± 0.001	270	1.166	2.449	0.476
	6 Bituminous sandstone	1.247 ± 0.003	2.456 ± 0.006	0.508 ± 0.001	246	1.120	2.468	0.454
	7 Bituminous sandstone	2.179 ± 0.007	2.308 ± 0.012	0.944 ± 0.004	246	---	---	---
	8 Bituminous sandstone	1.369 ± 0.005	2.429 ± 0.010	0.564 ± 0.003	270	0.887	2.488	0.356
	9 Grey conglomerate	1.206 ± 0.011	2.464 ± 0.014	0.489 ± 0.003	270	1.172	2.454	0.478
A2	10 Black shale (Kupf.)	1.192 ± 0.004	2.459 ± 0.005	0.485 ± 0.002	256	1.185	2.459	0.482
	11 Black shale (Kupf.)	1.194 ± 0.002	2.459 ± 0.004	0.485 ± 0.001	256	1.184	2.460	0.481
	12 Bituminous sandstone	1.189 ± 0.005	2.467 ± 0.006	0.482 ± 0.002	270	1.170	2.456	0.476
	13 Bituminous sandstone	1.201 ± 0.005	2.467 ± 0.007	0.487 ± 0.002	270	1.176	2.457	0.479
	14 Bituminous sandstone	1.186 ± 0.005	2.462 ± 0.004	0.482 ± 0.002	270	1.159	2.450	0.473
	15 Conglomerate	1.208 ± 0.006	2.468 ± 0.005	0.490 ± 0.003	270	1.174	2.452	0.479
B	16 Red mudstone	1.198 ± 0.004	2.473 ± 0.006	0.484 ± 0.001	270	1.186	2.469	0.481
	17 Fine white sandstone	1.186 ± 0.004	2.460 ± 0.006	0.482 ± 0.001	270	1.164	2.460	0.473
C	18 Red mudstone	1.191 ± 0.005	2.459 ± 0.005	0.484 ± 0.002	270	1.137	2.429	0.468
	19 Grey mudstone	1.207 ± 0.005	2.469 ± 0.007	0.489 ± 0.001	270	1.186	2.467	0.481
	20 Red mudstone	1.208 ± 0.004	2.482 ± 0.004	0.487 ± 0.002	270	1.193	2.466	0.484
	21 Red mudstone	1.208 ± 0.003	2.476 ± 0.007	0.488 ± 0.001	270	1.180	2.452	0.481
	22 Fine grey sandstone	1.199 ± 0.003	2.465 ± 0.007	0.486 ± 0.002	270	1.178	2.460	0.479
lit.	Kupferschiefer, Groningen (Wedepohl *et al.*, 1978)	1.190	2.463	0.483	256	1.182	2.464	0.480

Second, potential mineral sources of Pb in the Rotliegend sediments should be identified, and third, it should be investigated whether enough Pb could have been mobilized from these mineral sources to explain observed Pb concentrations in Rotliegend gas reservoir brines.

Since Pb minerals in gas production facilities have been deposited from reservoir brines coproduced with natural gas, their stable Pb isotopic signatures represent those of the reservoir brines (Schmidt *et al.*, submitted / **Chapter 6**). Comparison of the isotopic signatures of these deposits with signatures of Rotliegend sediments is done relative to the plumbotectonics model of Zartman and Doe (1981), in which four evolution curves represent the evolution of stable Pb isotope ratios in four terrestrial reservoirs: upper continental crust, lower continental crust, mantle, and an orogenic environment. The curves are the result of redistribution of U, Th and Pb during mixing of the terrestrial reservoirs in orogenic processes assumed to occur every 400 Ma (Zartman and Doe, 1981).

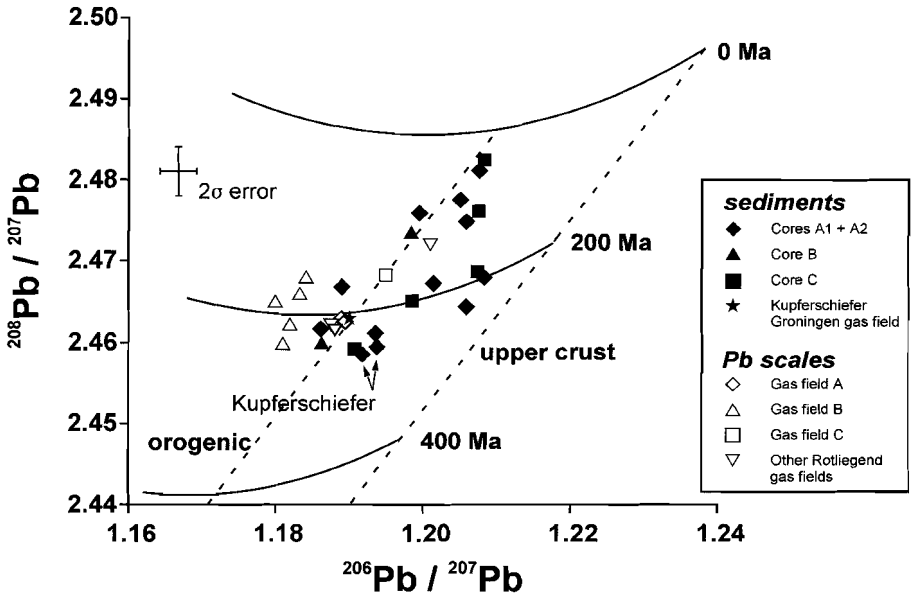

Figure 3.6 - Uncorrected stable Pb isotope ratios of sediments from this study, compared with ratios of Pb scales from production facilities of the same and other Rotliegend natural gas fields (Schmidt *et al.*, submitted / **Chapter 6**) and with Kupferschiefer sediments from the Groningen gas field (Wedepohl *et al.*, 1978). Error bars indicate average 2σ errors on isotopic ratios for sediments and scales.

Rotliegend and Kupferschiefer sediments from this study roughly cluster between orogenic and upper crust evolution curves, showing model ages of between 50 and 250 Ma (**Fig. 3.6**). Lead scales from a number of Rotliegend gas production facilities, including gas fields A, B and C from this study, cluster around the lower left end of the isotopic range presented by the

sediments. Within analytical errors part of the sediments and brines are in isotopic equilibrium, but most sediments appear to be enriched in both ^{206}Pb and ^{208}Pb compared to the brines. Upon correction for ingrowth of ^{206}Pb from ^{238}U and ^{208}Pb from ^{232}Th in sediments since their deposition, we see exactly the opposite: still part of the sediments and brines are in isotopic equilibrium, but now most sediments are depleted in ^{206}Pb and ^{208}Pb with respect to the brines (**Fig. 3.7**).

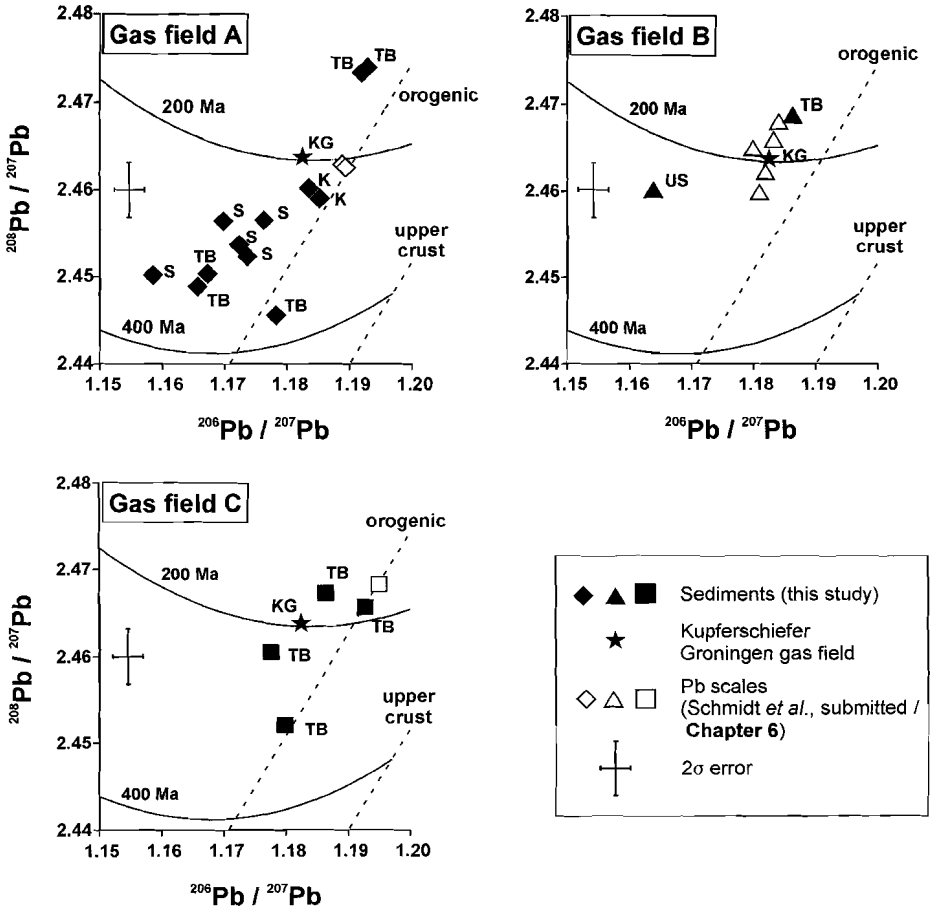

Figure 3.7 - Comparison of Pb isotope ratios of sediments, corrected for ingrowth of Pb from U and Th, and ratios of Pb scales, i.c. reservoir brines, for gas fields A, B and C from this study. Formation Members have been indicated for individual sediment samples. K: Kupferschiefer; KG: Kupferschiefer from the Groningen gas field (Wedepohl *et al.*, 1978); S: Slochteren; US: Upper Slochteren; TB: Ten Boer.

After correction, Slochteren and Ten Boer sediments from cores A1 and A2 mainly cluster around a model age of 300 Ma, while formation waters from this gas field are isotopically very similar to much younger Kupferschiefer sediments overlying the Rotliegend reservoir. Anomalous signatures of two Ten Boer mudstones from this field are probably due to analytical errors, in that too low detected U and Th concentrations cause a too small correction of isotope ratios. In gas fields B and C, reservoir sediments show younger corrected model ages than equivalent sediments from gas field A, but formation waters still plot at the youngest end of the corrected isotopic range of the sediments. Clearly, isotopic signatures of brines lie on the Pb evolution curve presented by the sediments. This indeed indicates large scale mobilization of Pb from the reservoir sediments into their formation waters between the time of deposition of the sediments and the present.

Having established that stable Pb isotope data support mobilization of Pb from Rotliegend sediments into Rotliegend brines, next mineral sources of this Pb should be identified in the sediments. Distribution of Pb in Dutch and German Rotliegend sediments from this study shows that in both oxidized and reduced sandstones, conglomerates and mudstones, most Pb is present in feldspars. Since feldspar dissolution occurred on a very wide scale in Dutch Rotliegend sediments (e.g. Lee *et al.*, 1989; Crouch *et al.*, 1996; Lanson *et al.*, 1996), distribution data support the hypothesis that Pb in Rotliegend gas reservoir brines was primarily derived from the dissolution of feldspars (Schmidt *et al.*, submitted / **Chapter 6**). In addition, some Pb in Rotliegend brines may have originated from dissolution of Fe-oxide coatings around sediment grains, as suggested by Carpenter *et al.* (1989). Fe-oxides in our samples generally contain only a small fraction of total Pb, but sometimes they may account for up to 20% of total Pb. This is in agreement with results for other red bed sediments. For instance, up to 20% of total Pb in Mexican Holocene-Pliocene red bed sediments was present in Fe-oxides, while remaining Pb was present in the silicate fraction of the sediments (Zielinski *et al.*, 1983). Fe-oxides fraction of British Permo-triassic red bed sandstones contained 3 to 20% of total Pb (Cave and Harmon, 1997).

Sequential extraction results further showed that in many of the Rotliegend sediments carbonates contain a significant portion of total Pb. However, it is not likely that carbonates in Rotliegend sediments contributed significantly to Pb in Rotliegend brines. Carbonates presently found in these sediments are either early cements precipitated from meteoric fluids (Gaupp *et al.*, 1993; Platt, 1994), or late stage carbonate cements, precipitated contemporarily with or after dissolution of feldspars and Fe-oxides (Pye and Krinsley, 1986; Platt, 1994). Carbonates in samples from this study are primarily late stage carbonates (Schmidt *et al.*, 2000 / **Chapter 2**), which therefore incorporated Pb previously mobilised from feldspars and/or Fe-oxides. Early carbonate cements, originating from meteoric waters and largely dissolved in our samples, will only have contained very small amounts of Pb. Finally, Hallager *et al.* (1991) suggested that Pb in Rotliegend brines was primarily derived from smectites as a result of their diagenetic transformation into illite. However, illite in Rotliegend sandstone gas reservoirs is mainly formed at the expense of kaolin-group minerals (e.g., Lee *et al.*, 1985; Pye and Krinsley, 1986; Lanson *et al.*, 1996). Kaolin-group minerals, like illite, generally contain only small amounts of Pb (Gmelin, 1976).

Finally, the question should be answered whether Rotliegend sediments contained enough Pb to account for observed high Pb concentrations in Rotliegend brines. A material balance calculation, such as applied by Doe *et al.* (1966), shows that Pb concentrations of about 100 ppm in Rotliegend gas reservoir brines can be quite simply explained by dissolution of feldspars and Fe-oxide grain coatings from Rotliegend sediments. From the Pb distribution in Rotliegend sandstones, mudstones and conglomerates and in other red bed sediments, an average Pb concentration of 10 ppm can be derived for an original Rotliegend sediment, with about 15% of the Pb present in Fe-oxides and 85% in feldspars. Assuming an average porosity of 10%, a reservoir brine density of about 1.0 $kg \cdot l^{-1}$ (at reservoir temperatures of about 100°C) and a sediment density of 2.3 $kg \cdot l^{-1}$, leaching of Pb by dissolving 40% of feldspars and 80% of Fe-oxide coatings will lead to a Pb concentration in the brine of:

$$[Pb]_{brine} = \frac{((0.40 \cdot 0.85) + (0.80 \cdot 0.15)) \cdot [Pb]_{rock} \cdot \rho_{rock}}{\phi \cdot \rho_{brine}} = 106 \ ppm$$

in which ϕ is the average sediment porosity fraction and ρ is density. Variations in leaching percentages, sediment porosities and Pb concentrations in sediments can have large effects on Pb concentrations in reservoir brines. For instance, dissolution of 50% of feldspars instead of 40% will lead to a Pb concentration in brines of 125 ppm. Therefore, reported Pb concentrations of 150 ppm in some Dutch Rotliegend reservoir brines do not seem anomalous, especially in reservoirs exhibiting large scale feldspar dissolution such as reported by Lanson *et al.* (1996).

Mobilization of Pb from the reservoir sediments was probably a single large scale event, since dissolution of feldspars and Fe-oxides in Rotliegend reservoirs is generally seen as a single event associated with the influx of acidic, Carboniferous fluids prior to emplacement of natural gas (Gaupp *et al.*, 1993; Lanson *et al.*, 1996). The observed range in isotopic compositions of Rotliegend reservoir brines (**Fig. 3.6**) may be due to isotopic differences between Rotliegend sediments in different reservoirs (**Fig. 3.7**), or to mixing of mobilized Pb with Pb either already present in the brines, or subsequently supplied by Zechstein fluids entering Rotliegend formations after 155 Ma (Lanson *et al.*, 1996).

Conclusions

Rotliegend sandstones, conglomerates and mudstones from three gas fields in the northern Netherlands and southern North Sea area and from outcrops in northern Germany show Pb concentrations comparable to average sandstones (7 ppm) and shales (20 ppm). Sequential extraction of Pb from these sediments shows that in sandstones 10-40% of total Pb is present in late stage diagenetic carbonate cements, while 52-75% is present in feldspars from the residual minerals fraction. In conglomerates and mudstones feldspars are by far the most important Pb-bearing minerals, accounting for 77 -92% of total Pb. Elevated Pb concentrations

of around 30 ppm in bituminous sandstones from one of the gas fields are due to the presence of Pb-sulphide associated with the bitumens. In Dutch and German Kupferschiefer, Pb-sulphides and silicates are the most important Pb-bearing mineral fractions. The exchangeable Pb fraction can be neglected in all investigated sediment types, but Fe-oxides may account for up to 20% of total Pb in Rotliegend sediments.

Correction of stable Pb isotope signatures of the reservoir sediments for ingrowth of Pb from decay of U and Th since their deposition provides a Pb evolution curve of the sediments. Isotopic signatures of Pb minerals deposited from brines of the same reservoirs plot on this Pb evolution curve, supporting large scale mobilization of Pb from Rotliegend sediments into Rotliegend brines. Sequential extraction data and diagenetic considerations lead to the conclusion that Pb in the brines was primarily derived from feldspars in the Rotliegend sediments, while some of it may have been derived from Fe-oxide grain coatings. Material balance calculations show that Pb concentrations in brines of about 100 ppm can be explained by dissolution of 40% of the feldspars and 80% of the Fe-oxide coatings of an average Rotliegend sediment containing 10 ppm Pb, of which 85% is present in feldspars and 15% in Fe-oxide grain coatings. Reported Pb concentrations of up to 150 ppm in brines can be accounted for by large scale feldspar dissolution, which has been reported for a number of Dutch Rotliegend gas reservoirs.

Mobilization of Pb from Rotliegend sediments was probably a single large scale event, controlled by diagenetic fluid fluxes. Heterogeneity of sediments or mixing of mobilized Pb with Pb from other sources may have caused current Pb isotopic differences between brines from different gas reservoirs.

Acknowledgement - The authors thank Nederlandse Aardolie Maatschappij B.V. for providing sediment samples. A.S. thanks NAM B.V. for the sponsorship of his PhD project of which this study forms a part.

Appendix 3.1

The leaching experiments were performed using HDPE centrifuge tubes in an ultrasonic bath. After each leaching step, leachates and washing solutions were separated from the residues by centrifugation and filtrated through a 0.20 µm Millipore filter. Final solutions were stored in HDPE flasks. Before analysis, final solutions from steps 1 to 4 were diluted 10 to 20 times in order to reduce total salinity. The leaching procedure was carried out according to the following recipe:

Step 1: Samples were leached with 10 ml 1 M $MgCl_2$ of pH 7 at room temperature for 1 h. Residues were washed twice with 10 ml distilled water, which was added to the leachates. Final solutions were adjusted to 100 ml with 4.5% HNO_3 and stored until ICP-MS analysis.

Step 2: Residues from step 1 were leached at room temperature for 5 h with 5 ml 1 M ammonium acetate, adjusted to pH 4.5 with 96% acetic acid. Residues were washed twice with 10 ml distilled water, which was added to the leachates. Final solutions were adjusted to 100 ml with 4.5% HNO_3 and stored until analysis.

Step 3: About 4 ml 30% H_2O_2 was added to the residues from step 2 and allowed to react at 60°C until no more gas development could be seen. Subsequently 5 ml 30% H_2O_2 was added to the suspensions which were left overnight at 60°C. Before centrifugation and filtration, suspensions were heated to 80°C for 10

minutes to destruct remaining H_2O_2, and 5 ml 1 M ammonium acetate of pH 5 was added. Residues were washed twice with 5 ml 1M ammonium acetate, and once with 5 ml distilled water. Ammonium acetate and distilled water were added to the leachates, and final solutions were adjusted to 100 ml with 4.5% HNO_3 and stored until analysis.

Step 4: Residues from step 3 were leached at 70°C for 24 h with 6 ml of Tamm's reagent (12.6 g oxalic acid and 24.9 g ammonium oxalate in 1 l of solution) at pH 3. After centrifugation, the solid residues were dried in a stove at 80°C and weighed. About 2 ml H_2O_2 (30%) and 1 ml HNO_3 (65%) were added to the leachates, which were then treated in a microwave evaporator. Final solutions were put in to a HDPE flask with 2 ml 65% HNO_3, adjusted to 25 ml with distilled water and stored until analysis.

Step 5: About 0.25 g of the dried residues from step 4 were put in sealed teflon containers and totally dissolved by acid digestion ($HCl/HF/HNO_3/HClO_4$) in a microwave oven for 2 h. Final solutions were adjusted to 50 ml with distilled water and stored until analysis.

Appendix 3.2

Correction of stable Pb isotope ratios in sediments is only possible on the assumption that no leaching or enrichment of U, Pb or Th occurred after deposition of the sediments. Ingrowth of Pb from U and Th in sediments is described by the law of radioactive decay. In a closed system, the general equation for the ingrowth of for instance ^{206}Pb from ^{238}U is:

$$[^{206}Pb]_{ingrowth} = [U]_{sediment} \cdot \left(\frac{U_{238}}{U_{tot}}\right)_T \cdot \left(e^{\lambda \cdot T} - 1\right)$$

where the concentration of ^{206}Pb due to ingrowth from decay of its parent nuclide ^{238}U is determined by the U concentration in the sediment, the fraction of ^{238}U atoms of total U in the sediment at the time T of deposition, and the decay constant λ of ^{238}U. For ^{206}Pb, ^{207}Pb and ^{208}Pb in a closed system the following equations apply:

$$[^{206}Pb]_{ingrowth} = [U]_{sediment} \cdot \left(\frac{U_{238}}{U_{tot}}\right)_T \cdot \left(e^{0.00015513 \cdot T} - 1\right)$$

$$[^{207}Pb]_{ingrowth} = [U]_{sediment} \cdot \left(\frac{U_{235}}{U_{tot}}\right)_T \cdot \left(e^{0.00098485 \cdot T} - 1\right)$$

$$[^{208}Pb]_{ingrowth} = [Th]_{sediment} \cdot \left(e^{0.000049866 \cdot T} - 1\right)$$

where element concentrations are expressed as moles·kg^{-1} and T stands for the age of deposition of the sediments in Ma. Because ^{238}U and ^{235}U have different half lives, their fractions of total U vary with time. Therefore, ^{238}U and ^{235}U fractions must be corrected, as must the U concentration in the sediment, which has decreased due to radioactive decay (Karam and Leslie, 1999). In the same way, the Th concentration in the sediments should be corrected. However, geologically speaking all our sediments have rather young and very similar ages. Therefore, in our calculations we have used the present ^{238}U and ^{235}U fractions of 0.99276 and 0.00720, respectively, while also U and Th concentration corrections have been neglected.

Application of for instance the corrected ^{235}U fraction for a sediment with an age of 270 Ma, which is 0.90% in stead of the present 0.72%, would result in maximum corrections in Pb isotope ratios in the order of only 0.0002 compared to standard deviations on the analyses in the order of ±0.006 .

Calculated concentrations of stable Pb are subtracted from present stable Pb isotope concentrations, and the resulting concentrations directly allow calculation of stable Pb isotope ratios of the sediments at the time of their deposition. Because ^{204}Pb could not be determined accurately in all sediments, this isotope is not taken into account here. This introduces an error in the correction calculations of about 1.2%, which is equal to the average ^{204}Pb concentration of samples with the lowest Hg contents.

Correction calculations are illustrated here with the example of sample 4. Analysed $^{206}Pb/^{207}Pb$, $^{208}Pb/^{207}Pb$ and $^{206}Pb/^{208}Pb$ ratios of this sandstone correspond to a present stable Pb isotope distribution of 25.65% ^{206}Pb, 21.39% ^{207}Pb, and 52.96% ^{208}Pb. With a total Pb concentration of 9.3 ppm, isotope concentrations amount to $2.30 \cdot 10^{-5}$ mole·kg^{-1} ^{206}Pb, $1.91 \cdot 10^{-5}$ mole·kg^{-1} ^{207}Pb, and $4.74 \cdot 10^{-5}$ mole·kg^{-1} ^{208}Pb. From U and Th concentrations of the sample, $6.31 \cdot 10^{-6}$ mole·kg^{-1} U and $1.00 \cdot 10^{-5}$ mole·kg^{-1} Th, Pb isotope ingrowth concentrations can be calculated as $2.68 \cdot 10^{-7}$ mole·kg^{-1} ^{206}Pb, $1.38 \cdot 10^{-8}$ mole·kg^{-1} ^{207}Pb, and $1.36 \cdot 10^{-7}$ mole·kg^{-1} ^{208}Pb. Subtracting ingrowth concentrations from measured concentrations gives Pb isotope concentrations which result in the following ratios at the time of deposition of the sandstone: $^{206}Pb/^{207}Pb = 1.167$, $^{208}Pb/^{207}Pb = 2.450$, and $^{206}Pb/^{208}Pb = 0.476$. Calculated corrections for this sample amount to 0.026, 0.011 and 0.009 respectively, roughly 2 to 5 times the 2σ standard deviations of the original analyses. Standard deviations (2σ) in the U, Th and Pb ICP-MS analyses of ± 2% result in total errors of corrected isotopic ratios of about twice the 2σ standard deviations of the original analyses.

References

Boyle, R.W., 1959. Some geochemical considerations on lead-isotope dating of lead deposits. Econ. Geol. 54, 130-135.

Bunzl., K., Kretner, R., Schramel, P., Szeles, M. and Winkler, R., 1995. Speciation of ^{238}U, ^{226}Ra, ^{210}Pb, ^{228}Ra, and stable Pb in the soil near an exhaust ventilating shaft of a U mine. Geoderma 67, 45-53.

Carpenter, A.B., 1989. Occurrence of lead- and zinc-rich brine in the Rotliegendes formation, the Netherlands. Abstr. Prog. Geol. Soc. Am. 21(6), 315.

Cave, M.R. and Harmon, K., 1997. Determination of trace metal distributions in the iron oxide phases of red bed sandstones by chemometric analysis of whole rock and selective leachate data. The Analyst 122, 501-512.

Crespo, M.T., Perez del Villar, L., Jimenez, A., Pelayo, L., Quejido, A. and Sanchez, M., 1996. Uranium isotopic distribution in the mineral phases of granitic fracture fillings by a sequential extraction procedure. Appl. Rad. Isot. 47, 927-931.

Crouch, S.V., Baumgartner, W.E.L., Houlleberghs, E.J.M.J. and Walzebuck, J.P., 1996. Development of a tight gas reservoir by a multiple fracced horizontal well: Ameland-204, the Netherlands. In: H.E. Rondeel, D.A.J. Batjes and W.H. Nieuwenhuijs (Eds.), Geology of gas and oil under the Netherlands. Kluwer Academic Publishers, Dordrecht, pp. 93-102.

Doe, B.R., Hedge, C.E. and White, D.E., 1966. Preliminary investigation of the source of lead and strontium in deep geothermal brines underlying the Salton Sea geothermal area. Econ. Geol. 61, 462-483.

Gatehouse, S., Russell, D.W. and Van Moort, J.C., 1977. Sequential soil analysis in exploration geochemistry. J. Geochem. Expl. 8, 483-494.

Gaupp, R., Matter, A., Platt, J., Ramseyer, K. and Walzebuck, J., 1993. Diagenesis and fluid evolution of deeply buried Permian (Rotliegende) gas reservoirs, Northwest Germany. AAPG Bull. 77, 1111-1128.

Gmelin, 1976. Blei, Teil A2a. Gmelin Handbuch der Anorganischen Chemie, Springer-Verlag, Berlin.

Hallager, W.S., Carpenter, A.B. and Campbell, W.L., 1991. Smectite clays in red beds as a source of base metals. Abstr. Progr. Geol. Soc. Am. 23, 31-32.

Harland, W.B., Armstrong, R.L., Cox, A.V., Craig, L.E., Smith, A.G. and Smith, D.G., 1990. A geologic time scale 1989. Cambridge University Press, Cambridge, 263 pp.

Hartmann, M., 1963. Einige geochemische Untersuchungen an Sandsteinen aus Perm und Trias. Geochim. Cosmichim. Acta 27, 459-499.

Hartree, R. and Veizer, J., 1982. Lead and zinc distribution in carbonate rocks. Chem. Geol. 37, 351-365.

Karam, P.A. and Leslie, S.A., 1999. Calculations of background beta-gamma radiation dose through geologic time. Health Physics 77, 662-667.

Knoke, R., 1968. Elementverteilung im Liegenden des Kupferschiefers. Contrib. Min. Petrol. 17, 347-366.

Kucha, H., 1985. Feldspar, clay, organic and carbonate receptors of heavy metals in Zechstein deposits (Kupferschiefer-type), Poland. Trans. Instn. Min. Metall. (Sect.B: Appl. Earth Sci.) 94, 133-156.

Lanson, B., Beaufort, D., Berger, G., Baradat, J. and Lacharpagne, J.-C., 1996. Illitization of diagenetic kaolinite-to-dickite conversion series: late-stage diagenesis of the lower Permian Rotliegend sandstone reservoir, offshore of the Netherlands. J. Sedim. Res. 66, 501-518.

Lee, M., Aronson, J.L. and Savin, S.M., 1985. K/Ar dating of time of Gas emplacement in Rotliegende Sandstone, Netherlands. AAPG Bull. 69, 1381-1385.

Lee, M., Aronson, J.L. and Savin, S.M., 1989. Timing and conditions of Permian Rotliegende sandstone diagenesis, Southern North Sea: K/Ar and oxygen isotopic data. AAPG Bull. 73, 195-215.

McCann, T., 1998. The Rotliegend of the NE German Basin: background and prospectivity. Petrol. Geosci. 4, 17-27.

Oszczepalski, S., 1986. On the Zechstein copper shale lithofacies and palaeoenvironments in SW Poland. In: G.M. Harwood and D.B. Smith (Eds.), The English Zechstein and related topics. Geological Society Special Publication 22. Geological Society, London, 171-182.

Platt, J.D., 1994. Geochemical evolution of pore waters in the Rotliegend (Early Permian) of northern Germany. Marine Petrol. Geol. 11, 66-78.

Pye, K. and Krinsley, D.H., 1986. Diagenetic carbonate and evaporite minerals in Rotliegend aeolian sandstones of the southern North Sea: their nature and relationship to secondary porosity development. Clay Min. 21, 443-457.

Schmidt, A.P., 1998. Lead precipitates from natural gas production installations. J. Geochem. Expl. 62, 193-200 (**chapter 5** of this thesis).

Schmidt, A.P., Hartog, F.A., Van Os, B.J.H. and Schuiling, R.D., 2000. Production of ^{210}Pb from a Slochteren Sandstone gas reservoir. Appl. Geochem. 15, 1317-1329 (**chapter 2** of this thesis).

Schmidt, A.P., Hartog, F.A., Van Os, B.J.H. and Schuiling, R.D., submitted. Origin and deposition of stable lead and ^{210}Pb from Dutch natural gas systems (**chapter 6** of this thesis).

Stäuble, A.J. and Milius, G., 1970. Geology of Groningen gas field, Netherlands. In: M.T. Halbouty (Ed.), Geology of giant petroleum fields. AAPG Mem. 14, 359-369.

Sun, Y. and Püttmann, W., 1996. Relationship between metal enrichment and organic composition in Kupferschiefer hosting structure-controlled mineralization from Oberkatz Schwelle, Germany. Appl. Geochem. 11, 567-581.

Tunn, W., 1975. Untersuchungen über Spurenelemente in Gasen aus deutschen Erdgas- und Erdöl-Feldern. Compendium Vorträge der Haupttagung der Deutsche Mineralölwissenschaft und Kohlechemie. Deutsche Gesellschaft fur Mineralölwissenschaft, 96-111.

Van Adrichem Boogaert, H.A. and Kouwe, W.F.P., 1993. Stratigraphic nomenclature of the Netherlands, revision and update by RGD and NOGEPA. Mededelingen RGD 50.

Van Wees, J.-D., Stephenson, R.A., Ziegler, P.A., Bayer, U., McCann, T., Dadlez, R., Gaupp, R.,

Narkiewicz, M., Bitzer, F. and Scheck, M., 2000. On the origin of the Southern Permian basin, Central Europe. Marine Petr. Geol. 17, 43-59.

Van Wijhe, D.H., Lutz, M. and Kaasschieter, J.P.H., 1980. The Rotliegend in the Netherlands and its gas accumulations. Geologie en Mijnbouw 59, 3-24.

Verdier, J.P., 1996. The Rotliegend sedimentation history of the southern North Sea and adjacent countries. In: H.E. Rondeel, D.A.J. Batjes and W.H. Nieuwenhuijs (Eds.), Geology of gas and oil under the Netherlands. Kluwer Academic Publishers, Dordrecht, 45-56.

Vidal, M. and Rauret, G., 1995. Use of sequential extractions to study radionuclide behaviour in mineral and organic soils. Quimica Analitica 14, 102-107.

Walraven, N., Van Os, B.J.H., Klaver, G.T., Baker, J.H. and Vriend, S.P., 1997. Trace element concentrations and stable lead isotopes in soils as tracers of lead pollution in Graft-De Rijp, the Netherlands. J. Geochem. Expl. 59, 47-58.

Wedepohl, K.H., 1956. Untersuchungen zur Geochemie des Bleis. Geochim. Cosmochim. Acta 10, 69-148.

Wedepohl, K.H., 1964. Untersuchungen am Kupferschiefer in Nordwestdeutschland; Ein Beitrag zur Deutung der Genese bituminöser Sedimente. Geochim. Cosmochim. Acta 28, 305-364.

Wedepohl, K.H., Delevaux, M.H. and Doe, B.R., 1978. The potential source of lead in the Permian Kupferschiefer bed of Europe and some selected paleozoic mineral deposits in the Federal Republic of Germany. Contrib. Min. Pet. 65, 273-281.

Zartman, R.E. and Doe, B.R., 1981. Plumbotectonics - The model. Tectonophysics 75, 135-162.

Ziegler, P.A., 1990. Geological Atlas of Western and Central Europe. Shell Internationale Petroleum Maatschappij BV, Den Haag.

Zielinski, R.A., Bloch, S. and Walker, T.R., 1983. The mobility and distribution of heavy metals during the formation of first cycle red beds. Econ. Geol. 78, 1574-1589.

Chapter 4

Experimental determination of the solubilities of Pb and water in methane - Transport of NORM constituents in natural gas

A.P. Schmidt and Th.W. De Loos

Abstract - Presence of lead precipitates containing unsupported ^{210}Pb in gas production facilities treating only a water saturated hydrocarbon gas phase, implies significant transport of Pb in this gas phase. We have measured solubilities of water and Pb in methane in equilibrium with a saturated $PbCl_2$ solution under natural gas production conditions, using a gas saturation system with a cold trap. Pb solubilities in methane, calculated from water solubilities in methane and Pb concentrations in condensed water, range from 0.1 to 2.5 $\mu g \cdot m^{-3}$ (STP). Although Pb solubilities were difficult to reproduce because of limitations posed by the experimental set-up, Pb solubility appears to increase with increasing temperature and decreasing pressure. Actual Pb concentrations in three out of four natural gas production samples are comparable to our experimentally determined solubilities in methane, and consistent with transport of Pb as a chloride compound. High organic acid concentrations in condensed water from a fourth production sample may indicate transport of Pb as an organic compound to explain the much higher Pb concentration than allowed by the maximum solubility in the experimental system. Measured Pb solubilities in methane and actual Pb concentrations in gas production samples correspond to Pb production rates of several tenths of grams to several grams per day for gas wells producing only a water saturated hydrocarbon gas phase. These rates enable significant deposition of ^{210}Pb-bearing Naturally Occurring Radioactive Matter (NORM) in gas production facilities.

To be submitted

Introduction

Lead concentrations in water coproduced with natural gas from Dutch Rotliegend, Zechstein and Triassic reservoirs range from 0.01 to 150 $mg \cdot l^{-1}$ (Schmidt *et al.*, submitted / **Chapter 6**). During production of natural gas, presence of liquid water and dissolved Pb in production facilities may result in the deposition of metallic Pb or Pb-sulphide, galena (Kaemmel *et al.*, 1978; Kolb and Wojcik, 1985; Schmidt, 1998 / **Chapter 5**; Schmidt *et al.*, subm. / **Chapter 6**). Most metallic Pb and galena deposits from Dutch gas production facilities may be termed NORM (Naturally Occurring Radioactive Materials), since they contain significant amounts of ^{210}Pb. Because ^{210}Pb in these NORM deposits is often 'unsupported', i.e. concentrations are higher than can be explained from *in situ* decay of ^{226}Ra and ^{222}Rn, stable Pb and ^{210}Pb must be collectively transported with natural gas.

High Pb concentrations in gas production water can be encountered when reservoir brines and hydrocarbons are produced in separate phases. In such a case, stable Pb and unsupported ^{210}Pb can be transported in the water phase. Depending on gas production rates, water/gas ratios, and Pb concentrations in formation water, produced total Pb may amount to several tens of kilograms per day. Many wells, however, never produce formation water during their life-time. All water produced from such wells has been condensed from the hydrocarbon gas phase as a result of temperature decreases along the production process. Since Pb deposits containing unsupported ^{210}Pb are also found in this type of wells (Schmidt *et al.*, subm. / **Chapter 6**), significant amounts of stable Pb and unsupported ^{210}Pb must be transported in the hydrocarbon gas phase.

Transport of Pb in a hydrocarbon gas phase has only been reported by Tunn (1975), who mentioned a Pb concentration of about 1 $\mu g \cdot m^{-3}$ (STP). Vapour pressures of inorganic Pb compounds such as Pb, PbS, or $PbCl_2$ are extremely low (Hörbe und Knacke, 1955), and apparently much too low to explain such a high concentration of Pb. However, (Pb,Bi)S (canizzarite) and $PbCl_2$ (cotunnite) are well known sublimates from volcanic fumaroles (e.g. Houtermans *et al.*, 1964; Tkachenko *et al.*, 1999). Thermodynamic modelling has shown that PbS and Pb-chloride compounds can be transported at a significant scale in fumarole gases (Bernard and Le Guern, 1986; Symonds and Reed, 1993). Tunn (1975) suggested that Pb in natural gas may be organically bound, or that part or all of the Pb was transported by coproduced formation water. However, even in organic-rich sediments such as peat natural background levels of organolead compounds cannot be detected at pg/g levels (Heisterkamp and Adams, 1998), illustrating the fact that biomethylation of Pb in nature has never been proven (Van Cleuvenbergen and Adams, 1990). Also, water found by Tunn (1975) appears not to be formation water, but condensed water from the hydrocarbon gas phase.

This paper describes the experimental determination of the solubilities of Pb and water in methane gas under natural gas production conditions. Experiments have been carried out in the ternary system $PbCl_2$-H_2O-CH_4 to exclude the presence of any organolead compounds. $PbCl_2$ was chosen because in gas reservoir brines chloride is generally by far the most abundant anion (e.g., Jacobs and Marquenie, 1991; Jacobs *et al.*, 1992). Experimental solubilities and solubilities empirically derived from Dutch gas production data are used to quantitatively discuss

the transport of Pb including ^{210}Pb in a hydrocarbon gas phase.

Materials and methods

Experimental setup

The solubility of Pb in methane gas was measured using a gas saturation system (**Fig. 4.1**). This system has been especially designed for gas-liquid solubility measurements and has been described in detail elsewhere (Stevens *et al.*, 1997). High pressure methane gas from a cylinder was passed through a regulating system (R) to obtain the desired experimental pressures. When necessary, the gas was first compressed by a compressor (C) to about 50 bars above the experimental pressures and fed into an equilibrium cell (E).

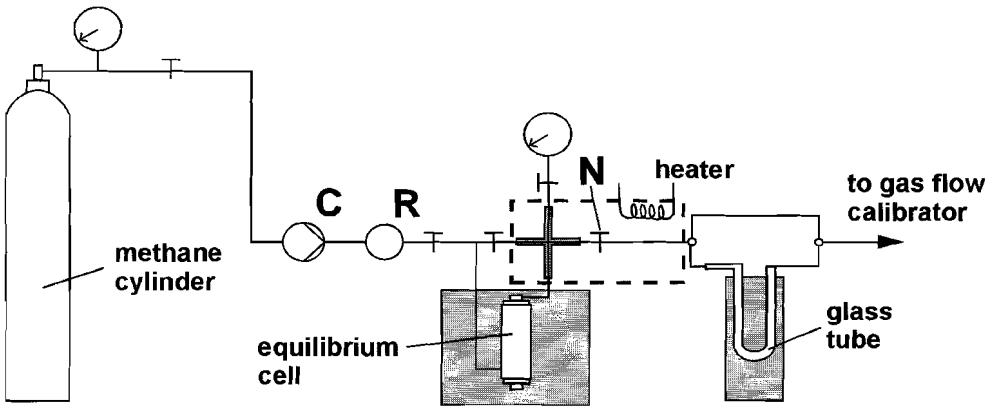

Figure 4.1 - Schematic diagram of the experimental set-up. C: compressor; R: regulating system; N: expansion valve (needle valve).

The cell was constructed of stainless steel pipe capped at each end and sealed with Viton O-rings (**Fig. 4.2**). The lower compartment of the cell was filled with approximately 32 ml of demineralized water and 3 g of $PbCl_2$, enough to maintain a saturated lead solution under all experimental conditions. The gas was dispersed by a metal sieve at the bottom of the cell and convection of the fluids around a small stainless steel open cylinder ensured saturation of the gas with the lead chloride solution. To prevent entrainment of liquid water and solid $PbCl_2$ from the cell, a demister, filled with glass wool and glass pearls, was placed in the upper compartment of the cell several centimeters above the water table. The cell was immersed in a thermostated bath. The temperature was measured by a calibrated digital Pt-100 temperature

sensor placed in the mantel of the equilibrium cell, with an accuracy of ± 0.01°C.

After leaving the equilibrium cell, the saturated gas was led to an expansion valve (needle valve N) at which the pressure was reduced to about 1 atm. The pressure in the cell was measured relative to atmospheric pressure using a Drück digital pressure indicator. During experiments, pressure was kept within ± 0.5 bar of the desired experimental pressure. After expansion, the gas was passed through a U-shaped glass tube, cooled to a constant temperature of -79°C by a mixture of solid CO_2 and ethanol. Thus, water vapour and dissolved Pb from the gas were trapped in the glass tube. Because of the extremely low solubility of water in methane gas at 1 atm and -79°C only a very small error was made. The section of tubing between the equilibrium cell and the glass tube was heated to at least 10°C above the temperature of the cell to prevent premature condensation of water.

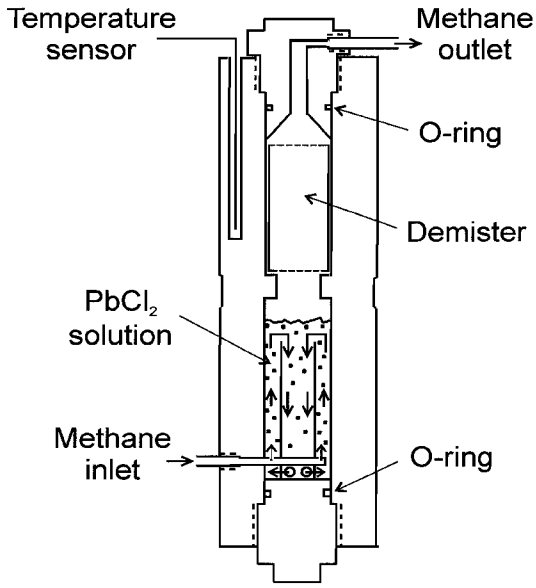

Figure 4.2 - Schematic representation of the equilibrium cell. Adapted from Stevens *et al.* (1997).

Solubility experiments

Every 1 to 3 experiments, depending on estimated water solubility of methane at chosen experimental conditions, the equilibrium cell and complete tubing between the cell and the glass tube were thoroughly cleaned with a three step treatment using water, ethanol and compressed air. Before each experiment, the glass tube was treated with an alkaline detergent solution followed by 2 M HCl. Subsequently, the tube was rinsed with water and ethanol, and dried in a stove at 110°C. Prior to the start of every experiment, gas was allowed to flow through the cell

for at least an hour to reach a steady state. The glass tube was weighed and the gas flow was led through the tube for a suitable period. Subsequently, the flow was diverted around the glass tube, which was weighed again. The amounts of condensed water varied from 250 mg to 1000 mg per experiment, weighing errors of 0.1 mg yielding a precision better than 0.1%. The water was poured into a glass vial, acidified with a few drops of ultrapur 65% HNO_3 and diluted to about 10 ml with demineralized water. Lead concentrations were analyzed with ICP-MS, using a VG Plasmaquad PQ 2+ instrument. Ten runs were measured for each sample. For mass bias correction NBS 981 standard was run after each batch of 6 samples. Precision (2σ) was better than 2%. Gas flow rates were maintained at approximately 110 ml of expanded gas per minute and measured using a Brooks Vol-U-meter calibrator with an accuracy better than 0.2%. Flow rates were normalized to STP (0°C and 1.013 bar) using laboratory barometer readings and temperature measurements of the gas made by a Pt-100 sensor inside the calibrator. Water solubilities in methane were calculated from amounts of condensed water and volumes of methane led through the glass tube. Solubilities of Pb in methane were calculated from water solubilities in methane and Pb concentrations in condensed water.

Severe corrosion of the stainless steel tubing section directly after the equilibrium cell urged replacement of this section several times in the course of the experiments. Corrosion was probably caused by cooling of tubings in between experiments, which resulted in the formation of a highly corrosive chloride-bearing water phase.

Results

Solubilities of water and Pb in methane were measured at temperatures of 80°C, 100°C, 120°C and 135°C, and at pressures of 50,100, 150 and 200 bar (gauge pressure), simulating natural gas production conditions (**Table 4.1**). Water concentrations in methane were reproducible within ± 13% for duplicate or triplicate measurements, average concentrations ranging from 5.05 $g \cdot m^{-3}$ (STP), measured at 100°C and 200 bar, to 52.90 $g \cdot m^{-3}$ (STP), measured at 135°C and 50 bar. As expected, water solubilities in methane increase with increasing temperature and decreasing pressure. Unfortunately, Pb solubilities in methane were only reproducible within one or two orders of magnitude. Measured solubilities vary from 0.016 to 2.270 $\mu g \cdot m^{-3}$ (STP) over the range of experimental conditions. Due to the low reproducibility, trends in Pb concentrations in methane with respect to temperature or pressure can only be interpreted with caution. In the following sections we will discuss these trends by careful investigation of the validity of the data.

Discussion

Validity of measured Pb solubilities in methane should first be checked by looking at the determined water solubilities. Water solubilities in methane from this study are in good agreement with experimentally determined water solubilities reported in the literature (**Fig. 4.3**).

Table 4.1 - Solubilities of water and Pb in methane.

T (°C)	Pressure (bar)	Water in gas ($g \cdot m^{-3}$, STP)	Pb in water (ppb)	Pb in gas ($\mu g \cdot m^{-3}$, STP)
80.00	50.0	7.494	7.0	0.053
80.00	50.0	7.702	< 0.1	------
100.22	50.0	19.471	15.1	0.295
100.00	50.0	16.746	35.0	0.586
100.22	100.0	8.458	48.6	0.449
100.00	100.0	9.911	5.5	0.054
100.22	150.0	6.704	32.1	0.215
100.00	150.0	7.020	6.5	0.046
100.00	200.0	5.327	41.5	0.221
100.00	200.0	4.836	25.4	0.123
120.04	50.0	34.424	31.7	1.093
120.00	50.0	32.754	0.8	0.025
120.00	50.0	28.150	10.4	0.293
120.20	101.2	17.527	56.2	1.002
120.00	100.0	18.402	32.0	0.588
120.03	100.0	17.723	< 0.1	-----
119.57	150.2	12.195	6.4	0.078
120.04	150.2	13.100	14.2	0.187
120.20	200.3	9.787	22.2	0.394
120.00	200.0	9.153	2.1	0.020
120.04	200.1	10.449	< 0.1	-----
135.00	50.0	52.044	16.6	0.864
135.00	50.0	53.626	42.3	2.270
135.00	50.0	53.023	12.3	0.650

It should be noted that solubilities by other workers (Olds *et al.*, 1942; Rigby and Prausnitz, 1968; Yarym-Agaev *et al.*, 1985; Yokoyama *et al.*, 1988) were all determined in the binary system CH_4-H_2O. However, lowering of the vapour pressure of water in our experiments due to the presence of $PbCl_2$, which has a solubility in water of about 0.18 M at 135°C (Malinin, 1957), is less than 1% and can be safely neglected. Therefore, agreement in water solubilities shows that measurements in this study have been conducted under equilibrium conditions. Errors in water solubilities, which were used to calculate Pb solubilities, can thus only explain a small part of the wide variation in Pb solubilities.

A second potential reason for large variation could be a failure of the demister in the equilibrium cell. Entrainment of tiny drops of water with the gas stream would considerably raise Pb concentrations in condensed water, without noticeably changing the amount of water trapped

in the glass tube. However, the same set-up was used successfully before at comparable flow rates (Stevens *et al.*, 1997). Moreover, a simple calculation shows that this effect would result in Pb concentrations in condensed water of several magnitudes higher than actually observed in the experiments. For instance, at 100°C water droplets with a total volume of 1 µl could have transported up to about 25 µg of Pb. On a volume of 0.25 ml of condensed water this would give a Pb concentration of 100 ppm, compared to measured concentrations of up to 56 ppb.

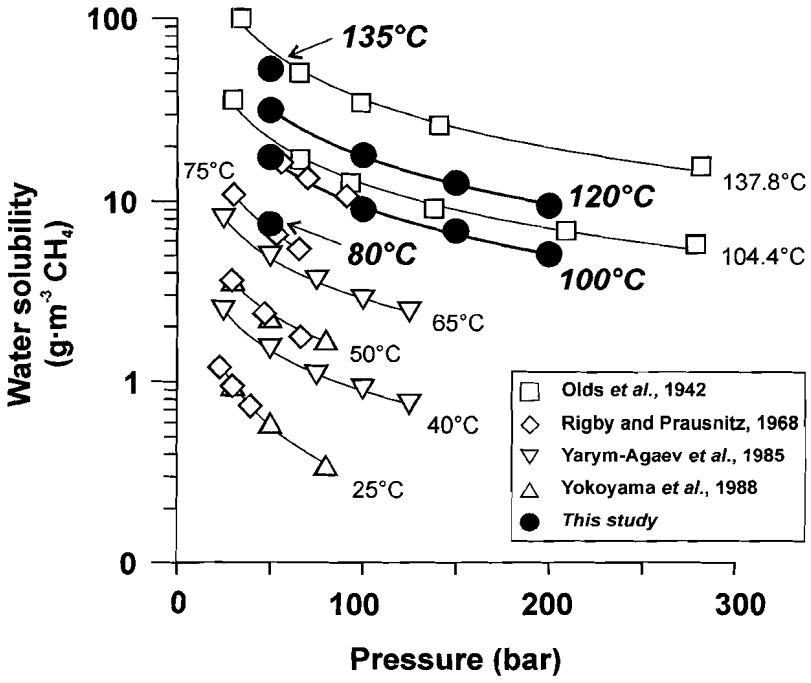

Figure 4.3 - Solubility of water in methane under natural gas production conditions.

The most likely explanation for observed variations in Pb solubilities is loss of Pb from methane gas in the first part of the glass tube. For reasons of construction, a temperature gradient from 10 to 20°C above the experimental temperature to -79°C existed over the first ten centimeters of the tube. Especially at low pressure and high temperature experiments, i.e. at high water solubilities, condensation of water from methane already started in this part of the glass tube. Early condensation of water was prevented as much as possible by manually heating this section of the set-up with a hair dryer. However, condensation could not always be

avoided, and early condensed water was re-evaporated in order to be condensed again further down the glass tube. Likely, Pb in early condensed water was not removed quantitatively in this process, and was lost by deposition onto the glass. Evidence for this explanation is provided by plots of Pb solubilities at varying temperatures and a constant pressure of 50 bar (**Fig. 4.4a**) and at varying pressures and constant temperatures of 100°C (**Fig. 4.4b**) and 120°C (**Fig. 4.4c**). Clearly, variation in Pb solubilities increases with increasing temperature and decreasing pressure, i.e. with increasing water content of methane and more chance of early condensation.

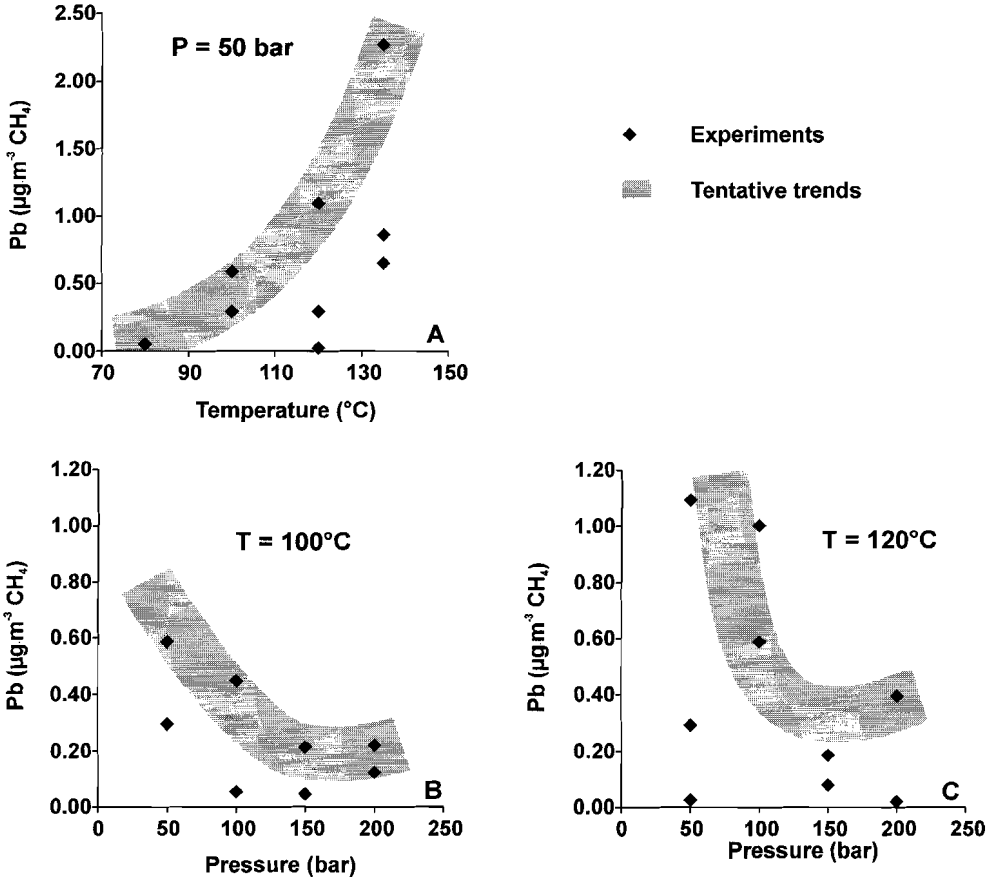

Figure 4.4 - Pb solubilities in methane and tentative trends at a pressure of 50 bar (A) and at temperatures of 100°C (B) and 120°C (C), all recalculated to STP.

Transport of Pb in natural gas

Assuming that the explanation given above is correct, the highest found Pb solubilities at certain P and T are the most reliable. Therefore, any trends in Pb solubilities over the range of investigated P and T conditions should be derived from these highest data points, although even these absolute values for solubilities are probably somewhat underestimated. At constant pressure, Pb solubility in methane tends to increase rapidly with increasing temperature (**Fig. 4.4a**). This can also be seen when trends in Pb solubilities at constant temperatures of 100°C and 120°C are compared (**Figs. 4.4b and 4.4c**). In addition, Pb solubility tends to decrease with increasing pressure, at least over the range from 50 to 150 bar. As can be expected, these trends are similar to observed trends in water solubility (**Fig. 4.3**). Of course, the presence of water vapour in methane has practically no influence on the solubility of Pb in methane, because both compounds are present in minute quantities compared to methane itself. The solubility minimum for Pb at 150 bar is rather speculative and probably non-existent. More Pb solubility data, especially at somewhat higher pressures than investigated in this study, could resolve this matter. Pressures in natural gas fields are often higher than 200 bar, but our set-up unfortunately limited the investigated range to 200 bar.

Although these trends are tentative, the data indicate that maximum amounts of Pb that could be transported with methane gas are in the order of 0.1 to 2.5 $\mu g \cdot m^{-3}$ (STP), determined at temperatures from 80°C to 135°C and pressures from 50 bar to 200 bar. Compositional differences of natural gas, which in reality also contains components such as N_2, CO_2 and higher hydrocarbons, will influence the maximum solubility of Pb. Moreover, transported amounts of Pb in natural gas will be less than according to theoretical Pb solubility, because gas reservoir brines are probably not saturated with $PbCl_2$ and deposition of Pb scales in the production facilities may have removed some of the Pb. Actual amounts of Pb that are transported in the gas phase are indicated by chemical compositions of condensed water from Dutch natural gas wells (**Table 4.2**).

Table 4.2 - Compositions of produced gas from four Dutch wells.

Formation	Zechstein	Zechstein	Upper Slochteren	Zechstein
Sampling date	06-05-1993	21-02-1994	05-03-1997	06-04-1999
Temperature (°C)	110	110	37	120
Pressure (bar)	27	59	343	200
Gas composition (%)				
CH_4	86.7	92.3	n.d.	n.d.
N_2	4.1	2.5	n.d.	n.d.
CO_2	6.5	3.1	n.d.	n.d.
H_2S	0.6	0.0	n.d.	n.d.
H_2O ($g \cdot m^{-3}$, STP)	8.7	11	0.25	10*

* Estimated from **Fig. 4.3**.

Water contents of the four gases closely agree with water solubilities in pure methane (**Fig. 4.3**). Pb contents of the gas samples, calculated from gas and condensed water compositions, are in the same order of magnitude as experimentally determined maximum solubilities, varying from 0.023 to 5.3 $\mu g \cdot m^{-3}$ (STP) (**Table 4.3**).

Table 4.3 - Condensed water composition and Pb content of natural gas from the four wells of Table 2.

Reservoir information				
Formation	Zechstein	Zechstein	Upper Slochteren	Zechstein
Sampling date	06-05-1993	21-02-1994	05-03-1997	06-04-1999
Temperature (°C)	110	110	37	120
Pressure (bar)	27	59	343	200
Condensed water composition (ppm)				
Na^+	4.2	88	410	69
K^+	< 1.0	15	640	70
Ca^{2+}	1.9	12	130	49
Mg^{2+}	1.5	3	9.8	11
Pb^{2+}	0.110	0.010	0.091	0.530
Cl^-	33	150	1170	280
Acetic acid	33	70	120	630
Propionic acid	n.d.	n.d.	46	200
*Calculated Pb content of gas ($\mu g \cdot m^{-3}$, STP)**	*0.96*	*0.11*	*0.023*	*5.3*

* calculated from H_2O content of gas (**Table 4.2**) and Pb content of condensed water.

Three of the condensed water samples fall in the P,T range of our measurements. When plotted in a diagram showing inferred Pb solubility trends, three out of four samples show Pb contents comparable to our experimentally determined Pb solubility (**Fig. 4.5**). In our experiments, Pb in the gas phase is probably present as $PbCl_{2\,(g)}$ or $PbCl_{4\,(g)}$, in analogy to Pb speciation in volcanic fumaroles of comparable temperatures (Symonds and Reed, 1993). Pb concentrations in the three production samples are therefore consistent with transport of Pb as a chloride compound. The fourth sample, however, appears to be oversaturated with Pb. High organic acid concentrations in condensed water from this sample may indicate transport of Pb as an organic compound.

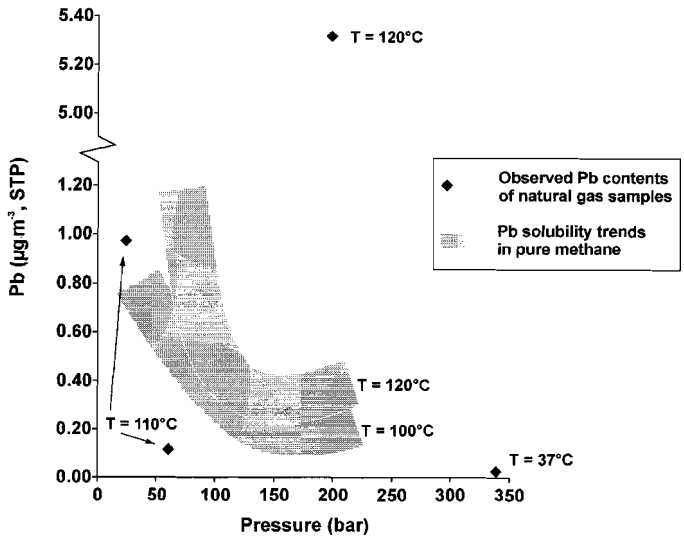

Figure 4.5 - Pb contents of Dutch natural gas samples compared to experimentally determined solubility in pure methane.

Implications for transport of NORM constituents in natural gas

As discussed in the previous section, actual concentrations of Pb transported in a hydrocarbon gas phase may amount to several $\mu g \cdot m^{-3}$ (STP). Therefore, total amounts of produced Pb in a hydrocarbon gas phase may range from several tenths of grams to several grams per day for a typical gas well with a daily production of 10^6 m^3 of gas. Clearly, these amounts are enough to enable significant deposition of metallic Pb or galena in gas production facilities on a production time scale. If ^{210}Pb is present in gas reservoir brines, ^{210}Pb can be transported together with stable Pb in the hydrocarbon gas phase. Coprecipitation of ^{210}Pb and stable Pb will then lead to the formation of NORM scales in production facilities.

Experimentally determined Pb concentrations in a hydrocarbon gas phase imply much higher vapour pressures of $PbCl_2$ than reported in literature (Hörbe and Knacke, 1955). This can be explained by the nonideal behaviour of supercritical methane, which significantly affects the solubility of heavy nonvolatile solids such as $PbCl_2$. In an ideal gas, solubility of a solid is defined as

$$y_i = \frac{P_i^{sat}(T)}{P}$$

where y_i is the mole fraction of the solid in the gas and $P_i^{sat}(T)$ is the sublimation or vapour pressure of the pure solid at the system temperature. Non-ideal behaviour of the gas is accounted for by the fugacity coefficient ϕ_i of the solid. At high pressure, the fugacity of the solid, which at low pressure is equal to P_i^{sat}, has to be corrected by the Poynting factor

$$e^{\frac{(P-P_i^{sat})V_i^{*S}}{RT}}$$

where V_i^{*S} is the molar volume of the pure solid and R the gas constant (McHugh and Krukonis, 1994). Introduction of this correction term leads to the following definition for the solubility of the solid:

$$y_i = \frac{P_i^{sat}(T) \cdot e^{\frac{(P-P_i^{sat})V_i^{*S}}{RT}}}{\phi_i \cdot P}$$

Because of these corrections, the solubility of a solid in a supercritical gas at about 50°C and 200 bar may be four to five orders of magnitude higher than in an ideal gas, as exemplified for the benzoic acid-CO_2 system by McHugh and Krukonis (1994).

Conclusions

Solubilities of Pb and water in methane have been measured in the system $PbCl_2$-CH_4-H_2O at temperatures from 80°C to 135°C and pressures from 50 bar to 200 bar, representing natural gas production conditions. Water concentrations in methane gas increase with increasing temperature and decreasing pressure, ranging from about 5 $g \cdot m^{-3}$ (STP), determined at 100°C and 200 bar, to about 53 $g \cdot m^{-3}$ (STP), determined at 135°C and 50 bar. Water solubilities are in good agreement with solubilities determined by other workers, showing that the equilibrium cell worked properly and that measurements represent equilibrium conditions.

Lead solubilities in methane were only reproducible within one or two orders of magnitude, likely because of constructional reasons causing repeated condensation and evaporation of water in the set-up. Nevertheless, accepting the limitations posed by our experimental set-up, tentative trends in Pb solubilities over the investigated temperature and pressure range could be established. Measured Pb solubilities in methane vary from 0.016 to 2.270 $\mu g \cdot m^{-3}$ (STP), solubilities increasing with increasing temperature and decreasing pressure.

Actual Pb concentrations in the hydrocarbon gas phase of four Dutch natural gas wells are comparable to experimentally determined Pb solubilities in pure methane. Water solubilities in the produced gas samples are not significantly affected by the presence of other components such as higher hydrocarbons and N_2, CO_2 and H_2S. In three out of four gas samples, Pb was probably transported as Pb-chloride compounds $PbCl_2$ and/or $PbCl_4$ in analogy to our

experiments and volcanic fumarole gases. Here, lower Pb concentrations than according to maximum solubilities could result from undersaturation of the gas reservoir brine with respect to $PbCl_2$, and/or loss of Pb from the hydrocarbon gas phase because of deposition in the production facilities before sampling of the condensed water. High concentrations of acetic and propionic acid in condensed water from a fourth gas sample may indicate transport of Pb as an organic compound to explain the Pb concentration much higher than maximum solubility in the experimental system.

Measured Pb solubilities and actual Pb concentrations in Dutch gas samples show that total amounts of Pb that can be produced with a water saturated hydrocarbon gas are in the order of several tenths of grams to several grams per day per well. These are minute quantities compared to amounts that can be produced by wells also producing reservoir formation waters. However, they enable significant deposition of metallic Pb or galena scales on a production time scale. If ^{210}Pb is present in gas reservoir brines, transport of ^{210}Pb together with stable Pb in the hydrocarbon gas phase may result in the deposition of NORM scales in production facilities.

Acknowledgement - The authors wish to thank Mr. Hans Grondel for valuable technical support and Mr. Wim Poot for general assistance with the experiments. Nederlandse Aardolie Maatschappij BV is thanked for providing chemical analyses of gases and condensed waters.

References

Bernard, A. and Le Guern, F., 1986. Condensation of volatile elements in high-temperature gases of Mount St. Helens. J. Volcan. Geotherm. Res. 28, 91-105.

Heisterkamp, M. and Adams, F.C., 1998. Simplified derivatization method for the speciation analysis of organolead compounds in water and peat samples using in-situ butylation with tetrabutylammonium tetrabutylborate and GC-MIP AES. Fres. J. Anal. Chem. 362, 489-493.

Hennet, R.J., Crerar, D.A. and Schwartz, J., 1988. Organic complexes in hydrothermal systems. Econ. Geol. 83, 742-764.

Houtermans, F.G., Eberhardt, A. and Ferrara, G., 1964. Lead of volcanic origin. In: A. Craig, S.L. Miller and G.J. Wasserburg (eds.), Isotopic and cosmic chemistry. North-Holland Publishing Company, Amsterdam, 233-243.

Hörbe, R. and Knacke, O., 1955. Zusammenstellung van Dampfdruckkurven und Erläuterung einiger Anwendungen. Erzmetall 8, 556-561.

Jacobs, R.P.W.M. and Marquenie, J.M., 1991. Produced water from gas/condensate platforms: environmental considerations. In: Proceedings of the First International Conference on Health, Safety and Environment, The Hague, The Netherlands. Society of Petroleum Engineers, 89-96.

Jacobs, R.P.W.M., Grant, R.O.H., Kwant, J., Marquenie, J.M. and Mentzer, E., 1992. The composition of produced water from Shell operated oil and gas production in the North Sea. In: J.P. Ray and F.R. Engelhart (Editors), Proceedings of the 1992 International Produced Water Conference, San Diego, California. Plenum Press, New York.

Kaemmel, T. et al., 1978. Sind $HgPb_2$ und (Hg,Pb), gebildet aus natürlichen Begleitkomponenten der Erdgase der Lagerstätten der Altmark, Minerale? Z. Angew. Geol. 24, 90-96.

Kolb, W.A. and Wojcik, M., 1985. Enhanced radioactivity due to natural oil and gas production and related radiological problems. Sci. Tot. Envir. 45, 77-84.

Lundegard, P.D. and Kharaka, Y.K., 1990. Geochemistry of organic acids in subsurface waters. In: D.C. Melchior and R.L. Bassett (Editors), Chemical modeling of aqueous systems II. ACS Symposium Series vol. 416. American Chemical Society, Washington DC, 169-189.

Malinin, S.D., 1957. The solubility of lead chloride in liquid and vapor phases of water. Geochem. 2, 69-76.

McHugh, M.A. and Krukonis, V.J., 1994. Supercritical fluid extraction: principles and practice, 2nd ed. Butterworth-Heinemann, Stoneham, MA.

Olds, R.H., Sage, B.H. and Lacey, W.N., 1942. Phase equilibria in hydrocarbon systems. Composition of the dew-point gas of the methane-water system. Ind. Eng. Chem. 34, 1223-1227.

Rigby, M. and Prausnitz, J.M., 1968. Solubility of water in compressed nitrogen, argon and methane. J. Phys. Chem. 72, 330-334.

Schmidt, A.P., 1998. Lead precipitates from natural gas production facilities. J. Geochem. Expl. 62, 193-200 (**chapter 5** of this thesis).

Schmidt, A.P., Hartog, F.A., Van Os, B.J.H. and Schuiling, R.D., submitted. Origin and deposition of stable lead and ^{210}Pb from Dutch natural gas systems (**chapter 6** of this thesis).

Stevens, R.M.M., Shen, X.M., De Loos, T.W. and De Swaan Arons, J., 1997. A new apparatus to measure the vapour-liquid equilibria of low-volatility compounds with near-critical carbon dioxide. Experimental and modelling results for carbon dioxide. J. Supercrit. Fl. 11, 1-14.

Symonds, R.B. and Reed, M.H., 1993. Calculation of multicomponent chemical equilibria in gas-solid-liquid systems: calculation methods, thermochemical data, and applications to studies of high-temperature volcanic gases with examples from Mount St. Helens. Am. J. Sci. 293, 758-864.

Tkachenko, S.I., Poorter, R.P., Korzhinskii, M.A., Van Bergen, M.J., Shmulovich, K.I. and Shteinberg, G.S., 1999. Mineral- and ore-forming processes in high-temperature fumarolic gases at Kudryavyi Volcano, Iturup island, Kuril archipelago. Geochem. Int. 37, 410-422.

Tunn, W., 1975. Untersuchungen über Spurenelemente in Gasen aus deutschen Erdgas- und Erdöl-Feldern. Compendium Vorträge der Haupttagung der Deutsche Mineralölwissenschaft und Kohlechemie. Deutsche Gesellschaft fur Mineralölwissenschaft, pp. 96-111.

Van Cleuvenbergen, R.J.A. and Adams, F.C., 1990. Organolead compounds. In: O. Hutzinger (Editor), Anthropogenic compounds. The handbook of environmental chemistry vol. 3-E. Springer verlag, Berlin.

Yarym-Agaev, N.L., Sinyavskaya, R.P., Koliushko, I.L. and Levinton, L.Y., 1985. Zh. Prikl. Khim. 58, 165-168.

Yokoyama, C., Wakana, S., Kaminishi, G. and Takahashi, S., 1988. Vapor-liquid equilibria in the methane-diethylene glycol-water system at 298.15 and 323.15 K. J. Chem. Eng. Data 33, 274-276.

Chapter 5

Lead precipitates from natural gas production facilities

Arthur P. Schmidt

Abstract - Over the last few years various Pb precipitates have been found in natural gas production facilities in the northern Netherlands and southern North Sea area during routine cleaning operations. Based on composition and morphology of these precipitates, the probable depositional processes are discussed. The lead precipitates can be divided into three categories based on morphology and composition: (1) thin crusts containing metallic Pb, barite and galena. These precipitates originate from untreated gas-water mixtures, and are found in pipes throughout production facilities; (2) annular, homogeneous precipitates of metallic Pb, formed from separated production water in pumps of production facilities; (3) suspended precipitates which are found either in the well tubing, or in pipes or valves downstream the facilities, originating from untreated gas-water mixtures. All Pb precipitates contain ^{210}Pb, whereas precipitates of both lead and barite contain ^{226}Ra as well. These Naturally Occurring Radionuclides (NORs) are most likely derived from U-enriched organic sediments or ^{226}Ra-enriched precipitates in or near the gas reservoirs.

Slightly modified from: Journal of Geochemical Exploration 62: 193-200 (1998)

Introduction

Precipitation of Pb has been reported from oil field brines in the USA, gas field brines in Germany and geothermal brines in the former Soviet Union. In Central Mississippi, well scale in tubing from two oil fields consisted of concentric rings of platy barite with an aggregate thickness of 3 mm, accompanied by grains of galena up to 20 µm in diameter. In one of the fields also discontinuous rings of metallic lead, up to 0.2 mm thick, were present. Well scale in a third field consisted almost entirely of metallic Pb, containing small angular fragments of steel (Carpenter *et al.*, 1974). In the Altmark region of East Germany, crusts of metallic Pb and Pb-mercury compounds (mm to cm size) have been discovered in both well tubing and surface installations of Rotliegend gas fields (Kaemmel *et al.*, 1978). In the Cheleken geothermal field, crusts of metallic Pb (1 to 5 mm thick) have been found on the inner surface of tubings over lengths of hundreds of metres. In addition, aggregates of clay and sand, cemented by metallic Pb, have been discovered around the perforation intervals. In some wells, Pb concentrations of 25 $mg \cdot l^{-1}$ at a depth of 1,450 metres had decreased to 3 $mg \cdot l^{-1}$ at the well head (Lebedev, 1972). In the same field, precipitation of laurionite (Pb(OH)Cl) has been reported in chloride solutions as a result of the mixing of metalliferous brines with alkaline Na-Cl-HCO_3-waters (Abramova and Zholnerovich, 1989). Laurionite precipitation has also been reported as a result of partial hydrolysis of chloride complexes of Pb, where brines were being discharged from Pliocene red bed strata in the upper part of the Cheleken anticline (Lebedev, 1983).

Recently, various Pb precipitates have been found in natural gas production facilities in the northern Netherlands and southern North Sea area. The presence of Pb in natural gas was first mentioned twenty years ago, when Tunn (1975) reported an average concentration of $1 \mu g \cdot m^{-3}$ (15° C, 1 atm) Pb in natural gas from northwest Germany. He suggested (1) that the Pb was derived from Pb-bearing reservoir rocks, and (2) that the Pb was either organically complexed in the gas, or brought to the surface with coproduced formation water. Kaemmel *et al.* (1978) made the same suggestions in order to explain the presence of metallic Pb scales in natural gas production facilities.

Very limited attention has been paid to the occurrence of Pb in natural gas. However, precipitation of Pb in natural gas production installations may cause serious problems. Each year, scale precipitation costs operators millions of dollars in maintenance, treatment, and lost production (Ford *et al.*, 1996). This report presents the first results from a study of Pb precipitates from gas production installations, and discusses the deposition processes. Knowledge of mobilisation, transport and deposition processes should ultimately lead to the development of geochemical engineering techniques preventing the precipitation of Pb in installations.

Sample description and analytical methods

Several types of precipitates were collected from six natural gas production facilities during routine cleaning operations in 1995 and 1996 (**Table 5.1**). In most facilities, produced gas is

obtained from the Rotliegend Formation. At location A, however, produced gas stems from Zechstein formations, at location E from reservoirs of Triassic age.

Table 5.1 - Lead precipitates from natural gas production facilities.

Sample No.	Sample type	Point of collection*	Location
1st category			
1	Thin metallic crust	Outlet waterbath heater	A
2-4	Thin metallic crusts	Inlet gas-water separator	A
5	Thin metallic crust	Inlet production manifold	A
2nd category			
6	Annular precipitate	Valve of re-injection pump	B
3rd category			
7	Unattached particles	Production water drain	C
8	Unattached particles	Flow control valve	D
9	Unattached particles	Tubing at perforation depth	E
10-11	Suspended solids	Production water filter	B
12	Reservoir material	Tubing at perforation depth	F

* see **Fig. 6.3** for explanation

The examined Pb precipitates can be divided into three categories, based on morphology, origin and provenance. The first category contains thin crusts which originate from gas-water mixtures, and which are found in pipes throughout the production facilities. Samples 1 to 5 can be classified in this category. They are brown to grey, metallic crusts (0.5 - 1 mm thick) that were taken from the inside of pipes at the inlet of the production manifold, at the outlet of the waterbath heater, and at the inlet of the gas-water separator (**Fig. 6.3**). Sample 6 forms the second category, which comprises annular precipitates that are formed from separated production water in pumps of production facilities. This sample is a grey, ring-shaped, metallic deposit (1 cm thick) which was found in the kill pump that was used to re-inject production water into the subsurface. The third category consists of unattached particles which are found either in the well tubing, or in pipes or valves downstream the facilities. Like the precipitates of the first category, they originate from gas-water mixtures. Samples 7 to 12 belong to this category. Precipitates 7, 8 and 9 are grey, metallic lumps of several cm in size. Sample 7 was found in a production water drain, sample 8 (21.33 g) was found stuck in a valve near the inlet of the gas-water separator, and sample 9 (1.5 kg) was removed from the well tubing at perforation depth. Samples 10 to 12 consist of small grains of coproduced reservoir material. Samples 10 and 11 are suspended solids, obtained from production water prior to re-injection on two consecutive days. Sample 10 was split into sieve-fractions from 45 µm to 850 µm. Sample 12, finally, was removed from the well tubing. This sample was also split into a number of sieve-fractions, of which fractions < 0.15 mm and 0.15 - 0.425 mm were studied.

In this study, mineralogy, bulk chemical composition and γ-ray activity of the samples were determined, together with compositions of individual phases in the samples. Qualitative X-ray diffraction analysis (XRD) was used to identify the mineralogy of the samples. Samples were

ground before XRD analysis, except for sample 6 from the second category and samples 7 and 9 from the third category. These samples could not be ground, and instead a polished surface was analysed by XRD. All samples were studied using scanning electron microscopy or electron microprobe analysis (SEM/EPMA). Samples 6, 7 and 9 were analysed in thin section, while the other samples were cemented onto aluminium mounts with a carbon adhesive, and coated with carbon prior to microprobe analysis. Inductively coupled plasma - mass spectroscopy (ICP-MS) and X-ray fluorescence spectrometry (XRF) were used to determine the amount of some selected elements in samples 2 through 8. All samples were analysed for Naturally Occurring Radionuclides (NORs), using standard γ-ray spectroscopy techniques (Knaepen *et al.*, 1995).

Results

The thin crusts all consist largely of Fe (**Table 5.2**), with Ba, Sr, S, Pb and Zn being the other major elements. Mineralogically the samples contain barite, galena and metallic Pb, adhering to an Fe-rich substrate. This subsurface probably consists of Fe-oxides from the inside of the pipes, which were in poor condition at the time of sampling. Small amounts of Pb-oxides, chloride salts and Pb-bearing calcite cover some samples, but no Zn-bearing minerals could be detected by XRD or microprobe analysis.

Table 5.2 - XRF and ICP-MS analyses of some selected elements in Pb precipitates (wt%).

Sample no.	Pb	Ba	Sr	S	Zn	Hg	Fe	Na	Al	Cl	Ca	Si	Total
2[a]	8.0	3.6	1.2	1.2	4.0	n.d.	17	n.d.	n.d.	n.d.	1.2	n.d.	35.7
3[a]	0.3	1.5	0.5	3.9	0.8	0.6	58	<0.5	<0.5	<0.5	1.0	<0.5	68.6
4[a]	10	12	4.6	5.4	2.5	0.03	34	<0.5	<0.5	<0.5	0.9	<0.5	71.4
5[a]	1.4	21	9.0	6.0	3.8	0.02	27	<0.5	0.6	0.8	1.2	<0.5	31.8
6[a]	93	n.d.	n.d.	n.d.	n.d.	n.d.	2.0	0.6	0.5	10	<1.0[b]	10.0	96.1
7[a]	48	n.d.	n.d.	0.4	0.5	n.d.	5.1	0.5	<1.0[b]	7.3	3.0	3.9	68.7
8[a]	85	<1.0[b]	n.d.	n.d.	n.d.	1.0	<1.0[b]	1.0	<1.0[b]	1.0	3.0	1.0	95.0

[a] XRF; [b] ICP-MS; n.d.: not detemined

Although all five samples are mineralogically similar, they are morphologically quite different. For instance, in sample 3, only a few particles of barite and galena (1-12 μm) are detectable on the Fe-oxide substrate. In sample 4, on the other hand, the substrate is covered with 1-10 μm size crystals of metallic Pb, Pb-oxides, galena and barite, and occasionally a larger particle of metallic Pb (up to 60 μm). Sample 2 shows a surface of platy and round Pb minerals (metallic Pb and Pb-oxides, 30 μm in diameter), with traces of Pb, Ca, Fe and Zn in the 'matrix' between the Pb minerals (**Micrograph 1**). The surface of sample 5 is composed of a random, wavy pattern of platey barite crystals (10-30 μm), with only a few 1 μm particles of metallic Pb on and

between the barite plates. In sample 1, finally, the rusty substrate is covered with 10-20 µm sized crystals of barite and some 1-10 µm sized Pb minerals. The presence of galena in samples 2 and 5, although revealed by XRD, was not confirmed by EPMA.

Micrograph 1 - Sample 2: Platy crystals of metallic Pb and Pb-oxides, stacked on an (invisible) substratum of rust. The fine crystalline matrix between the crystals contains Pb, Ca, Fe and Zn.

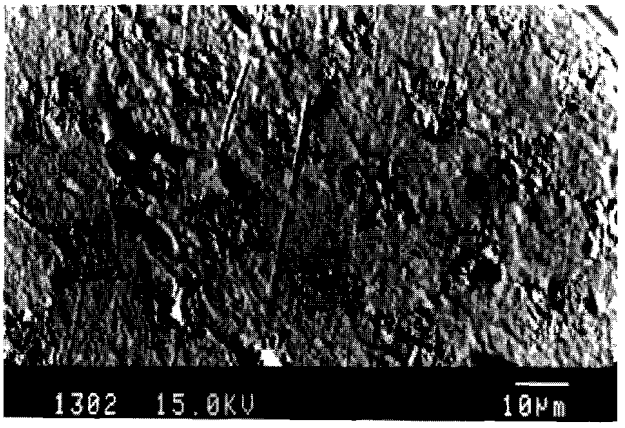

Micrograph 2 - Thin section of sample 6: A solid, homogeneous precipitate of metallic Pb, with some surface irregularities and inclusions of quartz and metallic iron particles. The grooves on the surface were caused by polishing the thin section with diamond paste in order to remove Pb-oxides.

Sample 6, the annular precipitate, is a homogeneous piece of metallic Pb (98 wt% Pb), with an outer layer of Pb-oxides (70-90 wt% Pb) and minor inclusions of organic material, Fe, Al and Cr, resulting in an overall Pb content of 93 wt%. **Micrograph 2** shows a polished cross section of the sample, with some surface irregularities and inclusions of quartz and metallic iron particles.

The suspended precipitates show a wide range of compositions and morphologies. Precipitate 7 is composed of about 65 wt% laurionite and 10 wt% calcite; no other crystalline

phases could be detected. Sample 8, on the other hand, shows the same composition and morphology as the annular precipitate. Small sand and clay particles have been trapped in the sample, together with earth alkaline compounds, some Fe-oxide and Hg. Sample 9, which at first glance looks very much like samples 6 and 8, is actually a porous aggregate of 0.2 - 20 mm sized clumps (**Micrograph 3**), consisting of 5-20 µm sized quartz and feldspar grains, cemented by metallic Pb (**Micrograph 4**).

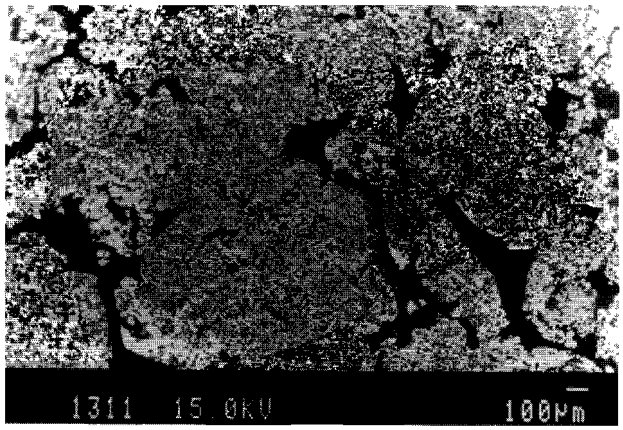

Micrograph 3 - Thin section of sample no. 9, showing a porous aggregate of 0.2 - 20 mm sized clumps, consisting of dark grains of reservoir material, cemented by white metallic Pb.

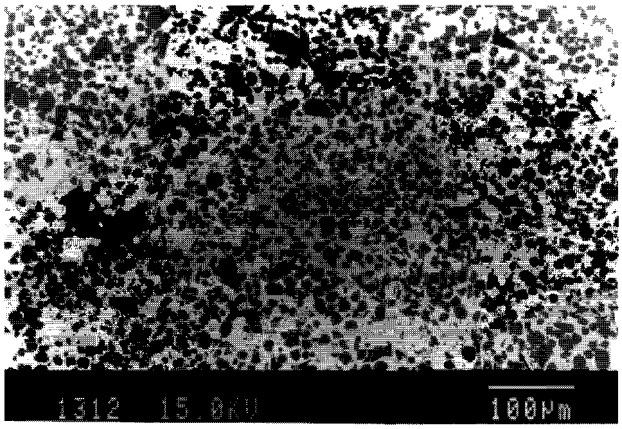

Micrograph 4 - Thin section of sample 9, showing dark grains of reservoir material cemented by white metallic Pb.

Samples 10, 11 and 12, finally, are very much alike, and consist of coproduced reservoir material, covered with a layer of precipitated crystals. Substantial amounts of metallic Pb, massicot (PbO), galena and hydrocerussite ($Pb_3(CO_3)_2(OH)_2$) occur in the larger sieve-fractions of sample 10, but the smaller fractions mainly consist of quartz and feldspar. **Micrograph 5** of

the 150 - 212 µm fraction reveals grains of quartz and feldspar, coated with 1-20 µm Pb minerals, some organic matter and a few particles of metallic iron and calcite. Sample 11, as expected, shows the same mineralogy and morphology as the combined sieve-fractions of sample 10. The fraction < 0.150 mm of sample 12 is mainly composed of quartz, calcite and galena. Respective volume percentages of 70, 30 and 1 for these compounds were estimated from SEM images. Accessory minerals are feldspar, sphalerite, barite, zircon and sylvite (NaCl). Calcite and quartz also form the main components of the fraction 0.150 - 0.425 mm. These grains are covered with small crystals of galena, metallic iron and calcite.

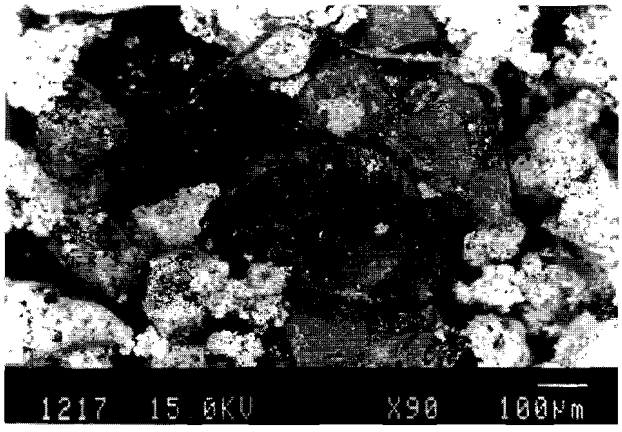

Micrograph 5 - Sample 10, consisting of suspended solids (150-212 µm sieve-fraction) obtained from production water. The grains of coproduced reservoir material are coated with metallic Pb, Pb-oxides and galena (white minerals), and some black organic matter (central grain).

Table 5.3 - NOR specific activities of Pb precipitates.

Sample no.	^{226}Ra (Bq·g^{-1})	^{210}Pb (Bq·g^{-1})
1	1500	380
2	600	620
3	200	50
4	2200	1370
5	2850	770
6	0.09 ± 0.02	288 ± 30
7	b.d.	860 ± 20
8	b.d.	950 ± 100
9	< 0.83	1590 ± 20
11	0.34 ± 0.03	271 ± 30
12 (< 150 µm)	1.67	217.5
12 (150 - 425 µm)	0.63	58.1

Interestingly, all samples contain Naturally Occurring Radionuclides (NORs) from the ^{238}U decay series (**Table 5.3**). The crustal precipitates show high γ-ray activities of both ^{210}Pb and ^{226}Ra, the other samples only show ^{210}Pb activities. Specific activities of ^{226}Ra range from 200 to 2850 $Bq \cdot g^{-1}$, which equals concentrations of 5.5 to 78 ppb. Pb-210 specific activities vary from 50 to 1590 $Bq \cdot g^{-1}$, equalling concentrations of 0.02 to 0.56 ppb.

Discussion and conclusions

Deposition processes

Most samples contain Pb-oxides, such as massicot or hydrocerussite. Since these compounds are typical weathering products of metallic Pb (Lin, 1996), they are probably caused by exposure of the precipitates to air during and after sampling. Only one sample (no. 7) contains laurionite, which is another corrosion product of metallic Pb (Aoyama, 1963). This compound is probably the result of a reaction between a metallic Pb precipitate and a combination of seawater and steam, used in a cleaning operation immediately before the sample was taken. Therefore, it is most likely that only three minerals originally precipitated in the production facilities: metallic Pb, barite and galena.

According to Carpenter *et al.* (1974), a reaction which probably causes the precipitation of metallic Pb from oil field brines is the oxidation of metallic iron from the facilities:

$$Pb^{2-} + Fe_{(metal)} \rightarrow Pb_{(s)} + Fe^{2+}$$

The same reaction has been proposed to explain the occurrence of metallic Pb scales in natural gas production facilities in Germany (Kaemmel *et al.*, 1978). Dissolution of Fe from the facilities is a matter of corrosion (Kharaka *et al.*, 1980), while Pb^{2+} can be precipitated from both condensed equilibrium water of the gas and coproduced formation water. Interestingly, the precipitation of metallic Pb scale in Central Mississippi well tubing is restricted to those wells which use pumps for the production of fluids (Carpenter *et al.*, 1974). Barite precipitation in the installations is probably related to the cooling of the condensed equilibrium water or the coproduced formation water as the gas rises to the surface, whereby $NaSO_4^-$ and $BaCl^+$ ions dissociate to form barite (e.g. Carpenter *et al.*, 1974):

$$NaSO_4^- + BaCl^+ \rightarrow BaSO_4 + Na^+ + Cl^-$$

Finally, precipitation of galena will occur if both Pb^{2+} and sulphide are present in the water or gas-water mixture.

A few remarks may be made about the conditions favouring the formation of the three types of precipitates. First, in this study, the thin crusts are restricted to one production facility. However, they are very similar to some of the scales reported from Germany, Central Mississippi and Cheleken, and are likely to be found in many more natural gas production facilities. Second, the annular metallic Pb precipitate was found in a pump used for brine disposal, which was also the case for metallic Pb scale in the Central Mississippi Raleigh field

(Carpenter *et al.*, 1974). Turbulence and pressure differences or intense corrosion caused by pumps seem to be important for the deposition of this kind of precipitates. Third, the suspended precipitates have probably been formed in the immediate vicinity of the perforations. Upon entering the well through these perforations, the gas is subjected to changes in pressure and temperature conditions, which could trigger precipitation of scale minerals. While some of the precipitates adhere to the well tubing, other precipitates are transported with the gas-water mixture into the surface facilities. Precipitation during transport of the fluids into the surface facilities is not likely to occur, because of the short residence times of the fluids in the facilities.

Naturally Occurring Radionuclides

An important question is the origin of the NORs incorporated in the examined precipitates. All Pb precipitates analysed in this study show γ-ray activities of ^{210}Pb, while the precipitates from location A, which include barite as well, show activities of both ^{210}Pb and ^{226}Ra (**Table 5.3**). Lead precipitates containing ^{210}Pb have never been reported, but barite scale containing ^{226}Ra is a common phenomenon in the oil and gas industry (e.g., Smith, 1987; Bassignani *et al.*, 1991; Ford *et al.*, 1996). Because of its chemical similarity to Ca, Ba and Sr, Ra is easily incorporated in barite. The sources of ^{226}Ra and ^{210}Pb in the examined precipitates must be looked for in or near the respective gas reservoirs (Smith, 1987). Uranium-enriched shales or coal measures are the most likely candidates (Smith, 1987), but ^{226}Ra-enriched precipitates in productive horizons may be important as well for ^{210}Pb (Lehnert and Just, 1979). Release of ^{226}Ra, ^{222}Rn and ^{210}Pb from these sources may lead to the accumulation of ^{226}Ra and ^{210}Pb in the precipitates formed in the production facilities.

Acknowledgement - The author would like to thank Dr. Sieger van der Laan for critically reading the manuscript and providing helpful suggestions.

References

Abramova, E.V. and Zholnerovich, V.A., 1989. Crystallization conditions of oxychlorides of copper and lead from thermal waters of the Cheleken Peninsula. Litol. Polezn. Iskop. 4, 123-130.

Aoyama, Y., 1963. The analysis of corrosion products by physical methods. Sci. Papers I.P.C.R. 57, 176-194.

Bassignani, A., Di Luise, G., Fenzi, A. and Finazzi, P.B., 1991. Radioactive scales in oil and gas production centers. In: Proc. 1st Int. Conference on Health, Safety and Environment, The Hague, 1991, v. 2. Society of Petroleum Engineers, The Hague, pp. 527-537.

Carpenter, A.B., Trout, M.L. and Pickett, E.E., 1974. Preliminary report on the origin and chemical evolution of lead- and zinc-rich oilfield brines in Central Mississippi. Econ. Geol. 69, 1191-1206.

Ford, W.G.F., Gadeken, L.L., Callahan, T.J. and Jackson, D., 1996. Solvent removes downhole NORM-contaminated $BaSO_4$ scale. Oil & Gas J. 94, 65-68.

Kaemmel, T., Müller, E.P., Krossner, L., Nebel, J., Unger, H. and Ungethüm, H., 1978. Sind $HgPb_2$ und (Hg, Pb), gebildet aus natürlichen Begleitkomponenten der Erdgase der Lagerstätten der Altmark, Minerale? Z. Angew. Geol. 24, 90-96.

Kharaka, Y.K., Lico, M.S. and Carothers, W.W., 1980. Predicted corrosion and scale-formation properties of geopressured geothermal waters from the northern Gulf of Mexico basin. J. Petrol. Techn. 32, 319-324.

Knaepen, W.A.I., Bergwerf, W., Lancee, P.J.F., Van Dijk, W., Jansen, J.F.W., Janssen, R.G.C., Kiezenberg, W.H.T., Van Sluijs, R., Tijsmans, M.H., Volkers, K.J. and Voors, P.I., 1995. State-of-the-art of NORM nuclide determination in samples from oil and gas production: Validation of potential standardization methods through an interlaboratory test programme. J.Radioanal. Nucl. Chem. 198, 323-341.

Lebedev, L.M., 1972. Minerals of contemporary hydrotherms of Cheleken. Geochem. Intern. 9, 485-504.

Lebedev, L.M., 1983. Cheleken hydrothermal system - a natural mineral-forming laboratory. Izv. Akad. Nauk SSSR, Ser. Geol. 7, 60-75.

Lehnert, K. and Just, G., 1979. Sekundäre Gammastrahlungsanomalien in Erdgasforder-sonden. Z. geol. Wiss. 7, 503-511.

Lin, Z., 1996. Secondary mineral phases of metallic lead in soils of shooting ranges from Orebro County, Sweden. Environm. Geol. 27, 370-375.

Smith, A.L., 1987. Radioactive-scale formation. J. Petr. Techn. 39, 697-706.

Tunn, W., 1975. Untersuchungen über Spurenelemente in Gasen aus deutschen Erdgas- und Erdöl-Feldern. In: Compendium Vorträge der Haupttagung der Deutsche Mineralölwissen-schaft und Kohlechemie. Deutsche Gesellschaft für Mineralölwissenschaft, 96-111.

Chapter 6

Origin and deposition of stable lead and ^{210}Pb from Dutch natural gas systems

Arthur P. Schmidt, F.A. Hartog, B.J.H. van Os and R.D. Schuiling

Abstract - Lead precipitates from gas production facilities in the Netherlands have been found to occur in three morphological types: thin crusts, annular precipitates, and unattached particles. Natural gas in the facilities is produced from Permian (Rotliegend and Zechstein) and Triassic reservoirs. The scales have lead concentrations of up to 93 wt%, and are primarily deposited as metallic lead and galena. Deposition of metallic lead is an electrochemical process associated with corrosion of steel, while deposition of galena is caused by supersaturation of the production fluids during gas production. All scales contain ^{210}Pb from the ^{238}U decay series. In most scales ^{210}Pb is almost completely unsupported by its radiogenic ancestors, implying direct transport of ^{210}Pb into production facilities followed by coprecipitation with stable lead in scales. ^{210}Pb is derived from U-enriched sediments within or near the productive horizons of the gas fields. Stable lead isotope ratios of the scales are in fact isotope ratios of the Permian and Triassic gas reservoir brines. The brines show model ages between 300 and 125 Ma. In Rotliegend reservoir brines, current lead isotope ratios result from the mixing of lead from at least three sources. Lead with a Late Carboniferous signature was derived from the dissolution of feldspars in Rotliegend sediments. Isotopically younger lead was already present in the Rotliegend pore waters and/or added by influx of Zechstein brines into Rotliegend gas reservoir sediments. In Triassic reservoirs, lead is mainly derived from the Triassic sediments themselves.

Submitted

Introduction

Precipitation of minerals from fluids is a common phenomenon in natural environments, and often a response to sudden changes in temperature and pressure conditions of a system. High pressure and temperature brines, for instance brines co-produced with hydrocarbons from oil and gas reservoirs, quickly become supersaturated when released to the earth's surface through artificial wells. During oil and gas production, the sudden decrease of temperature and pressure lowers the solubility of both solids and gases in the brines, which may cause precipitation of salts and metals throughout the production facilities. Common oil and gas field deposits are sulphates and carbonates of the alkaline-earth metals (e.g. Testa *et al.*, 1994).

Deposition of lead from natural brine systems has been reported from a number of settings. For instance, water production installations from the Cheleken Geothermal Field contained scales of metallic lead and laurionite (Pb(OH)Cl) (Lebedev, 1972; 1983), whereas galena (PbS) was found in a geothermal plant on the isle of Milos, Greece (Karabelas *et al.*, 1989). Only limited information on this subject has been reported by the oil and gas production industry. Precipitates from oil production installations in Central Mississippi consisted of galena and metallic lead (Carpenter, 1974). Metallic lead and lead-mercury amalgams have been found in an East German natural gas production installation (Kaemmel *et al.*, 1978), while metallic lead and galena were reported from North German gas installations (Kolb and Wojcik, 1985). The latter scales also showed increased activity concentrations of ^{210}Pb, from the ^{238}U natural decay series.

In the oil and gas industry, scales containing NORs (Naturally Occurring Radionuclides) are a well-known phenomenon. Especially scales containing ^{226}Ra from the ^{238}U natural decay series and ^{228}Ra from the ^{232}Th natural decay series are common and their origin is fairly well understood (e.g. Lysebo and Strand, 1997; Rood *et al.*, 1998). In contrast, little attention has been paid to lead-bearing scales containing ^{210}Pb from the ^{238}U natural decay series, and knowledge of these scales is still poor (Hartog *et al.*, 1995; 1996).

Geochemistry of lead in Dutch natural gas reservoir brines

Produced waters from Dutch North Sea gas fields are primarily acidic mixtures of very saline formation waters and fresh condensed water (Jacobs *et al.*, 1992), and the same holds for Dutch onshore gas fields. Lead concentrations in produced waters generally vary from 0.01 to 150 $mg.l^{-1}$ (F.A. Hartog, unpubl.). Chloride concentrations range from about 80 $mg.l^{-1}$ in condensed water to 189,000 $mg.l^{-1}$ in almost pure formation waters (Jacobs and Marquenie, 1991). Calculations show that in such brines over 85% of the dissolved Pb is complexed by chloride, and up to 6% of the Pb may be complexed by organic acid anions (Giordano and Kharaka, 1994), which are derived from the maturation of kerogen (e.g. Eglinton *et al.*, 1987). Complexation of lead by organic acid anions becomes more important with increasing acid anion concentration, and decreasing chloride concentration and temperature. In a slightly acidic, 18,000 $mg.l^{-1}$ Cl^- solution at 50°C, Pb complexation by acetate is more important than

complexation by chloride at concentrations of over 600 mg.l^{-1} acetate (Hennet *et al.*, 1988). Concentrations of organic acid anions in formation waters may reach 5,000 mg.l^{-} or more, especially between 80°C and 120°C, where acetate is usually the dominant organic acid anion (Lundegard and Kharaka, 1990). In 1989 Dutch offshore gas production waters showed an average concentration of 227 mg.l^{-1} of organic acid anions, of which 70 to 94% consisted of acetate (Jacobs *et al.*, 1992). Lead-sulphide complexes are only important at very low total Pb concentrations, in the order of 0.04 mg.l^{-1} (Kharaka *et al.*, 1987), or in H_2S saturated solutions (Nriagu, 1971).

Origin of Pb in Dutch natural gas reservoir brines

According to Carpenter (1989), high metal concentrations in Rotliegend brines are typical of brines associated with red beds and hydrocarbons such as in the Mississippi Salt Basin. He suggested that the lead and zinc in these brines were leached from poorly crystalline ferric iron oxides in the Rotliegend sediments (Carpenter, 1989). However, Hallager *et al.* (1991) argued that most of the base metals in Rotliegend brines were derived from smectitic clays rather than iron oxides. During compaction of the Rotliegend sediments, the diagenetic transition of smectites to illites released the metals into the pore waters. Finally, several studies suggest that lead in formation brines is derived from feldspars, which are important Pb-bearing minerals in clastic sediments. For instance, lead in Californian Salton Sea brines was probably mobilised during recrystallization of sediments, and especially feldspars, in the geothermal reservoir (Doe *et al.*, 1966; White, 1981). Rothbard (1982) reported destruction of detrital and authigenic K-feldspar prior to coprecipitation of kaolinite and galena in the aquifer unit for the southeast Missouri Pb district. Feldspar dissolution is a common feature in Dutch onshore Rotliegend sediments, together with diagenetic growth of illite and kaolinite (Lee *et al.*, 1989). Large scale feldspar dissolution and growth of kaolinite was also reported from the near-shore Dutch Rotliegend gas fields of Ameland (Crouch *et al.*, 1996) and the Broad Fourteens Basin (Lanson *et al.*, 1996). Feldspar dissolution and replacement by kaolinite and quartz probably occurred because of migration of acidic water from the Carboniferous Coal Measures into the overlying Rotliegend reservoir sediments (Gaupp *et al.*, 1993; Lanson *et al.*, 1996).

Lee *et al.* (1989) found indications for large scale groundwater movements in Dutch Rotliegend reservoirs between 200 Ma and 100 Ma. Initial formation waters had a large meteoric component, but around 150 Ma the formation waters had become enriched in ^{18}O, either because of fluids migrating into the Rotliegend together with natural gas, or because of brines from overlying Zechstein evaporites (Lee *et al.*, 1989). More recently, Lanson *et al.* (1996) showed that from deposition time (~275 Ma) to the Kimmerian orogeny (~155 Ma), Dutch Rotliegend sediments were penetrated by fluids from the Carboniferous Coal Measures. During and after the Kimmerian orogeny, influx of fluids from the overlying Zechstein Formation became important. Carpenter (1989) suggested that lead mobilized from Rotliegend sediments in the northeastern Netherlands contributed to deposition of large amounts of lead in the Kupferschiefer. However, there is an ongoing debate whether the Kupferschiefer was

mineralized during its deposition or by Rotliegend brines during late diagenesis (e.g. Cathles III *et al.*, 1993).

This paper presents detailed investigations on a large number of lead precipitates from Dutch natural gas production installations. Gas treated in these installations is derived from reservoirs producing either gas with free liquid reservoir brine or gas that is only saturated with water vapour. Investigations include mineralogy, lead isotopy, physical and chemical conditions for precipitation of the scales, and conditions for coprecipitation of NORs. Preliminary results on the characterization and deposition of some of the scales have been reported earlier (Schmidt, 1998 / **Chapter 5**). This study is focussed on the deposition mechanisms of Pb scales in natural gas production installations, and on the origin of stable lead and coprecipitated ^{210}Pb.

Sampling and methods

Sample description

Thirty-five scale samples were collected from ten natural gas production installations (locations A-J) in the onshore and offshore Netherlands during routine maintenance operations between 1993 and 1998 (**Table 6.1**). Natural gas fields are all situated in the Rotliegend desert area south of the desert lake margin (**Fig. 6.1**). Scales were taken from both surface facilities and downhole installation parts.

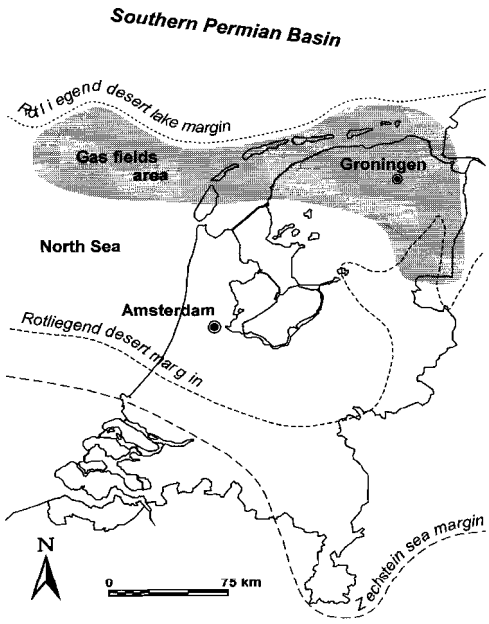

Figure 6.1 - Permian palaeogeographical map (after Ziegler, 1990; McCann, 1998) showing the area in which the sampled production installations onshore and offshore the Netherlands are situated.

Natural gas in these fields is produced from Permian or Triassic reservoir formations (**Fig. 6.2**). Three of the scales were still attached to the original steel installation parts that were replaced during the maintenance operations at locations F,G and I. No special care was taken for sample preservation, and some samples were analysed several years after being collected. Finally, a production water sample was taken from the water drain of installation B and stored in a plastic container after immediate dilution.

Table 6.1 - Lead precipitates from natural gas production facilities.

Sample no.	Location	Sampling point	Producing Member
Thin crusts			
1-3	A	Inlet production manifold	Z2 Carbonate
4	A	Inlet waterbath heater	Z2 Carbonate
5-6	A	Outlet waterbath heater	Z2 Carbonate
7-13	A	Inlet gas-water separator	Z2 Carbonate
14-17	A	Top separator	Z2 Carbonate
18-20	A	Outlet separator	Z2 Carbonate
21	F	Tubing	Slochteren
22	G	Outlet production manifold	Z2 Carbonate
Annular precipitates			
23	B	Flow control valve	Upper Slochteren
24	B	Water injection pump	Upper Slochteren
25	E	Tubing	Upper Volpriehausen Sandstone Detfurth Sandstone Basal Solling Sandstone
26	H	Tubing	Ten Boer Upper Slochteren
27	J	Outlet separator	Upper Slochteren
Unattached particles			
28	B	Production water filter	Upper Slochteren
29	B	Production water filter	Upper Slochteren
30	C	Gas-water separator	Upper Slochteren
31	D	Flow control valve	Upper Slochteren
32	F	Tubing, bottom of well	Slochteren
Scale covered steel installation parts			
33	F	Tubing	Slochteren
34	G	Outlet production manifold	Z2 Carbonate
35	I	Tubing	Upper Slochteren
Production brine			
36	B	Production water filter	Upper Slochteren

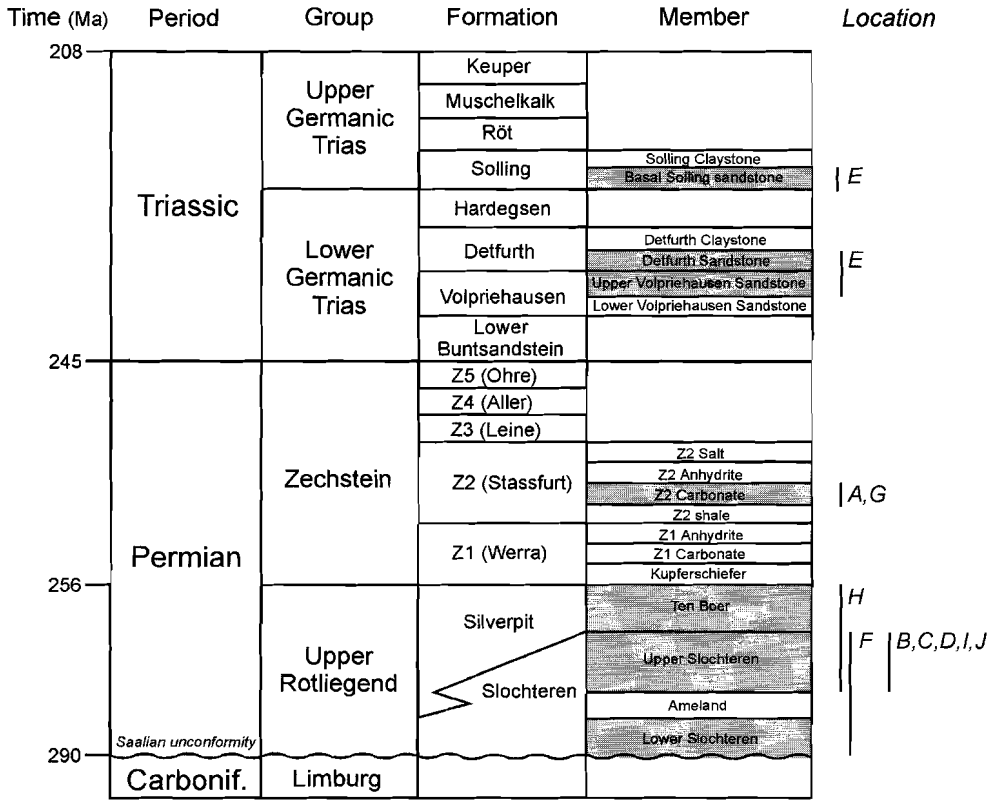

Figure 6.2 - Simplified stratigraphy of the reservoir formations from which gas is produced at the ten sampled facilities (after Van Adrichem Boogaert and Kouwe, 1993). Producing members are indicated in grey.

The scale samples were collected from different parts of the installations (**Fig. 6.3**), and can be divided into three morphological types as proposed earlier by Schmidt (1998). The first type are thin crusts up to 1 mm thick, covering the inside of pipes and tanks throughout the production installations. The second type are annular precipitates up to several centimeters thick, firmly attached to, and clogging tubing, pipes and valves. The third scale type is formed by unattached scale particles, several mm to cm in size, carried along with the production stream and deposited in areas of restricted flow such as production water filters, separators or the bottom of a well.

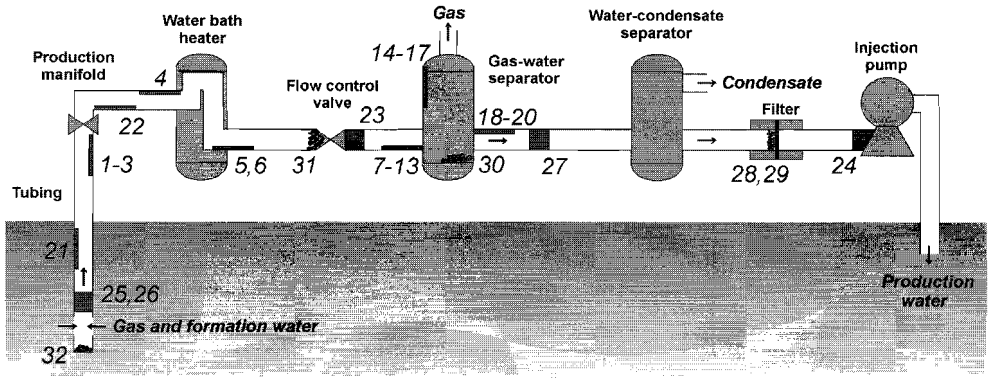

Figure 6.3 - Schematic view of a natural gas production facilities with sampling points of the lead scales indicated in Table 5.1.

Analytical techniques

Texture and mineralogical composition of the scale samples were studied using a Jeol JXA 8600 electron microprobe in back-scattered mode and wavelength dispersal analysis (WDS) at an accelerating voltage of 15 kV and a current of 10 nA. When possible, samples were analysed in polished thin section, otherwise small subsamples were cemented onto aluminium mounts with a carbon adhesive. Quantitative analyses on scale minerals were performed against in-house mineral standards using counting times of 20 s per element. Detection limits of the elements were on the order of 0.2 wt%. Reproducibility in repeat analyses of mineral standards was within 1% (2σ) for major elements.

Additionally, quantitative mineralogical analyses on some of the scales were performed using X-ray diffraction (XRD) coupled to Rietveld analysis. Most samples were ground before analysis, but samples with the highest lead contents were analysed in polished thin section.

Samples 1 to 32 were analysed for major and trace element composition using X-ray fluorescence spectrometry (XRF). However, samples with the highest lead contents could not be ground properly, and element concentrations had to be estimated from microprobe analyses. One liter of the production brine (sample 36) was heated in a HDPE beaker on a sand bath at 80°C until dryness, after which major and trace element concentrations were determined using XRF. Only concentrations of some selected elements in the scales and the brine are reported in this paper.

Subsamples of 0.020 to 0.030 g of the scales and the dry residu of the production brine were dissolved in 20 ml 4.5% suprapur HNO_3 and stored in ultra-clean HDPE flasks. Stable lead isotopes were measured with a VG Plasmaquad PQ 2+ ICP-MS at a concentration of about 50 ppb Pb. Ten runs were measured for each sample. For mass bias correction NBS 981 standard

was run after each batch of 6 samples. Relative standard deviations (1σ) for isotopic ratios are given in **Tables 6.2 and 6.4**. Variable Hg contents of the samples may have contributed to the observed higher standard deviations in ratios with respect to ^{204}Pb. Blanks of the 4.5% HNO_3 solution were also measured with ICP-MS and appeared to contain negligible amounts of Pb (< 20 ppt). Further details on the ICP-MS analysis procedure can be found in Walraven *et al.* (1997).

Finally, samples were analysed for NORs, using standard γ-ray spectroscopy techniques. Unless reported otherwise, radiometric analyses of ^{226}Ra and ^{210}Pb had a combined 2σ precision/accuracy of 10% (**Tables 6.2 and 6.4**). Details on spectroscopic techniques and derivation of the combined precision/accuracy have been reported elsewhere (Schmidt *et al.*, 2000/ **Chapter 2**).

Scale mineralogy and composition

Thin crusts

Thin crusts from location A (samples 1-20) mainly consist of various amounts of lead minerals, barite and calcite, precipitated on a substratum of iron-oxides from the inside of the pipes. Additional minerals such as sphalerite (ZnS) and anhydrite ($CaSO_4$) are present in minor amounts. Lead mineral assemblages are combinations of metallic lead, galena, hydrocerussite ($Pb_3(CO_3)_2Cl_2$), and lead oxides (e.g. PbO, PbO_2, and $Pb_5O_3(OH)_4$), with Pb concentrations in the crusts ranging from 0.3 wt% to 10 wt% (**Table 6.2**). Ba and Sr concentrations range up to 21 wt% and 9 wt% respectively, while Ca concentrations vary from 0 wt% to 2.7 wt%, with an outlier of 7.5 wt% for sample 6. Except for a few scales which contain only trace amounts of Ba or Sr, bulk analyses of the scales yield a fairly constant Ba:Sr mole ratio of about 63:37 (**Fig. 6.4**).

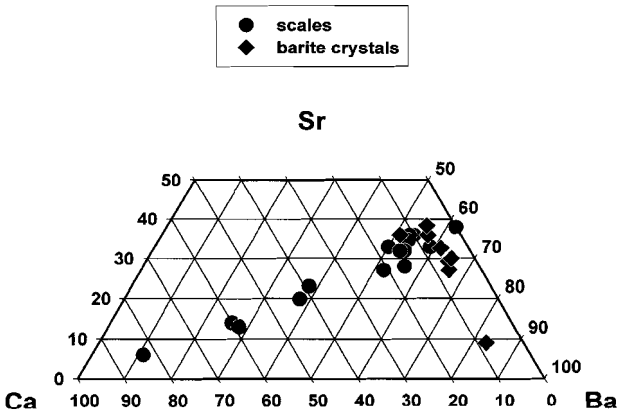

Figure 6.4 - Relative mole percentages of Ba, Sr and Ca in bulk scales and individual barite crystals within scales from location A. Corresponding Ba:Sr ratios in bulk scales and barite crystals show that most Ba and Sr in the scales are incorporated in barite. Most Ca is incorporated in calcite.

Table 6.2 - Activity concentrations of NORs, XRF analyses, and stable lead isotope ratios* in samples from location A.

Sample no.	^{226}Ra ($Bq.g^{-1}$)	^{210}Pb ($Bq.g^{-1}$)	$^{210}Pb/^{226}Ra$	Fe (wt%)	Pb (wt%)	S (wt%)	Ba (wt%)	Sr (wt%)	Ca (wt%)	Total (wt%)	$^{206}Pb/^{207}Pb$	$^{208}Pb/^{207}Pb$	$^{206}Pb/^{204}Pb$	$^{207}Pb/^{204}Pb$	$^{208}Pb/^{204}Pb$
Thin crusts															
1	2840	775	0.27	27	1.4	6.0	21	9.0	1.2	65.6	1.175 ± 0.003	2.449 ± 0.005	18.435 ± 0.052	15.687 ± 0.065	38.420 ± 0.150
2	2883	900	0.31	29	1.3	4.3	21	9.0	1.3	65.9	n.d.	n.d.	n.d.	n.d.	n.d.
3	1028	341	0.33	52	1.2	1.5	7.0	2.2	0.6	64.5	n.d.	n.d.	n.d.	n.d.	n.d.
4	2030	940	0.46	11	5.4	< d.l.	13	4.9	< d.l.	34.3	n.d.	n.d.	n.d.	n.d.	n.d.
5	1516	380	0.25	n.d.	n.d.	n.d.	n.d.	n.d.	n.d.	-	1.174 ± 0.003	2.456 ± 0.012	18.367 ± 0.046	15.648 ± 0.045	38.424 ± 0.142
6	250	197	0.79	39	3.8	3.1	3.3	1.2	7.5	57.9	n.d.	n.d.	n.d.	n.d.	n.d.
7	184	57	0.31	58	0.3	3.9	1.5	0.5	1.0	65.2	1.175 ± 0.004	2.451 ± 0.007	19.156 ± 0.162	16.309 ± 0.145	39.968 ±0.366
8	2483	901	0.36	30	1.5	4.8	17	7.0	1.7	62.0	n.d.	n.d.	n.d.	n.d.	n.d.
9	2833	1090	0.38	36	0.9	3.4	17	7.0	1.1	65.4	n.d.	n.d.	n.d.	n.d.	n.d.
10	578	632	1.09	17	8.0	1.2	3.6	1.2	1.2	32.2	n.d.	n.d.	n.d.	n.d.	n.d.
11	2203	1360	0.62	34	10	5.4	12	4.6	0.9	66.9	1.175 ± 0.004	2.450 ± 0.010	18.433 ± 0.097	15.690 ± 0.084	38.438 ± 0.233
12	746	605	0.81	14	5.5	1.4	3.6	1.4	1.1	27.0	1.175 ± 0.004	2.451 ± 0.006	18.393 ± 0.047	15.654 ± 0.051	38.372 ± 0.117
13	3016	1561	0.52	30	6.0	7.0	17	6.0	0.7	66.7	1.178 ± 0.003	2.455 ± 0.004	18.401 ± 0.023	15.626 ± 0.036	38.368 ± 0.137
14	12.4	9.1	0.73	58	1.4	3.2	0.2	< 0.1	1.1	63.9	n.d.	n.d.	n.d.	n.d.	n.d.
15	3.9	3	0.77	60	0.1	3.4	< 0.1	< 0.1	0.5	64.0	n.d.	n.d.	n.d.	n.d.	n.d.
16	0.3	0.5	1.67	64	0.0	0.5	< 0.1	< 0.1	2.2	66.7	n.d.	n.d.	n.d.	n.d.	n.d.
17	0.3	0.8	2.67	66	0.0	0.4	< 0.1	< 0.1	1.1	67.5	n.d.	n.d.	n.d.	n.d.	n.d.
18	729	347	0.48	43	3.7	2.8	4.3	1.3	2.7	57.8	n.d.	n.d.	n.d.	n.d.	n.d.
19	1087	780	0.72	49	8.5	2.9	6.0	2.0	0.7	69.1	1.175 ± 0.004	2.456 ± 0.007	18.358 ± 0.071	15.627 ± 0.066	38.376 ± 0.203
20	1327	784	0.59	46	8.0	3.4	7.0	2.7	0.6	67.7	n.d.	n.d.	n.d.	n.d.	n.d.

* Ratios are presented with 2σ standard deviations. < d.l. : below detection limit; n.d. : not determined

Microprobe analyses of individual barite crystals from the same crusts yield a corresponding average Ba:Sr mole ratio of 65:35 (**Table 6.3**, **Fig. 6.4**), which leads to the conclusion that almost all Ba and Sr in the scales are incorporated in precipitated barite. The amount of Ca coprecipitated in barite is also rather constant, but most Ca in the samples is incorporated in calcite. Detailed morphological information and micrographs of some of the thin crusts from location A have been published in an earlier paper (Schmidt, 1998). The only other thin crusts, from locations F and G, are very much like the crusts from location A. They show finely dispersed metallic lead, lead oxides and sphalerite (sample 21), and galena, barite, sphalerite and calcite (sample 22), on a substratum consisting of iron-oxides (**Table 6.4**).

Table 6.3 - Semi-quantitative microprobe analyses of barite crystals in unpolished grain mounts of samples from location A.

Barite crystal	Ba (wt%)	Sr (wt%)	Ca (wt%)	S (wt%)
1	36.4	12.3	1.0	11.4
2	35.3	2.4	1.0	10.8
3	27.5	8.0	0.8	8.5
4	34.1	8.9	1.0	8.5
5	33.4	10.0	0.7	9.0
6	41.9	17.2	1.5	9.1
7	35.5	15.7	1.2	n.d.
8	41.6	18.6	3.2	8.2

Annular precipitates

Four of the annular precipitates (samples 23 to 26) consist of metallic lead. Lead concentrations range from 85 to 93 wt%, due to partial weathering of the scales (**Table 6.4**). Although the four samples are macroscopically identical, the internal structure of sample 25 is different from the other three. Samples 23, 24 and 26 are solid pieces of lead, containing minor inclusions of organic material, and quartz and feldspar, probably from the gas reservoir formations. Parallel bands of slightly different composition inside sample 24, resembling growth rings, suggest a discontinuous precipitation process. Sample 25, on the other hand, is actually a porous aggregate of 0.2 - 20 mm sized lumps, consisting of 5-20 µm sized quartz and feldspar grains cemented by small needle-like crystals of metallic lead.

The fifth annular precipitate, sample 27, is very inhomogeneous of composition. One subsample, selected for this paper, contains metallic lead, lead oxides, and hydrocerussite. Major accompanying minerals are stolzite ($PbWO_4$), and another tungsten oxide ($KFe_{0.33}W_{1.67}O_6$). Lead concentration of this specific subsample is only 40 wt%, but W (11 wt%) and Cu (10 wt%) concentrations are remarkably high.

Table 6.4 - Mineralogy, Pb contents, ^{226}Ra and ^{210}Pb activities, and stable lead isotope ratios* of the samples from locations B to I.

Sample no.	Location	Mineralogy**	Pb (wt%)	^{226}Ra (Bq/g)	^{210}Pb (Bq/g)	$^{206}Pb/^{207}Pb$	$^{208}Pb/^{207}Pb$	$^{206}Pb/^{204}Pb$	$^{207}Pb/^{204}Pb$	$^{208}Pb/^{204}Pb$
Thin crusts										
21	F	Lo, Sph	n.d.	< 0.7	390 ± 16	1.189 ± 0.004	2.463 ± 0.008	18.670 ± 0.054	15.704 ± 0.024	38.679 ± 0.160
22	G	Ga, Ba, Sph, Ca	56	695	307	1.193 ± 0.002	2.471 ± 0.006	18.666 ± 0.061	15.643 ± 0.059	38.659 ± 0.163
Annular precipitates										
23	B	L	85***	< 0.02	380 ± 30	1.182 ± 0.003	2.462 ± 0.008	18.501 ± 0.053	15.654 ± 0.033	38.544 ± 0.073
24	B	L, Lo	93	0.09 ± 0.02	288 ± 30	1.181 ± 0.002	2.460 ± 0.009	18.484 ± 0.045	15.651 ± 0.045	38.501 ± 0.177
25	E	L	93	< 0.8	1590 ± 20	1.207 ± 0.003	2.474 ± 0.010	19.034 ± 0.059	15.765 ± 0.041	39.001 ± 0.136
26	H	L, Lo	90***	< 1.0	685 ± 12	1.188 ± 0.005	2.461 ± 0.013	18.654 ± 0.066	15.702 ± 0.078	38.649 ± 0.138
27	J	L, Lo, Ga, Sph, St	40	<0.02	203	1.187 ± 0.007	2.462 ± 0.011	18.621 ± 0.071	15.681 ± 0.090	38.610 ± 0.148
Unattached particles										
28	B	L, Ga, Lo, Hy	27	n.d.	n.d.	1.184 ± 0.006	2.468 ± 0.011	18.618 ± 0.081	15.724 ± 0.056	38.807 ± 0.154
29	B	L, Ga, Lo, Hy	41	0.34 ± 0.03	271 ± 30	1.180 ± 0.002	2.465 ± 0.006	18.579 ± 0.058	15.746 ± 0.049	38.814 ± 0.090
30	C	La, Lo, Ca	48	n.d.	860 ± 20	1.201 ± 0.002	2.472 ± 0.010	18.791 ± 0.055	15.647 ± 0.053	38.678 ± 0.182
31	D	Lo	85	n.d.	950 ± 100	1.195 ± 0.003	2.468 ± 0.007	18.745 ± 0.052	15.687 ± 0.043	38.720 ± 0.149
32	F	L	90***	< 0.5	348 ± 3	1.189 ± 0.004	2.463 ± 0.010	18.637 ± 0.060	15.670 ± 0.051	38.588 ± 0.178
Scale covered steel installation parts										
33	F	L, Ga	n.d.	< 0.5	348 ± 3	n.d.	n.d.	n.d.	n.d.	n.d.
34	G	Ga, Ba, Sph	n.d.	695	307	n.d.	n.d.	n.d.	n.d.	n.d.
35	I	Lo	n.d.	1.8 ± 0.1	204 ± 1	n.d.	n.d.	n.d.	n.d.	n.d.
Production brine										
36	B	NaCl	0.01	≤ 0.002	0.009 ±0.002	1.183 ± 0.003	2.466 ± 0.012	18.555 ± 0.043	15.681 ± 0.039	38.671 ± 0.189

* Ratios are presented with 2σ standard deviations. ** Ba: barite; L: metallic lead; Lo: lead oxides; Ga: galena; Sph: sphalerite; An: anhydrite; Ca: calcite; Hy: hydrocerussite; La: laurionite; St: stolzite; NaCl: rock salt. *** Estimated from microprobe analyses.

Unattached particles

Of the scale samples consisting of unattached particles, sample 32 contains only metallic lead (**Table 6.4**). Samples 28 and 29 consist of particles of metallic lead, associated with galena, lead oxides, and hydrocerussite ($Pb_3(OH)_2(CO_3)_2$). The lead particles, which were sieved from the production water stream, are mixed with various amounts of quartz and feldspar, co-produced from the gas reservoir. Some of these reservoir grains have been covered with a thin layer of lead particles. Samples 30 and 31, finally, resemble the annular precipitates, because their lead particles have a solid structure with minor inclusions of reservoir grains and metallic corrosion products. Sample 31 completely consists of lead oxides, sample 30 contains about 65 wt% laurionite ($Pb_2Cl_2(OH)_2$) and 10 wt% calcite, plus some lead oxide. In this sample, lumps of PbO are floating in a matrix of intergrown laurionite and calcite. All of these unattached particles have probably been formed somewhere upstream in the installations. While some of the precipitates adhere to the tubing, other precipitates are removed from their initial place of deposition and transported into the surface installations.

Lead scales on steel installation parts

Sample 33 is a typical example of an early stage annular precipitate, deposited on the inside of a piece of tubing (**Micrograph A**). A homogeneous layer of metallic lead is firmly attached to a corroded steel surface, separated by a very thin layer of Fe-oxides, mainly goethite and hematite. Sample 34 is an example of a cross section of a thin crust, consisting of tiny galena crystals in a matrix of mainly sphalerite, ZnS (**Micrograph B**). During preparation of the thin section, the crust became separated from its steel substratum, which is therefore not visible on the micrograph. However, it did not show any sign of corrosion. Sample 35 may be representative for an annular precipitate in its earliest stage. Small crystals of metallic lead are enclosed within an Fe-oxide rim covering the inside of a piece of severely corroded tubing. The corrosive layer seems to consist of several layers of Fe-oxides on top of each other, formed in different episodes (**Micrograph C**). Cracks within the corrosive rim are probably the result of dessication of the sample after removal from the installation.

Production brine from location B

Dissolved solids in the brine primarily consist of NaCl (> 2 wt%), and minor amounts of typical gas field brine metals such as Ba (13 ppm), Sr (250 ppm), Zn (100 ppm) and Pb (70 ppm).

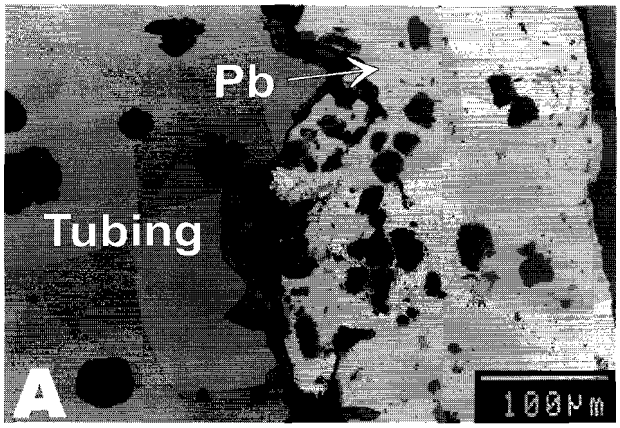

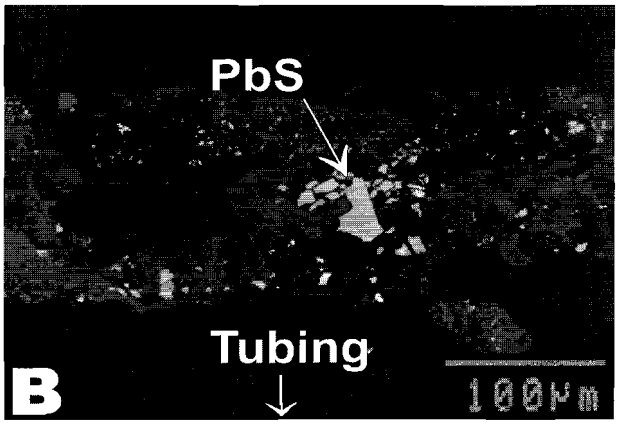

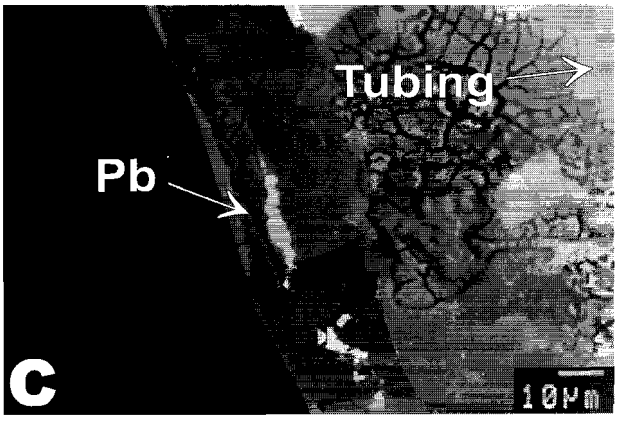

Micrographs showing scales attached to steel surfaces. **A**: a homogeneous layer of metallic lead with inclusions of quartz and feldpar is attached to a corroded steel surface, separated by a thin layer of Fe-oxides. **B**: Cross-section of a thin metal-like crust, consisting of galena crystals in a matrix of mainly sphalerite. During sample preparation, the crust became separated from the corroded steel tubing. **C**: Small crystals of metallic lead are enclosed within a layered Fe-oxide rim covering a piece of severely corroded steel tubing.

Naturally Occurring Radionuclides (NORs) and stable lead isotope ratios

All thin crustss from location A contain both ^{210}Pb and ^{226}Ra from the ^{238}U decay series (**Table 6.2**). Activity concentrations of ^{226}Ra range from 0.3 to 3016 $Bq.g^{-1}$, while ^{210}Pb activity concentrations vary from 0.5 to 1561 $Bq.g^{-1}$. Generally, $^{210}Pb/^{226}Ra$ activity concentration ratios in these samples are lower than 1. Scales from the other locations all contain significant amounts of ^{210}Pb, in the range of 203 $Bq.g^{-1}$ to 1590 $Bq.g^{-1}$ (**Table 6.4**). Except for sample 34 from location G, ^{226}Ra activity concentrations in these scales are negligible compared to those of ^{210}Pb, which means that almost all ^{210}Pb is 'unsupported'. This is also the case for the dry residu of the production brine from location B, since it shows a ^{210}Pb activity concentration of 0.009 $Bq.g^{-1}$ but no significant ^{226}Ra.

Except for samples 7 and 25, which show 'anomalously' high ^{206}Pb, ^{207}Pb and ^{208}Pb values compared to ^{204}Pb, stable lead isotope ratios of the scales fall within a narrow range (**Tables 6.2 and 6.4**): $^{206}Pb/^{207}Pb$ ranges from 1.174 to 1.207, $^{208}Pb/^{207}Pb$ from 2.449 to 2.474, $^{206}Pb/^{204}Pb$ from 18.358 to 18.791, $^{207}Pb/^{204}Pb$ from 15.626 to 15.765, and $^{208}Pb/^{204}Pb$ from 38.368 to 38.720. Since $^{206}Pb/^{207}Pb$ and $^{208}Pb/^{207}Pb$ ratios are not affected by variable Hg contents of the samples, and, for multiple samples from the same location, in a much closer range than the ratios with respect to ^{204}Pb, the former ratios will be used in the following discussion of the results.

Deposition of lead minerals in gas production facilities

Primary and secondary lead minerals

The investigated scales contain a large number of different lead minerals. In many samples metallic lead is accompanied by lead oxides and hydroxides, compounds that are not stable in a natural gas system, where oxygen fugacities are extremely low. Since lead oxides and hydroxides are typical weathering products of metallic lead (Lin, 1996), they are likely the result of oxidation of metallic lead precipitates upon cleaning the installations before sampling, and/or during and after sampling. The same holds true for hydrocerussite ($Pb_3(OH)_2(CO_3)_2$), which is also not stable under natural gas production conditions, but a typical secondary lead mineral in the presence of both O_2 and CO_2 (Edwards *et al.*, 1992). Laurionite, the main compound of sample 29, is a common corrosion product of metallic lead in a moist, salty environment (Aoyama, 1963). This mineral is probably the result of a reaction between a metallic lead precipitate and a combination of air, seawater and steam, used in a cleaning operation before sampling of the scale. The presence of PbO, itself an oxidation product of metallic lead, inside the laurionite matrix makes direct precipitation of lead chloride hydroxide complexes, such as have been detected in Red Sea brines (Tsai and Cooney, 1976), less viable. Secondary laurionite formation by reaction between metallic lead and ammonium chloride solutions (Badikov *et al.*, 1966) or between $PbCl_2$ and hydroxide solutions (Edwards *et al.*, 1992) are also not likely in a natural gas environment. Therefore, it is presumed that oxides, hydroxides,

chlorides and carbonates of lead formed under different conditions than metallic lead and galena. They are secondary in nature, while metallic lead and galena are primary scale minerals.

Electrochemical deposition of metallic lead

Metallic, or native, lead is a very rare mineral. Aggregates of small grains of native lead have been reported from the Polish Kupferschiefer, associated with galena and containing up to 8 wt% Cu and 2.4 wt% Zn (Sawlowicz, 1990). It was suggested that the native lead was precipitated in a micro-environment at relatively high pH and low sulphide concentration (Sawlowicz, 1990).

Deposition of metallic lead in oil and gas production installations is likely associated with corrosion of steel from the installations (Carpenter *et al.*, 1974; Kaemmel *et al.*, 1978). Corrosion of steel in aqueous media is an electrochemical process by which iron is dissolved according to the reaction

$$Fe_{(metal)} \rightarrow Fe^{2+} + 2e^-$$

(Kharaka *et al.*, 1980). In an acid aqueous environment like a natural gas system, where pH may range from about 4 to 6 and oxygen is absent, the electrons will react with hydrogen ions following the reaction

$$2H^+ + 2e^- \rightarrow H_{2\,(gas)}$$

(Kharaka *et al.*, 1980). However, when dissolved Pb is present in the system, the latter reaction may be replaced by the reaction

$$Pb^{2+} + 2e^- \rightarrow Pb_{(metal)}$$

(Carpenter *et al.*, 1974). Lead deposition on iron has been observed during laboratory experiments using lead silicate as a corrosion inhibitor for iron and zinc in an acetate buffered solution of pH 5.6. A porous layer of metallic lead was deposited onto the iron electrode at open circuit potential and in the absence of oxygen (Armstrong and Peggs, 1994). The corrosion rate of the iron was unaffected by the presence of the lead layer.

The investigated scale-covered steel parts from this study also indicate that corrosion of steel causes the precipitation of metallic lead scales. Iron is locally dissolved, which results in pitting corrosion of the steel (**Micrograph A**, **Fig. 6.5**). Subsequently, dissolved lead reacts with the electrons provided by the dissolution of iron, and metallic lead is precipitated onto the steel surface. The presence of water in pores between the tubing and the newly formed lead scale enhances the continuous dissolution of iron and a constant supply of electrons. Electron transport through the water and the metallic lead rim enables the rim to grow steadily on the outside, i.e. the inside of the steel pipe. Once a metallic lead deposit has started to grow in a specific site, uniform corrosion over the entire length of the steel tubing may provide a steady

flow of electrons towards that site. Upon opening of the tubing during maintenance operations, Fe^{2+} present in the water filled pores is rapidly oxidised and precipitated as Fe-oxides. The observed layering of the Fe-oxide rim in sample 22 and the enclosed crystals of metallic lead suggest that metallic lead was precipitated during gas production after at least one earlier maintenance operation.

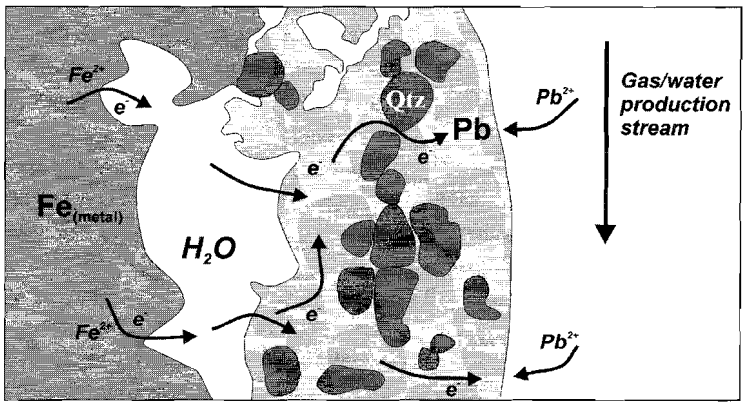

Figure 6.5 - Electrochemical precipitation of metallic lead on steel.

Potentials of the two half-reactions involved are greatly influenced by parameters such as temperature and composition of the metals and the corroding medium. For instance, the difference in (corrosion) potentials of Pb and Fe in a 3 wt% NaCl solution at 20°C is only about 0.18 V, compared with a difference in standard potentials of 0.31 V (Basalo, 1992). A simple calculation using the Nernst equation shows that in such a solution at 100°C, deposition of metallic lead on iron will occur at Fe^{2+}/Pb^{2+} chemical activity ratios of less than $7.2*10^4$. Well data from the investigated gas fields show that Fe concentrations in produced waters generally vary between 20 and 500 ppm (Hartog, unpubl.). Assuming that activity coefficients for Fe^{2+} and Pb^{2+} in produced waters are equal, Pb concentrations of at least 1 to 25 ppb are required for the reaction to take place. As reported above, Pb concentrations in produced waters generally vary between 0.01 and 150 $mg.l^{-1}$.

Deposition of galena

In contrast to deposition of metallic lead, precipitation of galena in natural gas installations is not an electrochemical process, but a matter of supersaturation. Solubility of sulphides such as galena or sphalerite in the gas-water system is both pressure and temperature dependent.

Because of changes in the equilibrium partitioning of H_2S and CO_2 between the gas and the water phase, decreasing pressure in production installations will cause exsolution of both CO_2 and H_2S from the water phase (Drummond and Ohmoto, 1985). This results in an increase of pH, which in turn leads to a higher HS^- concentration in the aqueous phase. Both effects favour the precipitation of galena by reactions such as:

$$PbCl_n^{2-n} + HS^- \rightleftharpoons PbS_{(s)} + H^+ + nCl^-$$

In order for this process to occur, the pH change must exceed the rate of H_2S exsolution from the water phase (Drummond and Ohmoto, 1985). The same process, under somewhat different conditions, is well known from geothermal plants. Here, sulphide deposition preferentially occurs during flashing, i.e. when a pressure drop causes sudden boiling of the produced aqueous fluid (e.g. Skinner *et al.*, 1967; Christanis and St. Seymour, 1995). Decreasing temperature during gas production also favours precipitation of galena, because lead chloride complexes become more stable with increasing temperatures (Seward and Barnes, 1997).

In acidic H_2S saturated solutions, where lead is predominantly complexed by bisulphide (Nriagu, 1971), the situation is somewhat different. Here, an increase in pH due to pressure release would result in an increased complexation of lead by bisulphide, increasing the solubility of galena (Drummond and Ohmoto, 1985).

Conditions influencing lead scale deposition

As has been mentioned above, the precipitation of lead scales requires the presence of Pb^{2+} ions in an aqueous phase in the production installations. Therefore, when gas is produced together with liquid formation water, and a hydrocarbon gas phase and a water phase coexist throughout the production system, lead scale deposition may occur anywhere in the installations because of the omnipresence of dissolved lead species. However, when produced gas is only saturated with water vapour, lead scale deposition depends on the chemical activity of lead in the gas phase, and the condensation of water from the hydrocarbon gas phase during production. In the second case, lead must initially be present in the gas phase. Indeed, Tunn (1975) reported an average Pb concentration of $1 \mu g.m^{-3}$ (NPT) in water saturated natural gas from Northwest Germany.

Since deposition of metallic lead is an electrochemical process related to corrosion, use of different steel types in installations should have an effect on this type of scaling. Corrosion behaviour of steel depends for instance on its Cr content (e.g., Vera *et al.*, 1994). Indeed, from the three steel samples in this study, samples 33 and 35 are covered with (oxidised) metallic lead scale. In both cases ordinary carbon-steel without any Cr was used. However, no metallic lead was observed in the scale on the third steel sample, no. 34, which contains a significant amount of Cr. Fluid flow velocity is also known to influence corrosion rates of steel (Vera *et al.*, 1994), and could have an effect on deposition rates of metallic lead. Precipitation of galena may also be influenced by fluid flow velocity, but not by steel grades.

Naturally Occurring Radionuclides in lead scale minerals

Coprecipitation of ^{226}Ra and ^{210}Pb

The presence of ^{226}Ra, and/or ^{228}Ra, in gas and oil field scales is well-known and can be explained by coprecipitation of Ra isotopes with Ba, Sr and Ca in sulphates and carbonates (e.g. Rood *et al.*, 1998). Pb-210 in scales can have three different origins (Hartog *et al.*, 1996); the third one mentioned here represents the most important source of ^{210}Pb for lead scales investigated in this study.

1. *In situ* decay of ^{226}Ra, present in sulphate and carbonate scales. If this is the only process operating, the age of the scales can be calculated from the ^{210}Pb ingrowth, since the emanation factor for ^{222}Rn in these scales is very low (Rood *et al.*, 1998).

2. *In situ* decay of ^{222}Rn, provided that the radon has a sufficient long residence time in the facilities. This process is well-known from Natural Gas Liquid fractionating units, such as de-propanisers, in which radon can become highly concentrated because of boiling point similarity (Van der Heijde *et al.*, 1977). After several years of operation 'invisible' ^{210}Pb deposits are found in some plants with high activity concentrations (Taylor and Cleghorn, 1996). The same phenomenon has been observed in LPG rail cars (Bland and Chu, 1996), in which dust particulates showed ^{210}Pb activities of about 10 $Bq.g^{-1}$. Because of high solubilities of radon in both liquid hydrocarbons and water, presence of liquid films on the inside of tubings and other installation parts may significantly enhance residence times of ^{222}Rn in production facilities.

3. Transport of 'unsupported' ^{210}Pb with production fluids. No or too little ^{226}Ra or ^{222}Rn are present to account for the observed ^{210}Pb activity and ^{210}Pb may be coprecipitated with non-radioactive lead also present in the fluids. Until recently, transport of unsupported ^{210}Pb was not recognized as a separate source of natural radioactivity in oil and gas industry scales, but in the last few years attention has been focussed on this important phenomenon (Hartog *et al.*, 1995; 1996).

Transport of unsupported ^{210}Pb is by far the most important source of natural radioactivity in the lead scales investigated in this study. All annular precipitates and unattached scale particles, plus the thin crust from location F, contain mostly unsupported ^{210}Pb. The scales do not contain any ^{226}Ra, and *in situ* decay of ^{222}Rn can only explain a small part of the high ^{210}Pb activities observed since distribution coefficients for radon in a gas-liquid system are presumably very high.

The thin crust from location G contains both ^{210}Pb and ^{226}Ra. Assuming that its initial ^{210}Pb concentration was zero, the age of the scale can be calculated from its $^{210}Pb/^{226}Ra$ activity concentration ratio using the formula:

$$t = \frac{\ln(1 - A_{Pb}/A_{Ra})}{\lambda_{Pb}}$$

The scale shows a $^{210}Pb/^{226}Ra$ activity concentration ratio of 0.44 ± 14%, which corresponds to *in situ* decay of ^{226}Ra over a period of about 18.5 ± 3.5 years. Since the time interval between

shutdown of the installation and sampling of the scale is about 20 years, it appears that no unsupported ^{210}Pb was coprecipitated with galena in this thin crust. ^{226}Ra in the crust was probably coprecipitated in barite and/or calcite.

The thin crusts from location A also contain both ^{210}Pb and ^{226}Ra. Since gas production from the field took place over a period of six years, while another 12 years passed between final shutdown of the installation and analysis of the samples, ingrowth of ^{210}Pb from *in situ* decay of ^{226}Ra alone would have led to current ^{210}Pb/^{226}Ra activity concentration ratios between 0.31 and 0.43. However, when 2σ confidence levels are taken into account, the samples show a range of ^{210}Pb/^{226}Ra ratios from 0.25 ± 0.04 to 2.67 ± 0.38 (**Table 6.2**). Ratios for at least 11 out of 20 samples fall outside the range predicted from their age, indicating that these scales must also contain a certain amount of unsupported ^{210}Pb, coprecipitated during deposition of the scales. This can also be seen in **Fig. 6.6**, which shows ^{210}Pb activity concentrations of the samples corrrected for *in situ* decay of ^{226}Ra over a time interval of 15 years, the average age of the scales. After correction for ^{210}Pb ingrowth, 14 out of 20 scales show initial, i.e. unsupported, ^{210}Pb activity concentrations. In addition, since lead isotope fractionation during scale precipitation is not likely, good correlation between unsupported ^{210}Pb activity concentrations and total Pb concentrations (**Fig. 6.6**) indicates a fairly constant unsupported ^{210}Pb over stable Pb ratio in the production fluids from which the scales precipitated. Again, some of the supposedly unsupported ^{210}Pb may actually result from *in situ* decay of ^{222}Rn in liquid hydrocarbon and/or water films on the inside of installation parts.

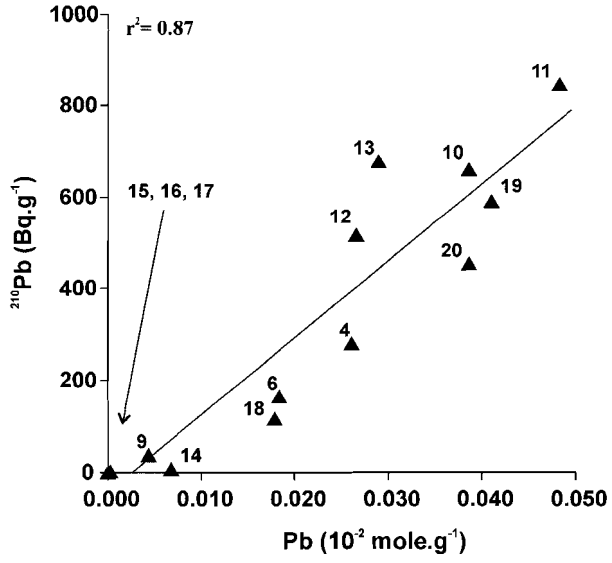

Figure 6.6 - Activity concentrations of ^{210}Pb, corrected for *in situ* decay of ^{226}Ra over a period of 15 years, versus total Pb contents of the scales from location A. Corrected ^{210}Pb activity concentrations represent concentrations of unsupported ^{210}Pb, coprecipitated in the scales. Good correlation between initial ^{210}Pb and total Pb indicates a constant unsupported ^{210}Pb over total Pb ratio in the production fluids from which the scales precipitated.

Because ^{226}Ra in the scales from location A is probably coprecipitated in barite and/or calcite, a correlation should be found between ^{226}Ra activity concentrations of the scales and combined total Ba, Sr and Ca concentrations. Indeed, ^{226}Ra activity concentrations tend to go up with increasing combined concentrations of the earth alkaline metals Ba, Sr and Ca (**Fig. 6.7a**).

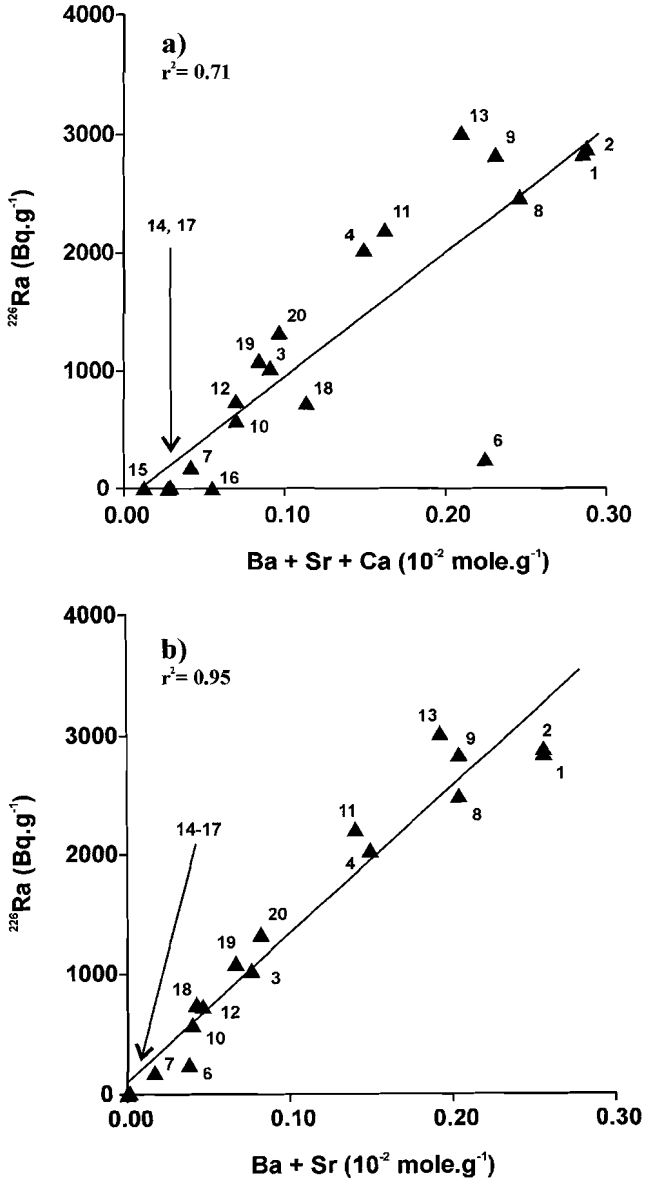

Figure 6.7 - ^{226}Ra activity concentrations versus (**a**) total Ba+Sr+Ca concentrations and (**b**) total Ba+Sr concentrations of the scales from location A.

However, correlation between ^{226}Ra activity concentrations and combined concentrations of Ba and Sr is much better (**Fig. 6.7b**). XRF analyses of the bulk scales combined with microprobe analyses of individual barite crystals in the same scales indicate that most Ca in the scales is present in calcite, whereas Ba and Sr are mainly present in barite. Therefore, it follows that ^{226}Ra is mainly incorporated in barite, and not in calcite. The same observation has been reported from Norway, where barium sulphate scales from production installations contained ^{226}Ra and ^{228}Ra, while carbonate scales did not (Lysebo and Strand, 1997). Most likely, when barium sulphates and calcium carbonates precipitate at the same time, radium prefers coprecipitation with the sulphates. The affinity between Ra^{2+} and especially Ba^{2+} follows from the similarity in ionic radii, electronegativities and electronic configurations (e.g., Curti, 1999). In addition, it has recently been shown that calcite/water distribution coefficients of Ra are very low, even at high (i.e. far above equilibrium) calcite precipitation rates (Rihs *et al.*, 1997).

Origin of ^{210}Pb and ^{226}Ra

The origin of ^{210}Pb in lead scales from production facilities was discussed at length in Schmidt *et al.* (2000) / **Chapter 2**. Because of the geologically very short half-life of ^{210}Pb, 22.3 a, the source of ^{210}Pb in production facilities must be looked for in or near the producing gas reservoirs. For Rotliegend reservoirs, three possible sources can be identified: the Carboniferous Coal Measures, the Zechstein Kupferschiefer, and solid bitumens in the Slochteren Sandstone reservoir itself. These different organic-rich sediments may all be enriched in uranium because of the affinity of uranium and organic matter. Uraniferous bitumen is believed to be the source of enhanced radionuclide levels in production waters from Texas and Ukrainian oil fields (Pierce *et al.*, 1964; Zhuravel, 1999).

Core studies from the reservoir at location F showed the presence of uraniferous bitumen in the Slochteren Sandstone, from which ^{210}Pb may be mobilized into production fluids as a result of fluid flow induced by gas production (Schmidt *et al.*, 2000 / **Chapter 2**). Sediment cores from the other Rotliegend locations in this study have not been examined in detail, and the presence of uraniferous bitumen in the reservoirs is not known. Well data provided by the oil company show the presence of the Kupferschiefer within several meters of the well perforations at locations C, D and I. In addition, at many locations Rotliegend reservoirs are formed by fault blocks. Here, Zechstein sediments, including the Kupferschiefer, are juxtaposed against the Rotliegend reservoirs. Fluid transport across these faults, as evidenced by widespread deposition of cements of Zechstein origin in Rotliegend sediments (e.g., Lee *et al.*, 1989; Gaupp *et al.*, 1993), may introduce Kupferschiefer U daughter nuclides into Rotliegend gas reservoir pore fluids. Carboniferous Coal Measures underlying the Rotliegend may be an alternative source of NORs when juxtaposed to Rotliegend gas reservoirs. However, no juxtaposition of Carboniferous to Rotliegend formations is known from the northern Netherlands or southern North Sea area, although it occurs in northwestern Germany (Gaupp *et al.*, 1993).

The source of ^{210}Pb produced from the Z2 Carbonate reservoir at location A and the Triassic reservoir at location E can only be guessed at. Well data for these locations were not available,

so it cannot be excluded that any uranium enriched horizons are present within the wells' drainage areas. Such horizons have never been mentioned in literature on Dutch gas reservoirs, but uranium enrichments have been reported from several levels in the Solling Claystone Member of Northwest Germany, not far from location E (Trusheim, 1961; Röhling, 1991). At location A, the nearest uranium enriched sediment may be the Kupferschiefer. There, the vertical distance between the well perforations and the Kupferschiefer is around 80 m. Enhanced fluid flow induced by production of gas from the field may enable transport of ^{210}Pb from the Kupferschiefer to the area of the well perforations through fractures or along faults cutting the sediments.

^{226}Ra may be mobilized directly into reservoir fluids through alpha-recoil from uranium enriched sediments (e.g. Rama and Moore, 1984). In brines, ^{226}Ra is often found far in excess of its parent nuclides due to its high solubility (e.g. Kronfeld *et al.*, 1993). Ra chloride complexes could account for up to 60% of total dissolved Ra in brines (Zukin *et al.*, 1987). At location A, where both ^{210}Pb and ^{226}Ra were coprecipitated in the scales, these radionuclides were probably derived from the same source in or near the reservoir formations. In the case of location G, where apparently no ^{210}Pb was coprecipitated in galena in the scales, the origin of produced ^{226}Ra from the Z2 Carbonate is uncertain. Perhaps the presence of ^{226}Ra and the absence of ^{210}Pb in the production fluids can be explained by the difference in half-lives between the two radionuclides. Because of its relatively long half life of about 1600 years, ^{226}Ra can be transported over much longer distances than ^{210}Pb.

Origin of stable lead in scales

As we have seen, Pb concentrations in formation waters from Dutch gas reservoirs can be as high as 150 $mg.l^{-1}$ (F.A. Hartog, unpubl.). Lead in Rotliegend brines may be leached from poorly crystalline ferric iron oxides in the Rotliegend sediments (Carpenter, 1989), or derived from Rotliegend smectites by their diagenetic transition to illites during compaction of the sediments (Hallager *et al.*, 1991). Dissolution of Rotliegend feldspars by Carboniferous, acidic waters flushing the sediments is another potential source of lead. Since stable lead isotope ratios of the scales must be the same as the isotope ratios in the production brines, these ratios may shed light on the origin of lead in the brines. For better comparison of scales within the same gas fields and between different fields we use $^{208}Pb/^{207}Pb$ and $^{206}Pb/^{207}Pb$ ratios (**Tables 6.2 and 6.4**) because they have the lowest relative standard deviations of the determined ratios.

Lead isotope ratios of scales from the same reservoir are identical within the standard deviations of the analyses (**Tables 6.2 and 6.4**). In addition, the agreement between the four scales and the reservoir brine from location B shows that lead isotope ratios of scales are indeed the same as the isotope ratios of the brines from which the scales are deposited. There is no direct relationship between stable lead isotope ratios of the scales and the age of the gas reservoir formations from which the lead is produced (**Fig. 6.8**). Scales from the two Zechstein reservoirs have a very different lead isotopy from one another, as do the scales from most Rotliegend reservoirs. Only the scales from Rotliegend reservoirs F, H and J show nearly the

same isotope ratios, remarkably corresponding to isotope ratios of Kupferschiefer sediments from the Groningen gas field as reported by Wedepohl *et al.* (1978). Because gas fields F, H and J are also nearest to the Groningen gas field (**Fig. 6.1**), lead in these brines and in the local Kupferschiefer sediments probably share the same history.

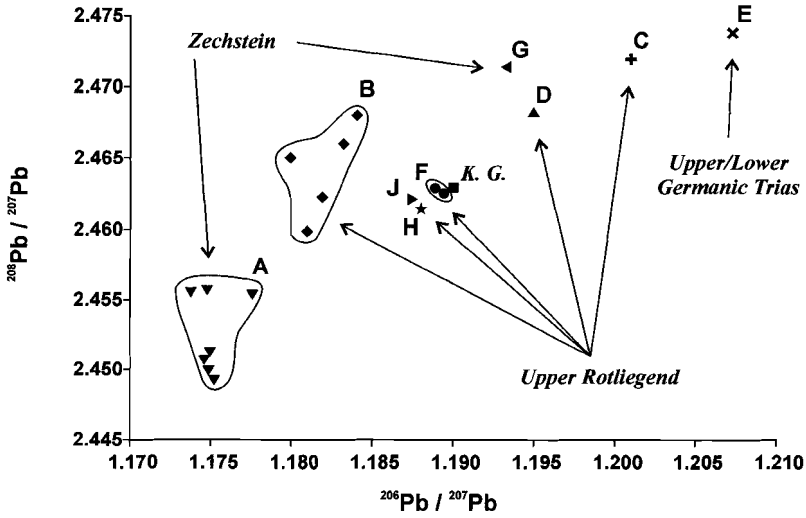

Figure 6.8 - Stable lead isotope ratios for lead scales from locations A through J, compared to Kupferschiefer (K.G.) sediment from the Groningen gas field (from Wedepohl *et al.*, 1978). Names indicate gas reservoir sediments at the different locations.

The origin of lead in reservoir brines from this study becomes clearer when isotope ratios of the scales are plotted in the plumbotectonics model by Zartman and Doe (1981). In this model, four evolution curves represent the evolution of stable lead isotope ratios in four terrestrial reservoirs: upper continental crust, lower continental crust, mantle, and an orogenic environment. The curves are the result of redistribution of U, Th and Pb during mixing of the terrestrial reservoirs in orogenic processes occurring every 400 Ma (Zartman and Doe, 1981). Comparing the ratios of the scales to the evolution curves defined by the model, the data imply an orogenic signature for the lead (**Fig. 6.9**). Hammer *et al.* (1987), who applied the same model to East-German Kupferschiefer sediments, also found an orogenic signature for their samples. According to the model, the scales from this study have ages between 300 Ma and 125 Ma. Moreover, the scales appear to follow the 'orogenic' evolution line, starting from a Late Carboniferous age for location A to an Early Cretaceous age for location E. Combining the ages of the scales, or reservoir brines, with those reported for large scale groundwater movements in Dutch Rotliegend gas reservoirs (Lee *et al.*, 1989; Lanson *et al.*, 1996), we come to the following reconstruction for the origin of lead in gas reservoir brines in the northeastern Netherlands.

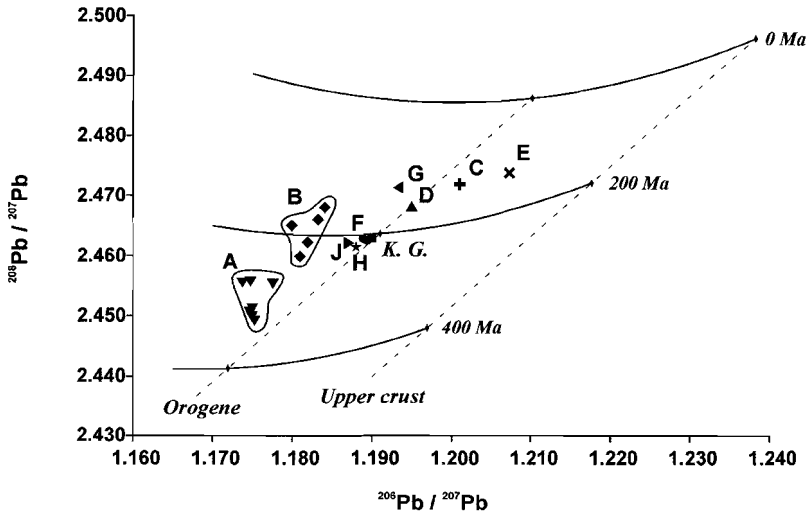

Figure 6.9 - $^{208}Pb/^{207}Pb$ versus $^{206}Pb/^{207}Pb$ evolution diagram for lead scales from locations A through H and Groningen Kupferschiefer (K.G., from Wedepohl *et al.*, 1989). Isochrons and signatures 'Orogene' and 'Upper crust' refer to lead evolution lines from the model of Zartman and Doe (1981).

We suggest that between 200 Ma and 150 Ma lead was released from Rotliegend sediments and added to Rotliegend formation waters by the same process that caused dissolution of K-feldspars in Rotliegend sediments (Lanson *et al.*, 1996). During the first major gas emplacement in the Rotliegend reservoirs in northeastern Netherlands, between 200 Ma and 150 Ma (Van Wijhe *et al.*, 1980), large amounts of volatile organic acids accompanied natural gas derived from the Late Carboniferous Coal Measures. When natural gas became trapped in Rotliegend reservoirs, local formation waters became acidic by uptake of organic acids. Subsequently, dissolution of feldspars by these acidic formation waters mobilized lead from the Rotliegend sediments. Because Dutch Rotliegend sediments mostly consist of redeposited Carboniferous sediments (Van Wijhe *et al.*, 1980), mobilized lead had a Carboniferous isotopic signature. Mixing of this lead with isotopically younger lead already present in the Rotliegend pore fluids, and/or later addition of younger lead, resulted in the present wide range of lead isotopic signatures of Rotliegend formation waters. A likely source of younger lead is the U-enriched Kupferschiefer directly overlying the Rotliegend formations. Large scale influx of Zechstein brines into Dutch Rotliegend sediments widely occurred after 155 Ma (Lanson *et al.*, 1996) and influx may still be going on, especially in places where Zechstein formations are juxtaposed to Rotliegend sediments.

Lead isotopic signatures of formation waters from Zechstein and Triassic reservoirs in northeastern Netherlands are more difficult to explain. Natural gas in these reservoirs is also believed to be generated in the Carboniferous Coal Measures (e.g. Van de Sande *et al.*, 1996;

Bruijn, 1996). Therefore, influx of organic acids with natural gas into Triassic reservoirs may have mobilized lead from the Triassic 'red bed' sediments themselves. Uranium-enriched horizons within these sediments (e.g. Trusheim, 1961) may have added isotopically younger lead to the Triassic formation waters. However, Zechstein carbonates do not contain any significant lead-bearing minerals such as feldspars, and mobilisation of lead from these sediments by organic acids is unlikely. Influx of lead-bearing Rotliegend brines may explain the present lead isotopic signatures, but more data on Zechstein lead scales and formation waters are needed to solve this matter.

The agreement in lead isotopy between reservoir brines at locations F, H and J and the Kupferschiefer from the nearby Groningen gas field suggests isotopic equilibrium between brines and Kupferschiefer sediments in this area. Since the amount of lead present in Rotliegend formation waters largely exceeds that in the about 50 cm thick Kupferschiefer, this equilibrium means that in the northeastern Netherlands Rotliegend metal-rich brines indeed contributed to deposition of base metals in the Kupferschiefer, as suggested by Carpenter (1989) and Cathles III *et al.* (1993). Moreover, lead deposition in the Dutch Kupferschiefer was mainly postgenetic, since large scale mobilisation of lead from Rotliegend sediments happened only after 200 MA.

Conclusions

Detailed investigation of a large number of lead precipitates from gas production facilities in the Netherlands showed the presence of three morphologically different types of scale: thin crusts, annular precipitates, and unattached particles. The scales consist of a wide assembly of lead minerals. Based on production history of the gas fields, redox conditions, and chemical composition of the scales, most lead minerals are considered to be of a secondary nature. Only metallic lead and galena were initially deposited in the facilities, together with phases such as barite, calcite and sphalerite.

Deposition of metallic lead is an electrochemical process associated with corrosion of the production facilities. Lead ions dissolved in the production fluids take up electrons liberated by dissolution of iron from steel parts of the installations. Gas production conditions in the Dutch facilities generally favour the precipitation of metallic lead, but the use of Cr-steel instead of carbon steel seems to inhibit the deposition process. Unlike the deposition of metallic lead, deposition of galena is both temperature and pressure dependent. Decreasing temperature during gas production lowers the stability of lead chloride complexes in the production fluids, while decreasing pressure leads to an increase in pH due to the exsolution of CO_2. Both changes may lead to supersaturation and precipitation of galena. When liquid formation water is produced together with gas, lead scale deposition may occur anywhere in the production facilities because of the omnipresence of lead ions in an aqueous phase. However, when produced gas is only saturated with water vapour, lead scale deposition depends on the chemical activity of lead in the gas phase and the condensation of water from the hydrocarbon gas phase during production.

All scale samples contained ^{210}Pb from the ^{238}U natural decay series. Scales from eight out of ten locations contained only 'unsupported' ^{210}Pb; there is no ^{226}Ra in the scales which might account for the presence of ^{210}Pb, while the residence time of ^{222}Rn in the gas phase in the facilities is not sufficient to build up a significant ^{210}Pb activity in the scales. However, ^{222}Rn in liquid phases of hydrocarbons and/or water may have contributed some ^{210}Pb. Samples from the remaining two locations also contained ^{226}Ra. ^{210}Pb in the single sample from one of these two locations proved to be completely the result of decay of ^{226}Ra originally coprecipitated in the scale. Samples from the other of the two locations contained both unsupported ^{210}Pb and ^{210}Pb from in-situ decay of ^{226}Ra. As in the scales containing only ^{210}Pb, some of the ^{210}Pb may have resulted from *in situ* decay of dissolved ^{222}Rn. Here, ^{226}Ra showed a good correlation with combined total Ba and Sr concentrations of the scales, indicating that the greater part of ^{226}Ra was coprecipitated in barite, not in calcite. When both barite and calcite precipitate at the same time, ^{226}Ra apparently prefers coprecipitation in barite. This would be expected based on the great similarity between Ra and Ba. All radionuclides in the scales are derived from U-bearing organic-rich sediments in or near the productive horizons. In Rotliegend reservoirs, U-enriched bitumens and/or the Zechstein Kupferschiefer are the most likely sources of produced ^{210}Pb. The Kupferschiefer also likely provides both ^{226}Ra and ^{210}Pb in scales from Zechstein gas fields, while locally U-enriched shales are the most likely sources of ^{210}Pb in Triassic production facilities.

Stable lead isotope ratios of scales are in fact isotope ratios of reservoir brines from which these scales have been deposited. Different locations show distinctive lead signatures, with model ages ranging from 300 to 125 Ma. Isotope ratios in Rotliegend brines are the result of mixing of lead from at least three sources. Organic acids accompanying natural gas from Carboniferous source rocks mobilized lead with a Carboniferous signature by dissolution of feldspars from Rotliegend sediments. This lead became mixed with isotopically younger lead, already present in Rotliegend pore waters and/or added in the course of influx of Zechstein brines into Rotliegend formations. Scales from three Rotliegend gas fields have almost identical signatures. Close correspondence to the signature of Kupferschiefer sediments in a nearby gas field implies that Rotliegend brines contributed to postgenetic deposition of metals in the Zechstein Kupferschiefer. The very young age of the Triassic reservoir brine in this study may have been caused by mobilisation of lead from the Triassic sediments themselves and addition of lead from U-enriched shales.

Acknowledgement - The authors would like to thank Dr. S.R. van der Laan for valuable dicussions and comments on the manuscript. Nederlandse Aardolie Maatschappij (NAM B.V.) is thanked for providing scale and production water samples, as well as geological and production data.

References

Aoyama, Y., 1963. The analysis of corrosion products by physical methods. Sci. Papers I.P.C.R. 57, 176-183.

Armstrong, R.D. and Peggs, L., 1994. The behaviour of lead silicate as a corrosion inhibitor for iron and zinc. Corr. Sci. 36, 749-757.

Badikov, V.V., Godovikov, A.A. and Pavlyuchenko, 1966. Synthesis of laurionite under hydrothermal conditions. Doklady Akad. NAUK SSSR 69, 132-135.

Basalo, C., 1992. Water and gas mains corrosion, degradation and protection. Ellis Horwood series in corrosion and its prevention. Horwood, New York.

Bland, C.J. and Chiu, N.W., 1996. Accumulation of ^{210}Pb activity on particulate matter in LPG rail cars. Appl. Rad. Isot. 47, 925-926.

Bruijn, A.N., 1996. De Wijk gas field (Netherlands): reservoir mapping with amplitude anomalies. In: H.E. Rondeel, D.A.J. Batjes and W.H. Nieuwenhuijs (Eds.), Geology of gas and oil under the Netherlands. Kluwer Academic Publishers, Dordrecht, pp. 243-253.

Carpenter, A.B., Trout, M.L. and Pickett, E.E., 1974. Preliminary report on the origin and chemical evolution of lead- and zinc-rich oilfield brines in entral Mississippi. Econ. Geol. 69, 1191-1206.

Carpenter, A.B., 1989. Occurrence of lead- and zinc-rich brine in the Rotliegendes formation, the Netherlands. Abstr. Progr. Geol. Soc. Am. 21(6), 315.

Cathles III, L.M., Oszczepalski, S. and Jowett, E.C., 1993. Mass balance evaluation of the late diagenetic hypothesis for Kupferschiefer Cu mineralization in the Lubin basin of southwestern Poland. Econ. Geol. 88, 948-956.

Christanis, K. and St. Seymour, K., 1995. A study of scale deposition: an analogue of meso- to epithermal ore formation in the volcano of Milos, Aegean arc, Greece. Geothermics 24, 541-552.

Crouch, S.V., Baumgartner, W.E.L., Houlleberghs, E.J.M.J. and Walzebuck, J.P., 1996. Development of a tight gas reservoir by a multiple fracced horizontal well: Ameland-204, the Netherlands. In: H.E. Rondeel, D.A.J. Batjes and W.H. Nieuwenhuijs (Eds.), Geology of gas and oil under the Netherlands. Kluwer Academic Publishers, Dordrecht, pp. 93-102.

Curti, E., 1999. Coprecipitation of radionuclides with calcite: estimation of partition coefficients based on a review of laboratory investigations and geochemical data. Appl. Geochem. 14, 433-445.

Doe, B.R., Hedge, C.E. and White, D.E., 1966. Preliminary investigation of the source of lead and strontium in deep geothermal brines underlying the Salton Sea geothermal area. Econ. Geol. 61, 462-483.

Drummond, S.E. and Ohmoto, H., 1985. Chemical evolution and mineral deposition in boiling hydrothermal systems. Econ. Geol. 80, 126-147.

Edwards, R., Gillard, R.D. and Williams, P.A., 1992. Studies of secondary mineral formation in the PbO-H_2O-HCl system. Min. Mag. 56, 53-65.

Eglinton, T.I., Curtis, C.D. and Rowland, S.J., 1987. Generation of water-soluble organic acids from kerogen during hydrous pyrolysis: implications for porosity development. Min. Mag. 51, 495-503.

Gaupp, R., Matter, A., Platt, J., Ramseyer, K. and Walzebuck, J., 1993. Diagenesis and fluid evolution of deeply buried Permian (Rotliegende) gas reservoirs, Northwest Germany. AAPG Bull. 77, 1111-1128.

Giordano, T.H. and Kharaka, Y.K., 1994. Organic ligand distribution and speciation in sedimentary basin brines, diagenetic fluids and related ore solutions. In: J. Parnell (Ed.), Geofluids: Origin, migration and evolution of fluids in sedimentary basins. Geological Society of London Special Publications 78, pp. 175-202.

Hallager, W.S., Carpenter, A.B. and Campbell, W.L., 1991. Smectite clays in red beds as a source of base metals. Abstr. Progr. Geol. Soc. Am. 23, 31-32.

Hammer, J., Hengst, M., Pilot, J. and Roesler, H.J., 1987. Pb-Isotopenverhältnisse des Kupferschiefers der Sangerhäuser Mulde; Neue Untersuchungsergebnisse. Chemie der Erde, 46: 193-211.

Hartog, F.A., Knaepen, W.A.I. and Jonkers, G., 1995. Radioactive lead: an underestimated issue? API / GRI NORM conference, Houston, USA, pp. 59-69.

Hartog, F.A., Jonkers, G. and Knaepen, W.A.I., 1996. The encounter and analysis of Naturally Occurring Radionuclides (NORs) in gas and oil production and processing, 7th International Symposium on Oil Field Chemicals, Geilo, Norway, pp. 17-20.

Hennet, R.J., Crerar, D.A. and Schwartz, J., 1988. Organic complexes in hydrothermal systems. Econ. Geol. 83, 742-764.

Jacobs, R.P.W.M. and Marquenie, J.M., 1991. Produced water from gas/condensate platforms: environmental considerations. First international conference on health, safety and environment. Society of Petroleum Engineers, The Hague, The Netherlands, pp. 89-96.

Jacobs, R.P.W.M., Grant, R.O.H., Kwant, J., Marquenie, J.M. and Mentzer, E., 1992. The composition of produced water from Shell operated oil and gas production in the North Sea. In: J.P. Ray and F.R. Engelhart (Eds.), 1992 International Produced Water Conference, San Diego, California. Plenum Press, New York.

Kaemmel, T., Müller, E.P., Krossner, L., Nebel, J., Gommern, U.H. and Ungethüm, H., 1978. Sind $HgPb_2$ und (Hg,Pb), gebildet aus natürlichen Begleitkomponenten der Erdgase der Lagerstätten der Altmark, Minerale? Z. Angew. Geol. 24, 90-96.

Karabelas, A.J., Andritsos, N., Mouza, A., Mitrakas, M., Vrouzi, F. and Christanis, K., 1989. Characteristics of scales from the Milos geothermal plant. Geothermics 18, 169-174.

Kharaka, Y.K., Lico, M.S. and Carothers, W.W., 1980. Predicted corrosion and scale-formation properties of geopressured geothermal waters from the northern Gulf of Mexico basin. J. Petrol. Tech. 32, 319-324.

Kharaka, Y.K., Maest, A.S., Carothers, W.W., Law, L.M., Lamothe, P.J. and Fries, T.L., 1987. Geochemistry of metal-rich brines from central Mississippi Salt Dome basin, U.S.A. Appl. Geochem. 2, 543-561.

Knaepen, W.A.I., Bergwerf, W., Lancee, P.J.F., Van Dijk, W., Jansen, J.F.W., Janssen, R.G.C., Kiezenberg, W.H.T., Van Sluijs, R., Tijsmans, M.H., Volkers, K.J. and Voors, P.I., 1995. State-of-the-art of NORM nuclide determination in samples from oil and gas production: Validation of potential standardization methods through an interlaboratory test programme. J. Radioanal. Nucl. Chem. 198, 323-341.

Kolb, W.A. and Wojcik, M., 1985. Enhanced radioactivity due to natural oil and gas production and related radiological problems. Sci. Tot. Envir. 45, 77-84.

Kronfeld, J., Minster, T. and Ne'eman, E., 1993. ^{238}U-series disequilibrium in the Upper Cretaceous oil shales of Israel as the primary source for the Dead Sea's ^{226}Ra anomaly. Terra Nova 5, 563-567.

Lanson, B., Beaufort, D., Berger, G., Baradat, J. and Lacharpagne, J.-C., 1996. Illitization of diagenetic kaolinite-to-dickite conversion series: late-stage diagenesis of the lower Permian Rotliegend sandstone reservoir, offshore of the Netherlands. J. Sedim. Res. 66, 501-518.

Lebedev, L.M., 1972. Minerals of contemporary hydrotherms of Cheleken. Geochem. Int. 9, 485-504.

Lebedev, L.M., 1983. Cheleken hydrothermal system - a natural mineral-forming laboratory. Izv. Akad. Nauk SSSR, Ser. Geol. 7, 60-75.

Lee, M., Aronson, J.L. and Savin, S.M., 1989. Timing and conditions of Permian Rotliegende sandstone diagenesis, Southern North Sea: K/Ar and oxygen isotopic data. AAPG Bull. 73, 195-215.

Lin, Z., 1996. Secondary mineral phases of metallic lead in soils of shooting ranges from Orebro County, Sweden. Environm. Geol. 27, 370-375.

Lundegard, P.D. and Kharaka, Y.K., 1990. Geochemistry of organic acids in subsurface waters. In: D.C. Melchior and R.L. Bassett (Eds.), Chemical modeling of aqueous systems II. ACS Symposium Series. American Chemical Society, Washington, DC, pp. 169-189.

Lysebo, I. and Strand, T., 1997. NORM in oil production in Norway, International symposium on radiological problems with natural radioactivity in the non-nuclear industry, Amsterdam, the Netherlands.

Nriagu, J.O., 1971. Studies in the system PbS-NaCl-H_2S-H_2O: Stability of lead (II) thiocomplexes at 90°C. Chem. Geol. 8, 299-310.

Rihs, S., Condomines, M. and Fouillac, C., 1997. U- and Th-series radionuclides in CO_2-rich geothermal systems in the French Massif Central. J. Radioanal. Nucl. Chem. 226, 149-157.

Rood, A.S., White, G.J. and Kendrick, D.T., 1998. Measurement of ^{222}Rn flux, ^{222}Rn emanation, and $^{226,228}Ra$ concentration from injection well pipe scale. Health Phys. 75, 187-192.

Rothbard, D.R., 1982. Diagenetic history of the Lamotte Sandstone, southeast Missouri. International Conference on Mississippi Valley-Type Lead-Zinc Deposits, Rolla, Missouri, pp. 385-395.

Sawlowicz, Z., 1990. Native lead in the Polish Kupferschiefer. Neues Jahrb. Min. Mh. 8, 376-382.

Schmidt, A.P., 1998. Lead precipitates from natural gas production installations. J. Geochem. Expl. 62, 193-200 (**chapter 5** of this thesis).

Schmidt, A.P., Hartog, F.A., Van Os, B.J.H. and Schuiling, R.D., 2000. Production of ^{210}Pb from a Slochteren Sandstone gas reservoir. Appl. Geochem. 15, 1317-1329 (**chapter 2** of this thesis).

Seward, T.M. and Barnes, H.L., 1997. Metal transport by hydrothermal ore fluids. In: H.L. Barnes (Ed.), Geochemistry of hydrothermal ore deposits. John Wiley & Sons, Inc., New York, pp. 435-486.

Skinner, B.J., White, D.E., Rose, H.J. and Mays, R.E., 1967. Sulfides associated with the Salton Sea geothermal brine. Econ. Geol. 62, 316-330.

Taylor, G.L. and Cleghorn, M., 1996. Naturally occurring radioactive materials: Contamination and control in a world scale ethylene manufacturing complex, 8th Ethylene Producers Conference, pp. 309-323.

Testa, C., Desideri, D., Meli, M.A., Roselli, C., Bassignani, A., Colombo, G. and Fresca Fantoni, R., 1994. Radiation protection and radioactive scales in oil and gas production. Health Phys. 67, 34-38.

Trusheim, F., 1961. Über radioaktive Leithorizonte im Buntsandstein Norddeutschlands zwischen Ems und Weser. Erdöl Kohle 14, 797-802.

Tsai, P. and Cooney, R.P., 1976. Ultraviolet spectroscopic evidence for polynuclear lead (II) complexes in synthetic red sea brines. Chem. Geol. 18, 187-202.

Tunn, W., 1975. Untersuchungen über Spurenelemente in Gasen aus deutschen Erdgas- und Erdöl-Feldern. In: Compendium Vorträge der Haupttagung der Deutsche Mineralölwissenschaft und Kohlechemie. D. Gesellschaft fur Mineralölwissenschaft, pp. 96-111.

Van de Sande, J.M.M., Reijers, T.J.A. and Casson, N., 1996. Multidisciplinary exploration strategy in the northeast Netherlands Zechstein 2 Carbonate play, guided by 3D seismics. In: H.E. Rondeel, D.A.J. Batjes and W.H. Nieuwenhuijs (Eds.), Geology of gas and oil under the Netherlands. Kluwer Academic Publishers, Dordrecht, pp. 125-142.

Van der Heijde, H.B., Beens, H. and De Monchy, A.R., 1977. The occurrence of radioactive elements in natural gas. Ecotox. Environm. Safety 1, 49-87.

Van Wijhe, D.H., Lutz, M. and Kaasschieter, J.P.H., 1980. The Rotliegend in the Netherlands and its gas accumulations. Geologie en Mijnbouw, 59: 3-24.

Vera, J.R., Viloria, A., Castillo, M., Ikeda, A. and Ueda, M., 1994. Flow velocity effect on CO_2 corrosion of carbon steel using a dynamic field tester. In: B. Kermani (Ed.), Predicting CO_2 corrosion in the oil and gas industry. European Federation of Corrosion publications vol. 13. The Institute of Materials, London, UK, pp. 94-119.

Walraven, N., Van Os, B.J.H., Klaver, G.T., Baker, J.H. and Vriend, S.P., 1997. Trace element concentrations and stable lead isotopes in soils as tracers of lead pollution in Graft-De Rijp, the Netherlands. J. Geochem. Expl. 59, 47-58.

Wedepohl, K.H., Delevaux, M.H. and Doe, B.R., 1978. The potential source of lead in the Permian Kupferschiefer bed of Europe and some selected paleozoic mineral deposits in the Federal Republic of Germany. Contrib. Mineral. Petrol. 65, 273-281.

White, D.E., 1981. Geothermal systems and hydrothermal ore deposits. Econ. Geol. 75th Anniversary Volume, 392-423.

Zartman, R.E. and Doe, B.R., 1981. Plumbotectonics - The model. Tectonophysics 75, 135-162.

Zukin, J.G., Hammond, D.E., Ku, T. and Elders, W.A., 1987. Uranium-thorium series radionuclides in brines and reservoir rocks from two deep geothermal boreholes in the Salton Sea Geothermal Field, southeastern California. Geochim. Cosmochim. Acta 51, 2719-2731.

Chapter 7

Synthesis: Origin, transport and deposition of NORM in Dutch gas production facilities

Introduction

The omnipresence of Naturally Occurring Radionuclides (NORs) within the Earth is well-known. Since long, radioactive decay of NORs has been recognised as the primary source of our internal planetary heat, and driving force of volcanism and the movement of plates forming the Earth's crust. Since NORs are most abundant in the Earth's crust, from which all oil and gas are produced, it is no surprise to encounter NORs in the oil and gas industry.

Already at the beginning of the 20th century, it became clear that NORs can be produced together with hydrocarbons. In oil and gas production facilities, enhanced concentrations of some NORs can be found in the hydrocarbons themselves, in coproduced water, and in all kinds of hard and soft deposits such as scales and sludges. Production water and deposits containing NORs have been termed NORM, i.e. Naturally Occurring Radioactive Materials, or TENORM, i.e. Technologically Enhanced NORM. The presence of NORM in production facilities can face oil and gas companies with large additional costs in maintenance, treatment and lost production, while extra care has to be taken regarding the environment and the health of production personnel. Therefore, management of NORM is essential to the oil and gas industry. Understanding the origin and formation of NORM may assist to predict or even prevent NORM build-up in production facilities, leading to important risk and cost reductions.

This study was initialised to gain insight into the origin and distribution of NORs (U, Th and decay products) in hydrocarbon reservoirs, mobilisation and transport of NORs into production lines, and deposition of NORM in production facilities during production, processing and treatment of oil and gas. A lack of knowledge on the origin, transport and deposition of especially ^{210}Pb, from the ^{238}U natural decay series, and the observation that ^{210}Pb-bearing production waters and scales form an important, if not the most important, part of Dutch gas industry NORM, led to focussing of this study on the encounter of ^{210}Pb in the gas production industry. Dutch gas reservoir sediments were studied for the distribution and mobilisation of ^{210}Pb and stable Pb. Transport of Pb into production lines was investigated by combining oil company production data with laboratory experiments, while Pb scales were studied in order to elucidate deposition mechanisms and the origin and coprecipitation of ^{210}Pb in these scales. Additionally, stable Pb isotope ratios of both sediments and scales were used for reconstruction of the origin of stable Pb in Dutch gas reservoir formation waters.

Accumulation and distribution of NORs in sediments

Most important NORs in Dutch oil and gas industry NORM are ^{226}Ra, ^{222}Rn and ^{210}Pb, all from the ^{238}U natural decay series (**Chapter 1**). Radium, radon and lead are highly mobile elements under reducing oil and gas reservoir conditions, radon being a gas, radium and lead being very soluble in salty waters which dominate hydrocarbon reservoir formation waters. In spite of this mobility, slow fluid transport in reservoir rocks and relatively short half lives of ^{226}Ra, ^{222}Rn and ^{210}Pb imply that the sources of these NORs are restricted to the reservoir environments themselves. Since all ^{238}U daughter nuclides preceding ^{226}Ra are considered to be immobile under hydrocarbon reservoir conditions, U enrichments within sediments are the most likely sources of produced NORs (**Chapter 1**). Large differences in NORs production between multiple wells from single reservoirs underline the very local scale on which U may be enriched in hydrocarbon reservoir sediments. Due to the high affinity of U for organic matter, two scenarios for U enrichment of reservoir rocks are possible.

In the first scenario, U accumulates in organic-rich sediments due to slow sorption from ground waters (**Chapter 1**). Organic-rich sediments happen to be present near the majority of Dutch gas reservoirs, most of which are found in Rotliegend or Zechstein formations. The organic-rich Kupferschiefer marking the boundary between Rotliegend and Zechstein formations is a likely source of NORs produced from these reservoirs, especially when Rotliegend gas reservoirs are sealed by faults juxtaposing the Kupferschiefer to the Rotliegend (**Chapter 6**). This is often the case with Rotliegend gas reservoirs in the northern Netherlands and the Dutch continental shelf. Fluid transport across these faults, as evidenced by deposition of cements of Zechstein origin, may introduce Kupferschiefer U daughter nuclides into Rotliegend gas reservoir pore fluids (**Chapter 6**). Organic-rich Carboniferous Coal Measures underlying the Rotliegend may be an alternative source of NORs when juxtaposed to Rotliegend gas reservoirs. However, no juxtaposition of Carboniferous to Rotliegend formations is known from the northern Netherlands area, although it occurs in northwestern Germany.

In the second scenario, migration of a liquid hydrocarbon phase, expelled from a nearby, mature, source rock, leads to deposition of bitumens in future gas reservoir sediments. After deposition, but before emplacement of natural gas, hydrocarbons scavenge U from formation waters. Alternatively, hydrocarbons entering the reservoir sediments may already be enriched in U if they contain asphaltenes. In hydrocarbons, most U is contained in the heavy asphaltene fraction (**Chapter 1**).

Investigation of Rotliegend and Kupferschiefer sediments from a northeastern Netherlands gas reservoir indeed showed enrichment of U in the locally 0.5 m thick Kupferschiefer (**Chapter 2**). However, Rotliegend sandstone intervals impregnated with bitumen contained much higher U concentrations. Most of this uranium was present as U-oxides lining pores within the bitumen. Good positive correlation between organic carbon and U contents of the sandstones showed that U and bitumen entered the Rotliegend sandstones together. Dating of the U-oxide grains around 246 Ma and the presence of large amounts of Ba, Cu, Ni, Sn and Pb suggest a Kupferschiefer origin for the U-enriched hydrocarbon phase. In spite of the bitumen impregnation, porosity and permeability of these sandstones were not lowered significantly, allowing intensive contact between U-oxides and pore fluids. Therefore, in this particular gas well bituminous sandstones likely are a more important source of NORs than the rather impermeable Kupferschiefer (**Chapter 2**). The absence of U-enriched bitumen in sediments from a nearby well within the same gas field confirms the very local scale on which production of NORs may be significant.

The two other natural decay series, with parent nuclides ^{235}U and ^{232}Th, also contain isotopes of Ra, Rn and Pb, but for geochemical and physical reasons these do not contribute significantly to Dutch oil and gas industry NORM (**Chapter 1**). First, ^{235}U accounts for only 0.7% of total U, while ^{238}U forms the remaining 99.3%. Moreover, half lives of Ra, Rn and Pb daughter nuclides of ^{235}U are very much shorter than those of equivalent daughter nuclides of ^{238}U. Second, in most sediments Th is mainly present in clay minerals, at low background concentrations. Th has no affinity for organic matter, and can only become enriched in placer deposits, sediments containing high amounts of heavy minerals. However, no placer deposits are known to occur within or very close to Dutch oil and gas reservoirs.

Mobilisation of NORs from sediments

Mobilisation of ^{226}Ra, ^{222}Rn and ^{210}Pb from U-bearing sediments occurs through the α-recoil process, by which a newly formed daughter nuclide may be ejected from sediment grains into fluid-filled pores, and through leaching from lattice sites damaged by previous α-recoil processes. Direct α-recoil tends to be seen as somewhat more important than leaching (**Chapter 1**). Upon entering the pores, NORs may be removed from their source by diffusion and formation water transport. In contrast, under stagnant flow conditions ^{226}Ra and ^{210}Pb will be preferentially retained within the sediment because of re-adsorption onto sediment grains. Emanated ^{222}Rn will quickly decay into ^{210}Pb and also be removed from the pore fluids by adsorption.

Therefore, continuous production of NORs from natural gas reservoirs, which are considered to be closed systems, seems difficult. However, many Dutch Rotliegend reservoirs are not entirely closed systems. Reservoir fluids are effectively kept within the reservoir because of cap rocks or sealing faults, but this does not exclude influx of fluids from neighbouring formations into Rotliegend reservoirs. For instance, heavy brines from Zechstein formations may enter Rotliegend sediments containing less salty pore waters. These brines may introduce NORs from U decay in the Zechstein Kupferschiefer into Rotliegend pore waters, enabling co-production of these NORs with natural gas. Gas production will enhance fluid flow within the Rotliegend reservoir formations, thus promoting continuous influx of new Zechstein brines and NORs.

In addition, γ-ray analysis of NORs concentration activities in U-rich bituminous sandstones revealed a mechanism for mobilisation of ^{210}Pb from reservoir sediments into gas production fluids (**Chapter 2**). Successfull dating of the U-oxide grains in the bituminous sandstones by means of their stable Pb contents implies negligible loss of mobile U daughters since sorption of U on the organic matter. However, one of the bituminous sandstones showed significant disequilibrium between ^{226}Ra and ^{210}Pb. This loss of 30% of ^{210}Pb with respect to its parent ^{226}Ra must have occurred within the last ten years, most likely because of gas production from the reservoir. Enhanced fluid flow because of gas production enabled migration of ^{222}Rn, which has a much higher emanation than ^{226}Ra or ^{210}Pb, through bituminous sandstone pore waters. Upon decay of dissolved ^{222}Rn during migration, resulting ^{210}Pb was not re-adsorbed on the rock matrix, but transported further towards and into gas production lines.

Transport of NORs in production fluids

In the Netherlands, natural gas from Permian and Triassic reservoirs is generally produced in two systems: either as a single, water saturated, gas phase, or together with a liquid water phase. Some wells never produce a separate, liquid water phase during their life time, while in other cases water production starts within a few weeks after completion of the well.

Transport of NORM constituents in the two-phase system is easily understood: produced liquid water consists primarily of formation water, containing all kinds of salts, metals and soluble NORs. Because of complexation by chloride and/or organic acid anions, high amounts of stable Pb and ^{210}Pb, but also Ba, Sr and ^{226}Ra, can be transported into production facilities. Total dissolved Pb production rates of several tens of kilograms per day per well can be reached (**Chapter 4**). Transport of gaseous ^{222}Rn, which is very soluble in hydrocarbons and in formation waters, is possible in both gas and water phases. Finally, significant amounts of stable Pb and ^{210}Pb must also be produced in a water saturated hydrocarbon gas phase. This is supported by the fact that deposition of NORM scales is also observed in production facilities where all water produced is condensed from the hydrocarbon gas phase. Indeed, combination of experimental and oil company production data (**Chapter 4**) shows a Pb solubility of up to about 5 $\mu g.m^{-3}$ in a water saturated hydrocarbon gas phase, implying Pb production rates of several grams per day for a well producing 10^6 Nm^3 per day in a single gas phase system. In

such a system, Pb is probably transported in neutral complexes with chloride or organic acid anions, e.g. $PbCl_2^0$ or Pb-acetate^0.

NORM scales: deposition of stable Pb and coprecipitation of ^{210}Pb

Lead scales from gas production facilities in the Netherlands can be divided into three morphological types: thin crusts, annular precipitates, and unattached particles, which can be found throughout the facilities (**Chapter 5, 6**). Lead is primarily deposited as metallic Pb and/or galena (Pb-sulphide). Weathering of scales during removal and subsequent sample preparation cause the formation of a wide range of secondary Pb minerals such as oxyhydroxides or chloridehydroxides. Precipitation of galena occurs because of supersaturation of PbS in H_2S-bearing production fluids, due to decrease of pressure and temperature during production. Precipitation of metallic Pb is an electrochemical process, associated with corrosion of steel from production facilities. In this process, Pb^{2+} ions from production fluids react with electrons, liberated by dissolution of iron from steel installation parts. Corrosion potentials of Pb^{2+} and Fe^{2+} strongly depend among others on temperature and salinity of production fluids (**Chapter 6**). Under average Dutch gas production conditions, deposition of metallic lead requires a Fe^{2+}/Pb^{2+} chemical activity ratio of less than about 10^4-10^5. This requirement is generally met in Dutch natural gas production waters, allowing widespread precipitation of metallic lead. However, precipitation could be inhibited by the use of Cr-steel in installations, because it is much less corroded than ordinary steel. In a single gas phase production system, precipitation of galena and/or metallic Pb can only occur after initial condensation of water vapour. Liquid water is needed as a corrosive medium and for the presence of Pb^{2+} ions.

In most Pb-bearing NORM scales from Dutch gas facilities, ^{210}Pb is unsupported, i.e. directly coprecipitated with stable Pb in the scales. Ingrowth from *in situ* decay of ^{226}Ra cannot explain the observed ^{210}Pb activity concentrations, while short residence times of ^{222}Rn and production fluids in gas facilities exclude a substantial contribution from *in situ* decay of ^{222}Rn in the gas phase. Evidently, ^{210}Pb became separated from its parent ^{222}Rn, either because of separation of a liquid and a gas phase during transport to the surface, or because of transport distances too long for ^{222}Rn to survive (**Chapter 2**). However, due to its high solubility in water, decay of ^{222}Rn accumulated in for instance water tanks or in water films on the inside of tubing may explain part of the unsupported ^{210}Pb in scales covering the inside of these tanks and tubing.

In some cases, ^{210}Pb can be partly unsupported and partly derived from *in situ* decay of ^{226}Ra, or ^{210}Pb can be entirely due to *in situ* decay of ^{226}Ra, coprecipitated with Ba, Sr in sulphate minerals in the scales. In the latter situation, the ^{210}Pb/^{226}Ra activity ratio provides an age estimation for the scales.

NORM scales as a geological tool: origin of stable Pb in gas reservoir brines

Lead scales, often undesirable to the oil and gas industry, are an excellent tool for looking into

the hydrocarbon reservoirs. Namely, stable Pb isotope ratios of scales are identical to ratios of formation waters from which the scales are derived. Combined with Pb isotope ratios of reservoir sediments they provide new information on the history of both sediments and fluids in the reservoirs.

Based on their lead isotopy, formation waters from different gas fields in the northern Netherlands and the southern North Sea can be clearly distinguished from one another (**Chapter 6**). Lead isotopic model ages of the formation waters range from 300 Ma (Late Carboniferous) to 125 Ma (Early Cretaceous), and result from mixing of Pb from at least two identifiable sources and subsequent ingrowth from decay of U and Th in sediments. During the first major gas emplacement in Rotliegend and Zechstein reservoirs in the northeastern Netherlands, between about 200 Ma and 150 Ma, volatile organic acids accompanying natural gas from Carboniferous source rocks mobilised Pb by dissolving feldspars and Fe-oxides in Rotliegend sediments. These sediments, but especially feldspars in the sediments, contain enough Pb to explain Pb concentrations of 100 ppm or more currently observed in Rotliegend gas reservoir brines (**Chapter 3**). Since most Dutch Rotliegend sediments consist of redeposited Late Carboniferous sediments, large amounts of Pb with a Late Carboniferous isotopic signature were added to Rotliegend formation waters. This Pb became mixed with younger Pb already present and/or flowing in from the overlying Zechstein formation. This Pb probably originated from decay of U in the Zechstein Kupferschiefer. Influx of Zechstein brines into Rotliegend reservoir sediments happened on a very large scale after 155 Ma, but likely continued after entrapment of natural gas, until the present day (see 'Mobilisation of NORs from sediments').

Follow-up

Although this study has added new insights into the nature of ^{210}Pb and stable Pb associated with the production of natural gas, further research on a number of topics is needed to complete the picture. For instance, several possibilities for the origin of NORs in lead mineral scales have been identified, but only in a qualitative way. Quantification of NORs mobilisation from U-enriched sediments in or near producing gas reservoirs might enable the construction of geochemical models predicting NORs levels in production fluids. A second challenge comprises the speciation of Pb in a water saturated gas phase. Transport of Pb in neutral complexes of chloride and/or organic acid anions such as acetate is most likely, but has not been proven directly. Lead speciation in a gas phase, either experimentally measured or empirically derived from oil company production data, could help in controlling deposition of lead mineral scales in gas production facilities.

Recommendations from this study

The outcome of this study has several implications for the oil and gas industry. In view of the

conclusions above, a number of recommendations can be made regarding the production and deposition of NORM from natural gas reservoirs:

a) During development of a gas field, any potentially U-enriched sediments in or near the gas-bearing formations should be located in as much detail as possible. Localisation of organic-rich shales or bituminous horizons should be combined with extensive γ-ray logging and monitoring of Rn concentrations in exploration wells. In addition, stable Pb isotope signatures of well test production waters much younger than expected from the age of reservoir sediments may indicate the presence of U-enriched sediments in or near the gas reservoir.

b) When completing a well, perforations for the production of natural gas should not be made in, or within close distance of, any known organic-rich horizons, in order to reduce mobilisation of U daughter nuclides, especially ^{222}Rn and ^{210}Pb. Also, perforations should be avoided near faults where possibly U-enriched sediments are juxtaposed to gas-bearing horizons, to minimise the risk of continuous influx of NORs into the producing gas reservoir.

c) Deposition of metallic Pb and coprecipitation of ^{210}Pb in gas production facilities could be reduced by the use of Cr-steel or other types of steel less sensitive to corrosion than ordinary steel. Alternatively, steel installation parts, including well tubings, could be treated with a non-corrodable coating. Another approach would be to try and keep Pb in solution, by addition of complexing agents, by addition of Fe^{2+} in order to enlarge the Fe^{2+}/Pb^{2+} activity ratio in the fluids, or by application of an electrical potential to steel parts, high enough to prevent the transfer of electrons to Pb^{2+}. A third option would be to force deposition of metallic Pb at a location of choice under controlled conditions, for instance by offering a sacrificial electrode, or by passing the production fluids through a column charged with Fe particles.

d) Deposition of ^{210}Pb-bearing galena could be prevented if Pb and S levels in the production fluids are kept below the PbS solubility product. In gas fields producing no or only very low levels of H_2S this condition is almost always met. When produced gas contains significant levels of H_2S, pressure and temperature conditions in the production facilities could be set in such a way that galena deposition will preferentially take place at one easily accessible position in the facilities. It should be emphasised here that all possible remediations against deposition of metallic Pb or galena offered under c) and d) apply to wells producing both a gas and a liquid water phase. In facilities producing a single gas phase, controlling pressure and temperature conditions could also be used to stimulate or reduce condensation of water, without which no deposition of mineral scales seems possible.

Of course, these recommendations should be carefully judged on economic feasibility. Some options are much more expensive than other ones, and costs for NORM prevention or reduction should not outweigh costs associated with for instance the removal of NORM and cleaning and maintenance of production facilities, unless other aspects than just economic ones are or become more important, such as technical restraints, legislation or environmental regulations.

Samenvatting

Inleiding

De aanwezigheid van Natuurlijk Voorkomende Radionuclides (NVR) in de Aarde is alom bekend. De energie die vrijkomt bij hun radioactief verval is de voornaamste bron van aardwarmte, en de drijvende kracht van vulkanisme en de beweging van de schollen waaruit de aardkorst is opgebouwd. Aangezien we deze radioactieve deeltjes vooral in de aardkorst aantreffen, waaruit ook alle olie en gas worden gewonnen, is het niet verbazingwekkend dat we ze ook tegenkomen in de olie- en gasindustrie.

Al in het begin van de 20e eeuw, slechts enkele jaren na de ontdekking van het verschijnsel radioactiviteit, werd het duidelijk dat NVR kunnen worden mee geproduceerd met olie en gas. Verhoogde concentraties van sommige van deze elementen kunnen zowel in het geproduceerde olie en gas, als in mee geproduceerd water en allerlei afzettingen in productie-installaties voorkomen. Wanneer mee geproduceerd water of minerale afzettingen NVR bevatten worden ze aangeduid met de Engelse afkorting NORM, oftewel Naturally Occurring Radioactive Materials. De aanwezigheid van radioactieve stoffen in productie-installaties kan oliemaatschappijen voor extra onderhouds- en verwerkingskosten plaatsen, maar vraagt ook om extra beschermende maatregelen voor hun personeel en het milieu. Een goed beleid ten aanzien van NORM is daarom essentieel voor oliemaatschappijen. Kennis over de herkomst en het ontstaan van NORM kan bijdragen tot voorspellen of misschien zelfs voorkómen van NORM in productie-installaties, wat weer kan leiden tot een belangrijke vermindering van risico's en kosten.

Het onderzoek wat in dit proefschrift wordt beschreven is opgezet om inzicht te verkrijgen in de herkomst en verspreiding van NVR (uranium, thorium en hun vervalproducten oftewel dochternucliden) in olie- en gasreservoirs, in transport van NVR vanuit deze reservoirs naar en in de productie-installaties, en in de afzetting van NORM in de installaties. Vanwege geringe kennis over vooral lood-210 (^{210}Pb, een van de radioactieve dochterelementen van uranium-238), en vanwege het feit dat ^{210}Pb een van de belangrijkste NVR is die men in de Nederlandse gaswinningsindustrie tegenkomt, is dit onderzoek vooral gericht op ^{210}Pb in relatie tot de winning van aardgas. Omdat ^{210}Pb, een van de vele in de natuur voorkomende isotopen van lood, vrijwel altijd wordt aangetroffen samen met niet-radioactief ofwel stabiel lood, is de aanwezigheid van zowel ^{210}Pb als stabiel lood onderzocht in boorkernen uit Nederlandse gasvelden. Het transport van lood vanuit gasreservoirs in de diepe ondergrond naar en in productie-installaties is onderzocht door middel van laboratoriumexperimenten, waarbij de oplosbaarheid van lood in methaan is gemeten, het voornaamste bestanddeel van aardgas. Verder is een aantal verschillende typen minerale afzettingen van lood uit productie-installaties onderzocht om uit te vinden hoe deze worden afgezet en hoe ^{210}Pb in de afzettingen wordt ingebouwd. Tenslotte is de loodisotopen-samenstelling van zowel de sedimenten uit de boorkernen als van de minerale afzettingen gebruikt om de herkomst van stabiel lood in diep grondwater uit Nederlandse gasvelden te achterhalen.

Aanrijking en verspreiding van NVR in gasreservoirsedimenten

De belangrijkste NVR in NORM van de Nederlandse olie- en gasindustrie zijn radium-226, het gasvormig radon-222 en lood-210, alle drie afkomstig uit de radioactieve vervalreeks van de "moeder"nuclide uranium-238 (**tabel 1.1**). Hoewel de twee andere natuurlijke vervalreeksen, die van uranium-235 en thorium-232, ook isotopen van radium, radon en lood bevatten, zijn deze om geochemische redenen en/of vanwege hun zeer korte levensduur niet van belang voor de Nederlandse situatie (**hoofdstuk 1**).

Onder de zuurstofloze omstandigheden zoals die in olie- en gasreservoirs heersen, zijn de elementen radium, radon en lood erg mobiel. Radon omdat het een gas is, radium en lood vanwege hun goede oplosbaarheid in het meestal zeer zoute grondwater in olie- en gasreservoirs. Ondanks dat ze erg mobiel zijn, moeten radium, radon en lood die met olie en/of gas mee geproduceerd worden toch uit het reservoir zelf, of uit de directe omgeving afkomstig zijn, vanwege de zeer langzame grondwaterbewegingen in de diepe ondergrond en vanwege de relatief korte levensduur van de elementen. En aangezien alle elementen uit de vervalreeks tussen ^{238}U en ^{226}Ra immobiel zijn onder de reducerende omstandigheden zoals die in olie- en gasreservoirs heersen, is uranium in de reservoirsedimenten de meest waarschijnlijke bron van ^{226}Ra, ^{222}Rn en ^{210}Pb (**hoofdstuk 1**).

Grote verschillen in gehaltes mee geproduceerde NVR tussen meerdere putten uit dezelfde reservoirs geven aan dat uranium plaatselijk veel of juist heel weinig voor kan komen in de reservoirsedimenten. Door de grote affiniteit van uranium voor organisch materiaal zijn er twee manieren denkbaar om uranium, wat zelf slecht oplosbaar is in zuurstofloos grondwater, plaatselijk op te hopen in reservoirsedimenten. Ten eerste kan uranium zich langzaam ophopen in organischrijke sedimenten die het opnemen uit langs stromend, zuurstof houdend grondwater, voordat de olie en/of het gas in de sedimenten ophopen en alle zuurstof verdrongen wordt. Een waarschijnlijke bron van mee geproduceerde NVR met Nederlands aardgas is de organischrijke Kupferschiefer, een laag die voornamelijk is opgebouwd uit kalk en klei en de scheiding vormt tussen de voor Nederland belangrijkste gasreservoirgesteenten, de Rotliegend en Zechstein formaties (**Fig. 2.1 en 6.2**). Vooral wanneer de Kupferschiefer slechts door middel van een breuk van een Rotliegend gasreservoir wordt gescheiden, zoals in figuur 2.1, kunnen NVR vanuit de Kupferschiefer in grondwater langs en horizontaal door de breuk heen in het reservoir terechtkomen (**hoofdstuk 6**). De organischrijke steenkool houdende Carboonsedimenten onder het Rotliegend zouden op dezelfde manier een alternatieve bron van NVR kunnen zijn, ware het niet dat er in de Noord-Nederlandse ondergrond geen geologische situaties bekend zijn waarin een Rotliegend gasreservoir slechts door een breuk van het Carboon wordt gescheiden.

Ten tweede kunnen restanten van migrerende olie, bitumen genaamd, in een toekomstig gasreservoirgesteente worden afgezet. Indien deze restanten asphaltenen bevatten kunnen ze al rijk aan uranium zijn geweest voor hun afzetting (**hoofdstuk 1**); in het andere geval kunnen ze na hun afzetting uranium uit passerend grondwater hebben opgenomen, vóór de aankomst van het aardgas.

Onderzoek aan sedimenten uit boorkernen uit een Noordnederlands gasveld hebben inderdaad verhoogde concentraties uranium in de plaatselijk 0.5 m dikke Kupferschiefer aangetoond (**hoofdstuk 2**). Een aantal niveaus uit de Rotliegend sedimenten bevatten echter

bitumen met nog veel hogere uraniumgehaltes. Het uranium was vooral aanwezig in de vorm van kleine kristalletjes uraniumoxide langs poriën in het bitumen (**omslagfoto**). Het lineaire verband tussen het uranium en organisch-koolstofgehalte van deze gesteenten en de ouderdom van de uraniumoxide kristalletjes, 246 miljoen jaar, wijzen erop dat het bitumen al uranium bevatte toen het in het Rotliegend gesteente werd afgezet en dat het waarschijnlijk afkomstig is van de Kupferschiefer. De goede porositeit en permeabiliteit van het bitumineuze gesteente geven aan dat het bitumen in ieder geval in dit deel van het gasveld een belangrijker bron van NVR is dan de slecht waterdoorlatende Kupferschiefer (**hoofdstuk 2**). De afwezigheid van bitumen in een andere boorkern uit hetzelfde gasveld onderstreept de zeer plaatselijke schaal waarop productie van NVR met olie en/of gas belangrijk kan zijn.

Mobilisatie van NVR vanuit reservoirsedimenten

Mobilisatie van ^{226}Ra, ^{222}Rn en ^{210}Pb vanuit uranium houdende sedimenten gebeurt door middel van het "α-recoil" proces, waarbij een nieuw ontstaan dochteratoom door de energie van het vervalproces kan worden weggeschoten uit het sediment en in de met water en eventueel olie en/of gas gevulde sedimentporiën terechtkomt, of door uitlogen van de NVR vanuit plaatsen in kristalroosters die door eerdere α-recoil processen zijn beschadigd. Directe α-recoil mobilisatie wordt over het algemeen belangrijker geacht dan uitlogen (**hoofdstuk 1**). Normaal gesproken zullen gemobiliseerde NVR in gesloten olie- of gasreservoirs waar geen stroming in plaatsvindt vrijwel onmiddellijk geadsorbeerd worden aan het sediment. Veel Nederlandse Rotliegend gasreservoirs zijn echter toch toegankelijk voor grondwater van buitenaf, bijvoorbeeld voor het zeer zoute water vanuit de Zechstein formaties. Door deze stroming kunnen continu NVR afkomstig van bijvoorbeeld verval van uranium in de Kupferschiefer naar het Rotliegend gesteente getransporteerd worden. De productie van gas vanuit een reservoir gaat gepaard met een drukvermindering in het gesteente, die een dergelijke instroom van water van buitenaf in stand kan houden.

Stroming, opgewekt door gasproductie, is waarschijnlijk ook de reden van de selectieve mobilisatie en productie van ^{210}Pb vanuit uraniumrijke, bitumineuze Rotliegend gesteenten. In dit laatste proces wordt ^{222}Rn, wat vanwege zijn gasvormigheid een hogere "ontsnappingsgraad" heeft dan ^{226}Ra en ^{210}Pb, weggevoerd van het uraniumoxide waaruit het door α-recoil is gemobiliseerd. Op weg naar de gasput vervalt het naar ^{210}Pb wat op die manier mee geproduceerd kan worden met het aardgas (**hoofdstuk 2**).

Transport van NVR in gaswinningsvloeistoffen

In Nederland wordt aardgas over het algemeen in twee fysische systemen gewonnen: ofwel in een enkele, met water verzadigde, gasfase, ofwel samen met een vloeibare waterfase. Transport van NVR, maar ook van niet-radioactieve deeltjes zoals stabiel lood, in het tweefasensysteem is eenvoudig te verklaren: het mee geproduceerde water bestaat hoofdzakelijk uit grondwater uit het gasreservoir, waarin door het vaak hoge zout- en/of organische zuurrestgehalte onder andere grote hoeveelheden stabiel lood, ^{226}Ra en ^{210}Pb

kunnen voorkomen. Op deze manier kunnen hoeveelheden stabiel lood tot enkele tientallen kilo's per dag per gasput worden geproduceerd (**hoofdstuk 4**). Transport van het gasvormige ^{222}Rn, dat zowel in water als in koolwaterstoffen goed oplosbaar is, is zowel in het tweefasen- als in het één-fase systeem geen enkel probleem. Laboratoriumexperimenten en productiegegevens van Nederlandse aardgasvelden hebben aangetoond dat ook stabiel lood en ^{210}Pb in een met water verzadigde gasfase getransporteerd kunnen worden (**hoofdstuk 4**). Weliswaar ligt de maximale productie op ongeveer 5 gram lood per put per dag, maar dat is genoeg om de aanwezigheid van loodafzettingen in productie-installaties van die putten te kunnen verklaren (**hoofdstuk 6**). Hoewel het onderzoek dit niet heeft kunnen aantonen, is het zeer waarschijnlijk dat het lood in het aardgas aanwezig is in de vorm van elektrisch neutrale complexen met chloride- en/of zuurrest-ionen zoals acetaat.

Minerale NORM afzettingen: neerslag van stabiel lood en coprecipitatie van ^{210}Pb in gaswininstallaties

Loodafzettingen uit Nederlandse gaswininstallaties kunnen worden onderverdeeld in drie typen: dunne korsten, ringvormige afzettingen en los voorkomende deeltjes of stukken, die alle drie overal in de installaties kunnen worden aangetroffen (**hoofdstukken 5 en 6**). Het lood wordt in oorspronkelijk afgezet als metallisch lood of als loodsulfide, galeniet. Verwering en omzetting van de afzettingen zorgen ervoor dat ze bij onderzoek uit een heel scala aan secundaire loodmineralen blijken te bestaan.

Neerslag van galeniet wordt veroorzaakt door oververzadiging van PbS in de productievloeistoffen ten gevolge van druk- en temperatuurdalingen tijdens het productieproces. Afzetting van metallisch lood is een elektrochemisch proces, gerelateerd aan corrosie van staal uit de installaties. Dit proces verloopt alleen bij een lagere Fe^{2+}/Pb^{2+} ratio in het productiewater dan 10.000 tot 100.000, wat echter doorgaans het geval is. Ook is het proces sterk afhankelijk van onder andere de temperatuur en het zoutgehalte van de productievloeistoffen, en lijkt het gehinderd te kunnen worden door het gebruik van chroom houdend staal, wat veel corrosiebestendiger is dan gewoon staal (**hoofdstuk 6**). In gaswininstallaties die alleen met water verzadigd gas produceren, kunnen loodafzettingen alleen optreden als er door drukvermindering eerst vloeibaar water uit de gasfase condenseert. Dit water is nodig als corrosief medium en om lood- en eventueel ook zwavel-ionen in op te kunnen lossen.

In de meeste loodafzettingen uit Nederlandse gaswininstallaties is het ingebouwde ^{210}Pb direct mee neergeslagen met stabiel lood. De aanwezige hoeveelheid ^{210}Pb kan niet ter plekke ontstaan zijn uit verval van ^{226}Ra of ^{222}Rn, omdat er vaak geen of te weinig ^{226}Ra in de afzettingen aanwezig is, en de verblijftijd van ^{222}Rn in de installaties doorgaans te kort is. Vanwege de goede oplosbaarheid van ^{222}Rn in water kan een deel van het aanwezige ^{210}Pb in afzettingen op bijvoorbeeld de wand van wateropslagtanks wel uit *in situ* verval van ^{222}Rn verklaard worden. Soms ook is er wel voldoende ^{226}Ra in afzettingen aanwezig om alle of een gedeelte van het ^{210}Pb uit *in situ* verval te kunnen verklaren. In het laatste geval kan de ouderdom van de afzettingen worden afgeleid uit de verhouding $^{210}Pb/^{226}Ra$ (**hoofdstuk 6**).

NORM afzettingen als een geochemisch hulpmiddel: de herkomst van het lood in reservoirwaters

De loodafzettingen die de olie- en gasindustrie voor extra kosten en productieproblemen plaatsen, bieden de geochemicus een welkom kijkje in de olie- en/of gasreservoirs. De loodisotopensamenstelling van de afzettingen komt namelijk exact overeen met die van het grondwater uit de reservoirs. In combinatie met de loodisotopensamenstelling van de reservoirsedimenten leveren de afzettingen derhalve nieuwe informatie over de geschiedenis van zowel de sedimenten als het grondwater.

Met behulp van hun lood isotopie zijn grondwaters uit verschillende gasvelden in Noord-Nederland en het zuidelijk deel van de Noordzee duidelijk van elkaar te onderscheiden. Modellen leveren voor de waters een ouderdom op van 300 miljoen jaar (Laat Carboon) tot 125 miljoen jaar (Vroeg Krijt). Tijdens de vroegste fase in de Nederlandse geologie waarin aardgas reservoirs werden gevuld, tussen 200 en 150 miljoen jaar geleden, loste een groot deel van het lood uit veldspaten en ijzeroxidehuidjes in de reservoirgesteenten op door inwerking van organische zuren die met het gas mee werden aangevoerd vanuit de steenkoollagen in het Carboon. De reservoirsedimenten bevatten genoeg lood om de huidige concentraties van 100 ppm of meer lood in Rotliegend grondwaters te kunnen verklaren (**hoofdstuk 3**). Dit lood, dat een isotopensamenstelling bezat overeenkomend met Carboongesteentes, waaruit het Rotliegend immers voornamelijk is opgebouwd, werd vermengd met lood met een jongere signatuur dat al aanwezig was in het water of werd aangevoerd vanuit de bovenliggende Zechstein formaties. Aanvoer van water in Rotliegend gesteentes vanuit het Zechstein vond op grote schaal plaats na ongeveer 155 miljoen jaar geleden, maar is waarschijnlijk doorgegaan ook na de aankomst van aardgas in de reservoirformaties, tot op de dag van heden (**zie "mobilisatie van NVR..."**).

Aanbevelingen naar aanleiding van dit onderzoek

Hoewel dit onderzoek nieuwe inzichten heeft opgeleverd over ^{210}Pb en stabiel lood in relatie tot aardgaswinning, is er aanvullend onderzoek nodig om het beeld te completeren. Zo zou het bijvoorbeeld nuttig zijn om de herkomst van ^{210}Pb in loodafzettingen te kwantificeren. Met die kennis zouden modellen kunnen worden ontwikkeld om ^{210}Pb gehaltes in geproduceerd gas en water te kunnen voorspellen. Een andere uitdaging is het vaststellen van de speciatie van lood in aardgas. De aanwezigheid van elektrisch neutrale chloride- of zuurrestcomplexen is waarschijnlijk, maar niet bewezen. Kennis hierover zou de afzetting van lood in gaswininstallaties kunnen helpen beheersen of beïnvloeden.

De voornaamste aanbevelingen die vanuit dit onderzoek kunnen worden gedaan ten aanzien van productie en afzetting van NVR met aardgas zijn:

a) Tijdens de ontwikkelingsfase van een gasveld zouden organischrijke lagen, die in potentie veel uranium kunnen bevatten, in of nabij de reservoirformaties nauwkeurig in kaart moeten worden gebracht. Gammastralings- en radongehaltes in exploratieputten zouden gecombineerd kunnen worden met loodisotopen onderzoek aan reservoirwater afkomstig van productietests. Een jongere modelleeftijd dan verwacht zou kunnen wijzen op de aanwezigheid van

uraniumrijke afzettingen in of dichtbij de reservoirgesteenten.
b) Bij het voltooien van een productieput moet het aanbrengen van perforaties ter hoogte van organischrijke lagen zoveel mogelijk vermeden worden, om mobilisatie van NVR vanuit deze lagen tegen te gaan. Ook zouden perforaties zover mogelijk bij breuken vandaan moeten worden gezet die eventueel uranium houdende sedimenten scheiden van het reservoir.
c) De afzetting van metallische lood en coprecipitatie van ^{210}Pb zou kunnen worden teruggebracht door de toepassing van corrosiebestendiger chroom houdend staal in plaats van gewoon staal, of door aanbrengen van een corrosiebestendige coating op het staal. Een andere aanpak zou het in oplossing houden van het lood kunnen zijn, door toevoeging van complexvormende stoffen, door toevoeging van tweewaardig ijzer om de Fe^{2+}/Pb^{2+} ratio te verhogen, of door toepassing van een elektrische potentiaal op installatie-onderdelen. Een derde optie zou kunnen zijn om het lood daar neer te laten slaan waar je er makkelijk bij kunt om het te verwijderen, met weinig risico's en kosten.
d) De afzetting van ^{210}Pb-houdend galeniet zou door middel van druk- of temperatuur-modificaties in het productieproces kunnen worden beïnvloed, door ofwel oververzadiging van PbS in de productievloeistoffen te voorkomen, ofwel galeniet op een gunstige plek te laten neerslaan. Het moge overigens duidelijk zijn dat de onder c) en d) aangedragen opties betrekking hebben op gasputten die naast het aardgas ook vloeibaar water produceren. Voor putten die slechts met water verzadigd aardgas produceren is het tegengaan of juist op een bepaald plek stimuleren van watercondensatie met behulp van druk en/of temperatuur al voldoende om het vormen van loodafzettingen te beïnvloeden.

De hier gedane aanbevelingen moeten vanzelfsprekend beoordeeld worden op hun economische haalbaarheid. Sommige opties zijn duidelijk duurder dan andere, en kosten voor het tegengaan of stimuleren van NORM afzetting mogen niet veel hoger zijn dan de kosten die oliemaatschappijen nu maken voor het verwijderen van NORM en extra onderhoud en veiligheid. Tenzij ook andere factoren een rol spelen, zoals technische beperkingen, wetgeving of milieu-voorschriften.

Acknowledgements

Graag wil ik hier iedereen bedanken die heeft bijgedragen aan de totstandkoming van dit proefschrift. Allereerst mijn promotor, prof. dr. Olaf Schuiling, die mij de mogelijkheid bood om te promoveren op een zeer interessant en breed onderwerp. Daarnaast de leden van de "stuurgroep", samengesteld uit medewerkers van de Nederlandse Aardolie Maatschappij en de Shell onderzoekcentra in Rijswijk en Amsterdam, onder de bezielende leiding van mijn copromotor Andre Hartog van het Shell Research and Technology Centre Amsterdam.

Van de Faculteit Aardwetenschappen in Utrecht wil ik met name mijn tweede copromotor Sieger van der Laan bedanken, voor zijn immer stimulerende inbreng, en Peter van der Linde, die onmisbaar bleek als "vliegende keep" om alles op IT-gebied in goede banen te leiden. Verder alle collega AiO's, OiO's, postdocs en overige medewerkers van de vakgroep, later projectgroep, Geochemie, en de medewerkers van de bibliotheek, de audiovisuele dienst en het voormalige AGL.

Delen van dit onderzoek zijn uitgevoerd in samenwerking met en bij het Nederlands Instituut voor Toegepaste Geowetenschappen TNO en de Technische Universiteit Delft. Bij deze bedank ik alle betrokken medewerkers van het voormalig Geochemisch Laboratorium van NITG-TNO in Haarlem en van het Laboratorium voor Toegepaste Thermodynamica en Faseleer van de Faculteit Scheikundige Technologie en Materiaalkunde van de TU Delft.

Als laatste wil ik graag Odette bedanken. Zonder haar liefde, steun, geduld en vertrouwen was dit proefschrift niet tot stand gekomen.

Curriculum Vitae

Arthur Pieter Schmidt werd geboren op 24 november 1970 in Zwijndrecht. In 1983 begon hij zijn middelbare schoolopleiding aan het Willem de Zwijgercollege te Bussum. Deze opleiding werd in 1989 afgesloten met het VWO diploma. In datzelfde jaar begon hij met zijn studie aan de Universiteit van Amsterdam, waar hij in 1990 het propedeutisch examen Scheikunde behaalde. Hij zette zijn studie voort aan de Universiteit Utrecht, waar hij in 1995 het doctoraal examen Endogene Geochemie aflegde. Vanaf september 1995 werkte hij als Assistent in Opleiding bij de Vakgroep Geochemie van de Universiteit Utrecht, waar dit proefschrift tot stand kwam. Sinds mei 2000 werkt hij als onderzoeker bij het Ceramics Research Centre van Corus in IJmuiden.